Supplementary

Harnessing the Power of a Novel Triple Chelated Complex in Fermented Probiotic Dairy Products: A Promising Solution for Combating Iron Deficiency Anemia

Alexey Gvozdenko[1], Andrey Blinov[1], Alexey Golik[1], Zafar Rekhman[1], Andrey Nagdalian[2], Dionis Filippov[1], Alina Askerova[2], Nikita Bocharov[1], Elena Kastarnova [3], Faten Abdo Hassan[4*], Ammar AL-Farga[5], and Mohammad Ali Shariati[6*]

[1] Physical and Technical Faculty, North-Caucasus Federal University, 355017 Stavropol, Russia; agvozdenko@ncfu.ru (Alexey Gvozdenko); avblinov@ncfu.ru (Andrey Blinov); abgolik@ncfu.ru (Alexey Golik); zaarekhman@ncfu.ru (Zafar Rekhman); ddfilippov@ncfu.ru (Dionis Filippov); bochamocha26@yandex.ru (Nikita Bocharov).

[2] Laboratory of Food and Industrial Biotechnology, North-Caucasus Federal University, 355017 Stavropol, Russia; anagdalian@ncfu.ru (Andrey Nagdalian); vikalinka04@mail.ru (Alina Askerova).

[3] Veterinary Faculty, Stavropol Sate Agrarian University, Zootechnicheskiy Street 9, 355017, Stavropol, Russia elena-kastarnova@mail.ru (Elena Kastarnova)

[4] Faculty of Science, Department of Microbiology, Taiz University, Taiz, Yemen fatenhassan@taiz.edu.ye (Faten Abdo Hassan)

[5] Department of Biochemistry, College of Science,University of Jeddah, Jeddah, Saudi Arabia. alfergah83@gmail.com (Ammar AL-Farga)

[6] Scientific Department, Semey Branch of the Kazakh Research Institute of Processing and Food Industry, Gagarin Avenue 238G, Almaty 050060, Kazakhstan; shariatymohammadali@gmail.com (Mohammad Ali Shariati)

Corresponding author

Faten A. M. Hassan; fatenhassan@taiz.edu.ye ; Mohammad Ali Shariati: shariatymohammadali@gmail.com

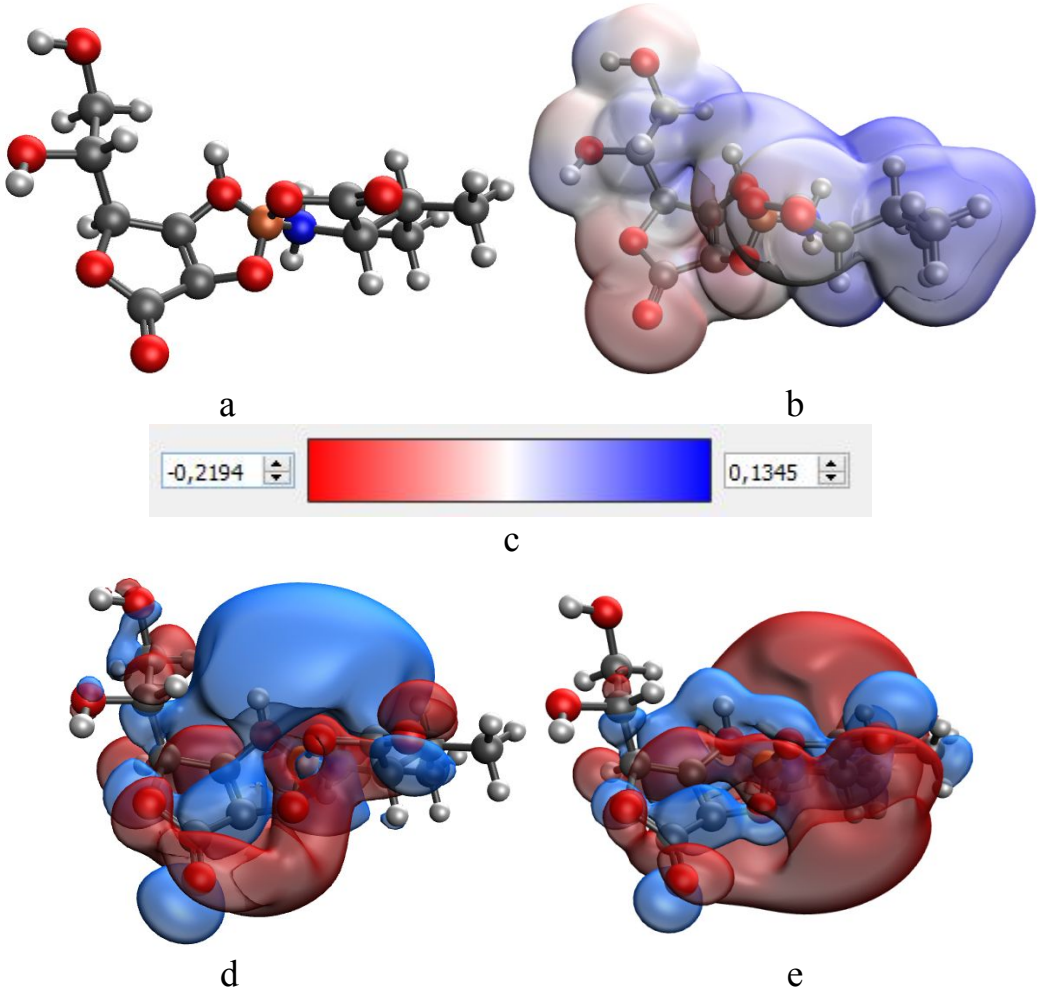

Figure S1. Results of modeling of iron ascorbate valinate through the amino and carboxyl groups of L-valine and hydroxyl groups attached to C2 and C3 carbon atoms of ascorbic acid: model of the molecular complex (a), electron density distribution (b), electron density distribution gradient (c), HOMO (d), LUMO(e)

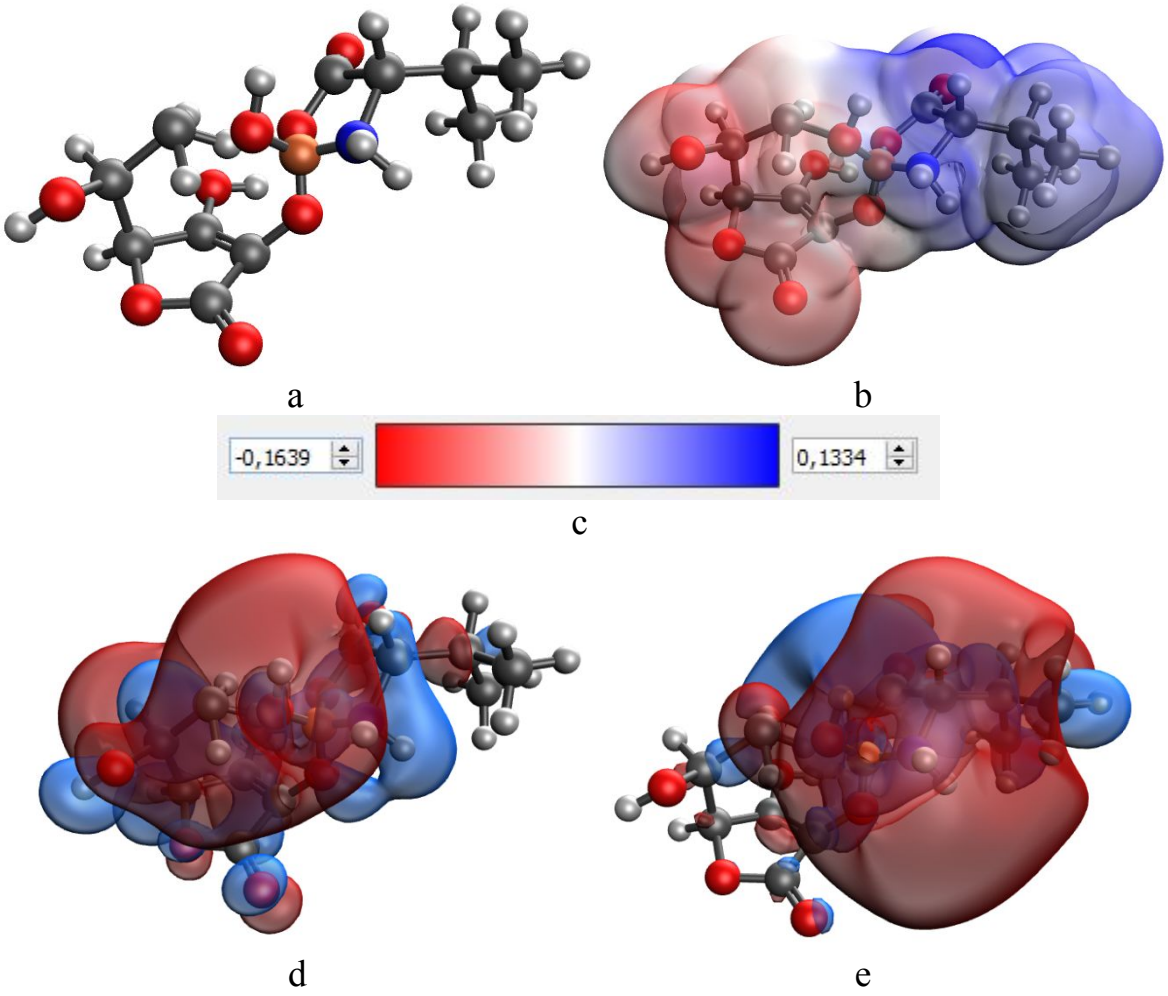

Figure S2. Results of modeling of iron ascorbate valinate through the amino and carboxyl groups of L-valine and hydroxyl groups attached to C2 and C6 carbon atoms of ascorbic acid: model of the molecular complex (a), electron density distribution (b), electron density distribution gradient (c), HOMO (d), LUMO(e)

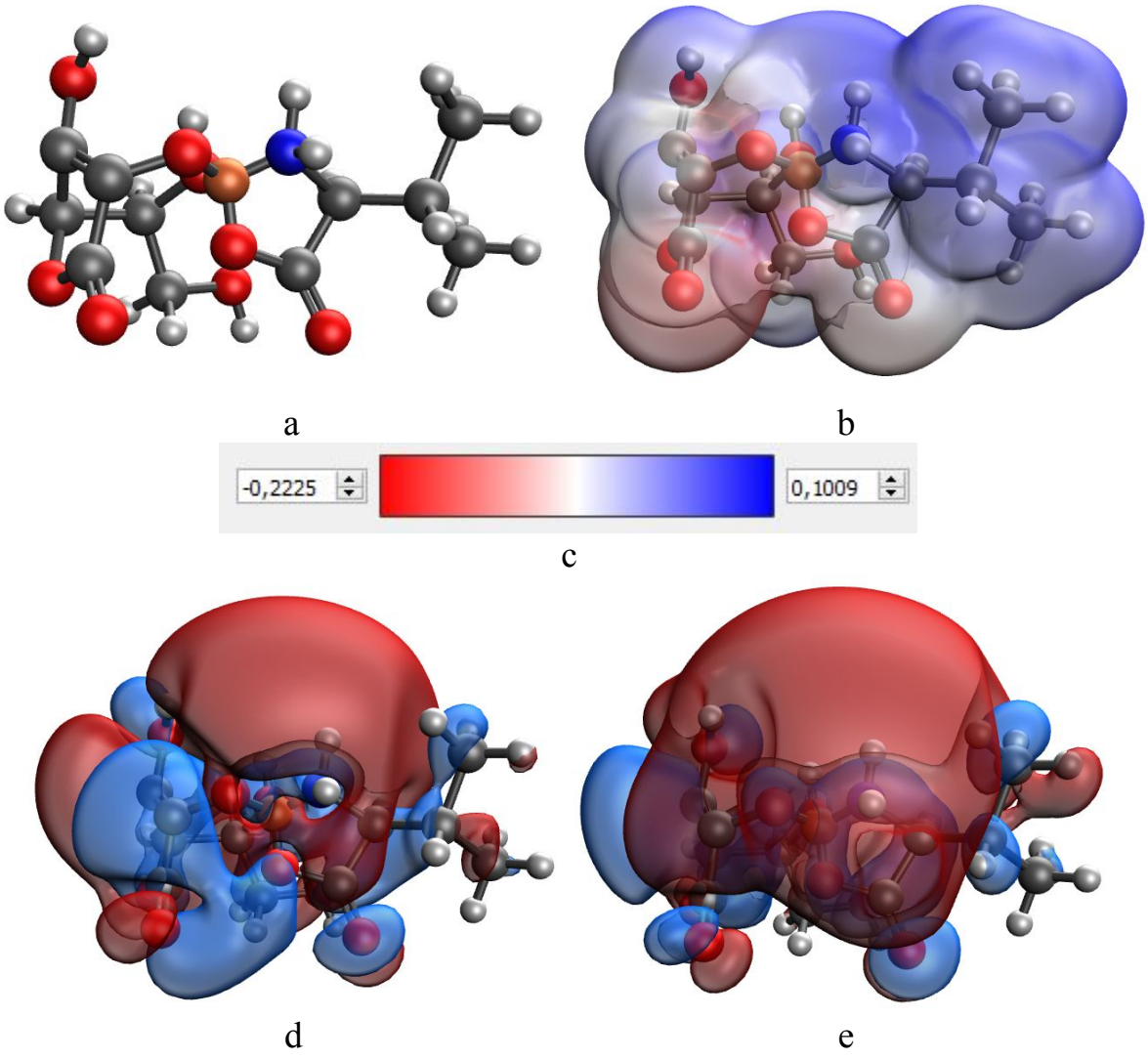

Figure S3. Results of modeling of iron ascorbate valinate through amino and carboxyl groups of L-valine and hydroxyl groups attached to C2 and C5 carbon atoms of ascorbic acid: model of the molecular complex (a), electron density distribution (b), electron density distribution gradient (c), HOMO (d), LUMO(e)

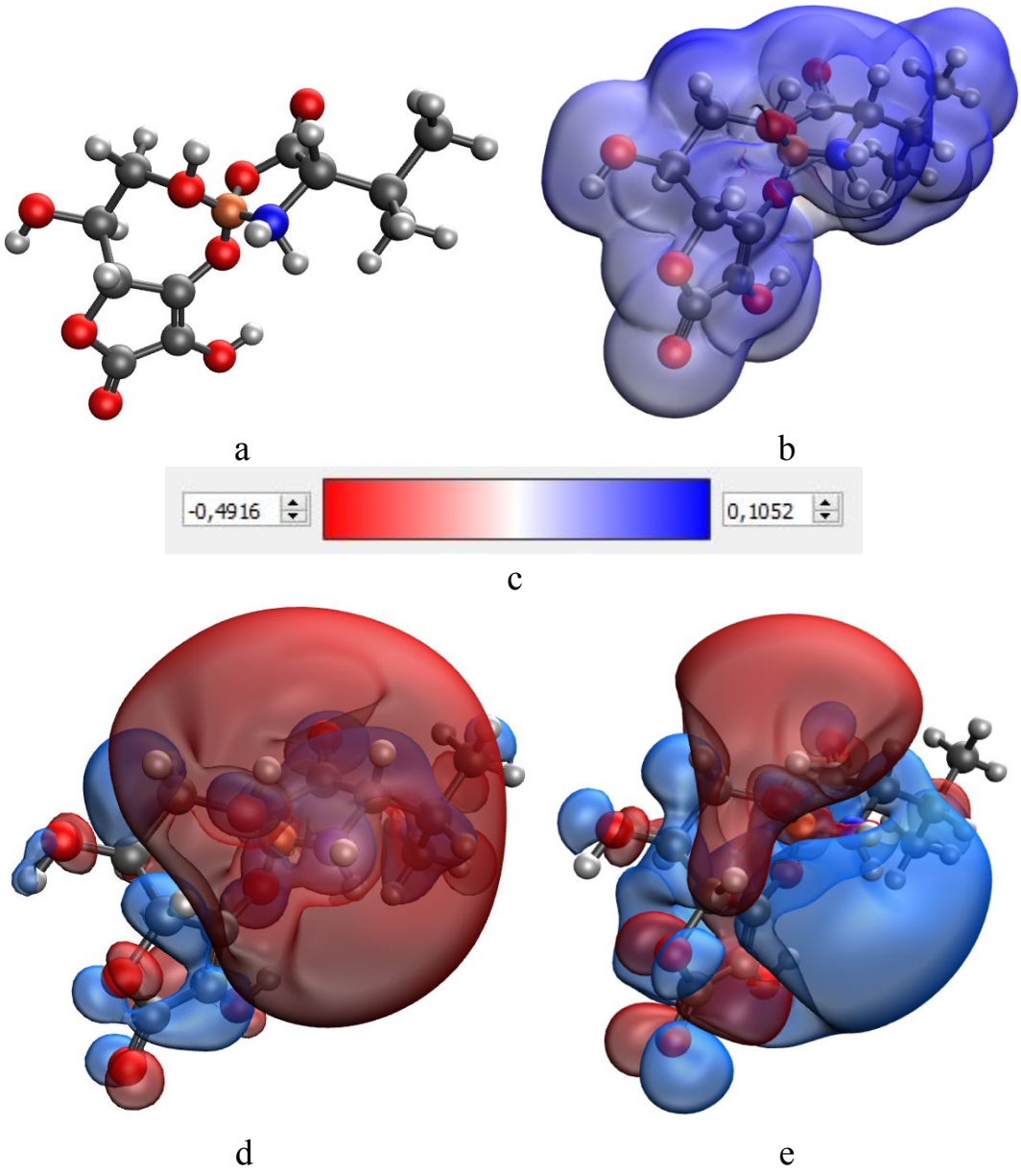

Figure S4. Results of modeling of iron ascorbate valinate through amino and carboxyl groups of L-valine and hydroxyl groups attached to C3 and C6 carbon atoms of ascorbic acid: model of the molecular complex (a), electron density distribution (b), electron density distribution gradient (c), HOMO (d), LUMO(e)

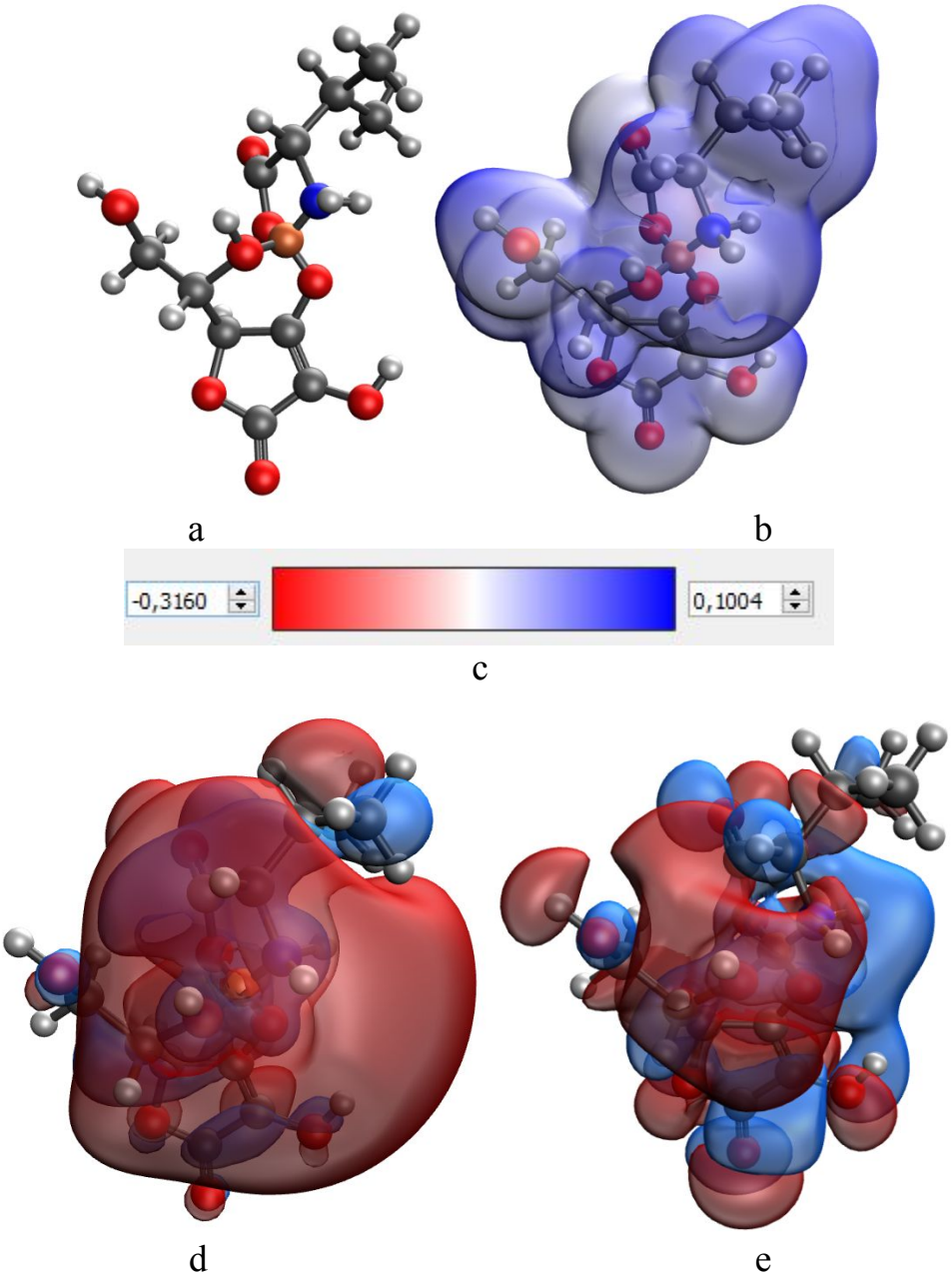

Figure S5. Results of modeling of iron ascorbate valinate through the amino and carboxyl groups of L-valine and hydroxyl groups attached to C3 and C5 carbon atoms of ascorbic acid: model of the molecular complex (a), electron density distribution (b), electron density distribution gradient (c), HOMO (d), LUMO(e)

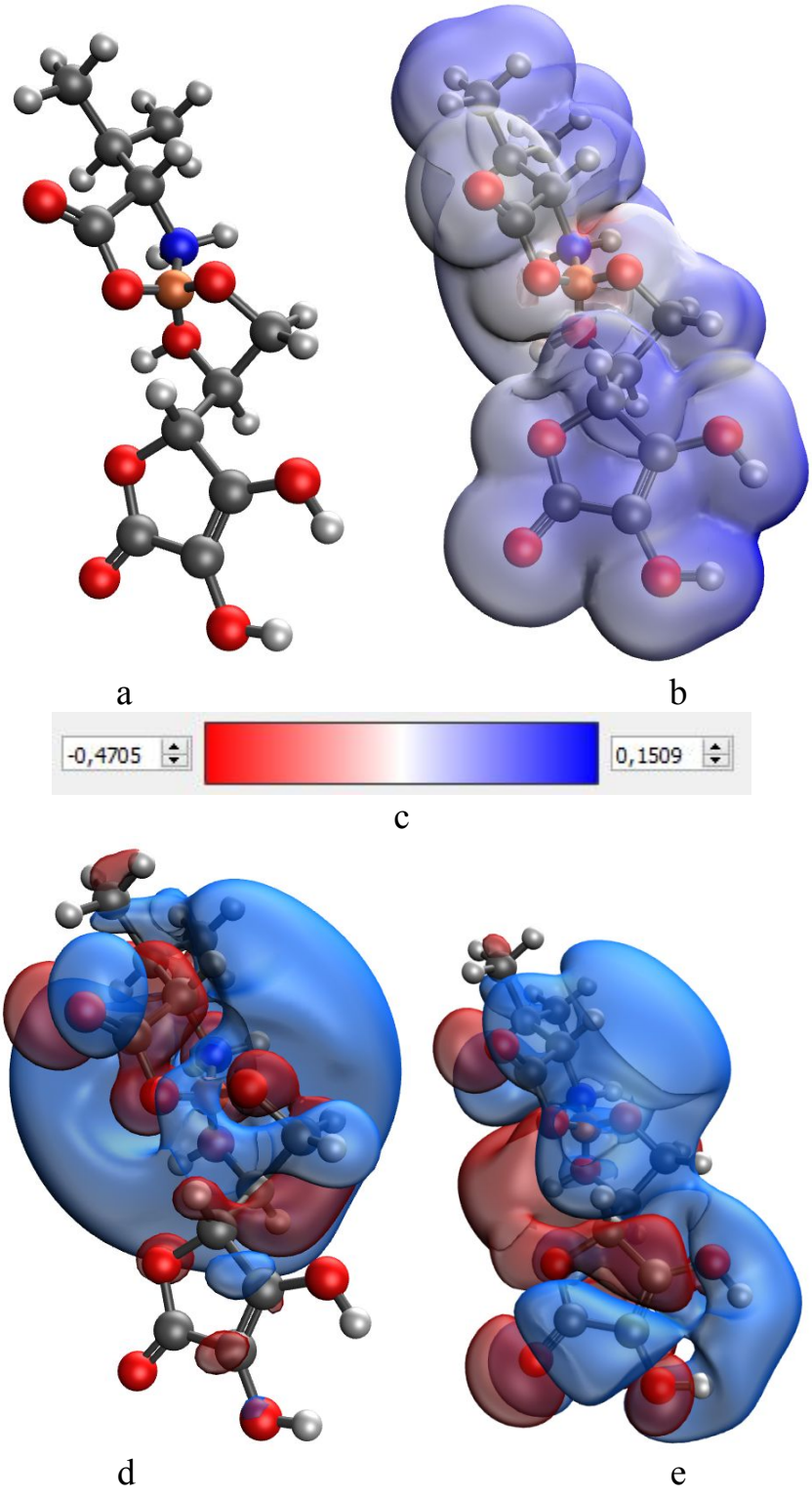

Figure S6. Results of modeling of iron ascorbate valinate through amino and carboxyl groups of L-valine and hydroxyl groups attached to C5 and C6 carbon atoms of ascorbic acid: model of the molecular complex (a), electron density distribution (b), gradient of electron density distribution (c), HOMO (d), LUMO(e)

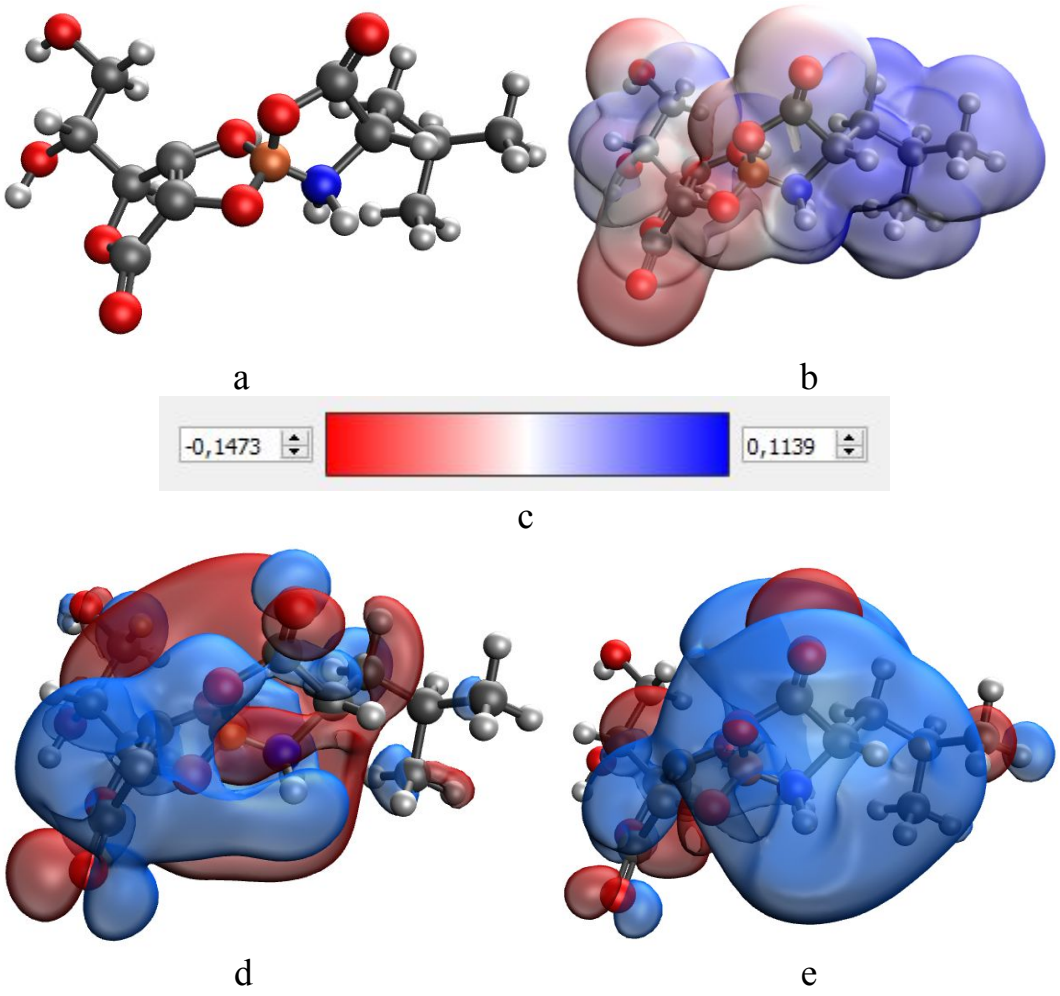

Figure S7. Results of modeling of iron ascorbate leucinate through amino and carboxyl groups of L-leucine and hydroxyl groups attached to C2 and C3 carbon atoms of ascorbic acid: model of the molecular complex (a), electron density distribution (b), electron density distribution gradient (c), HOMO (d), LUMO(e)

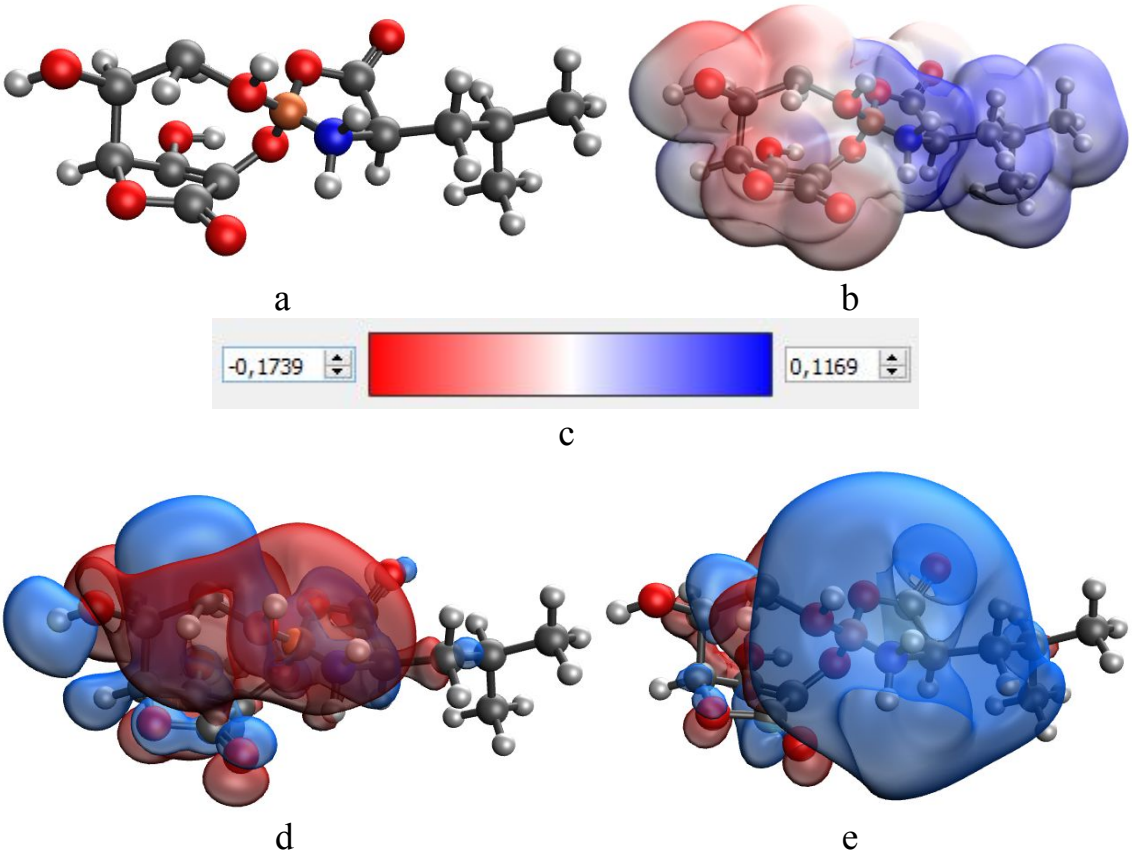

Figure S8. Results of modeling of iron ascorbate leucinate through amino and carboxyl groups of L-leucine and hydroxyl groups attached to C2 and C6 carbon atoms of ascorbic acid: model of the molecular complex (a), electron density distribution (b), electron density distribution gradient (c), HOMO (d), LUMO(e)

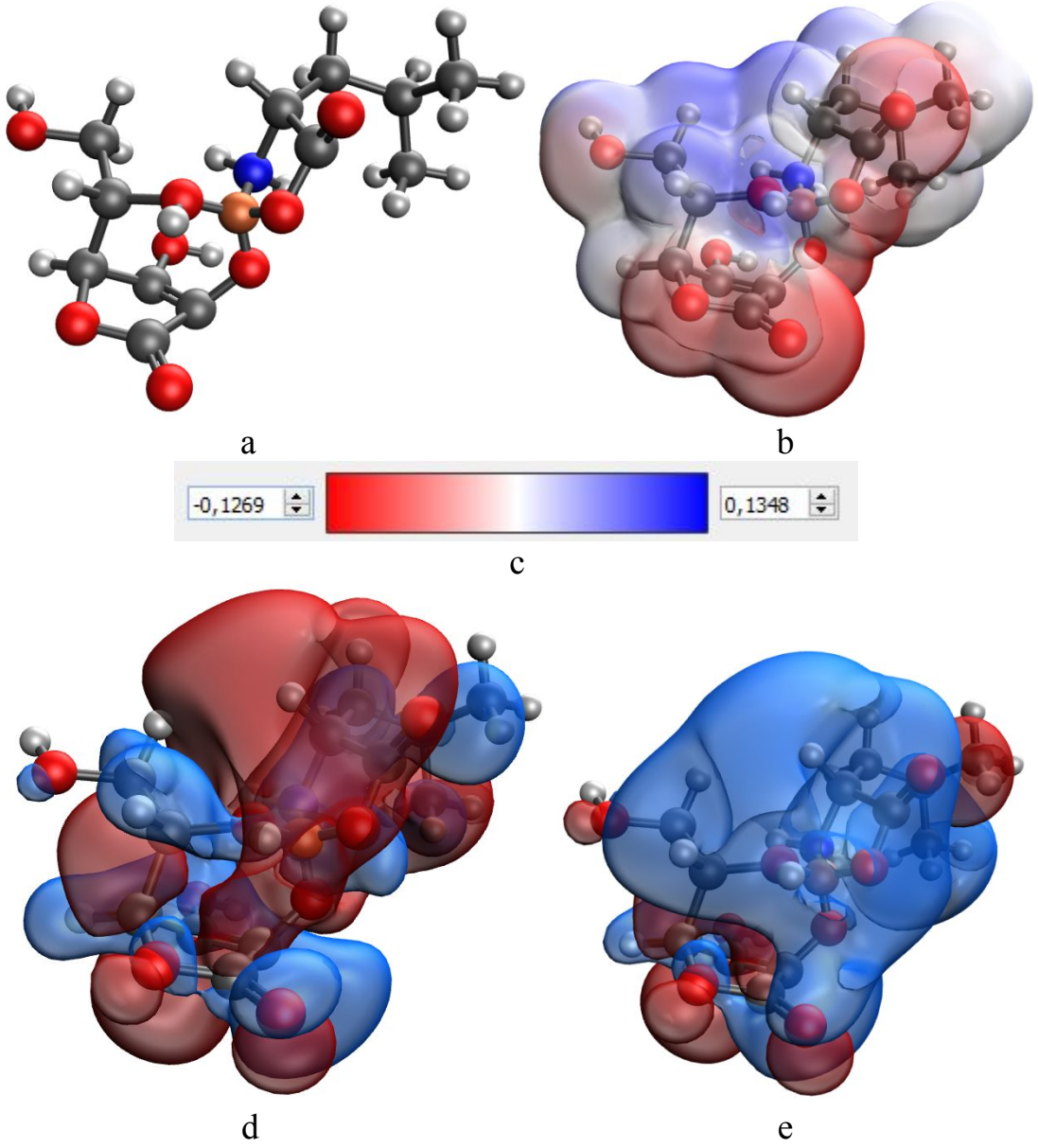

Figure S9. Results of modeling of iron ascorbate leucinate through amino and carboxyl groups of L-leucine and hydroxyl groups attached to C2 and C5 carbon atoms of ascorbic acid: model of the molecular complex (a), electron density distribution (b), electron density distribution gradient (c), HOMO (d), LUMO(e)

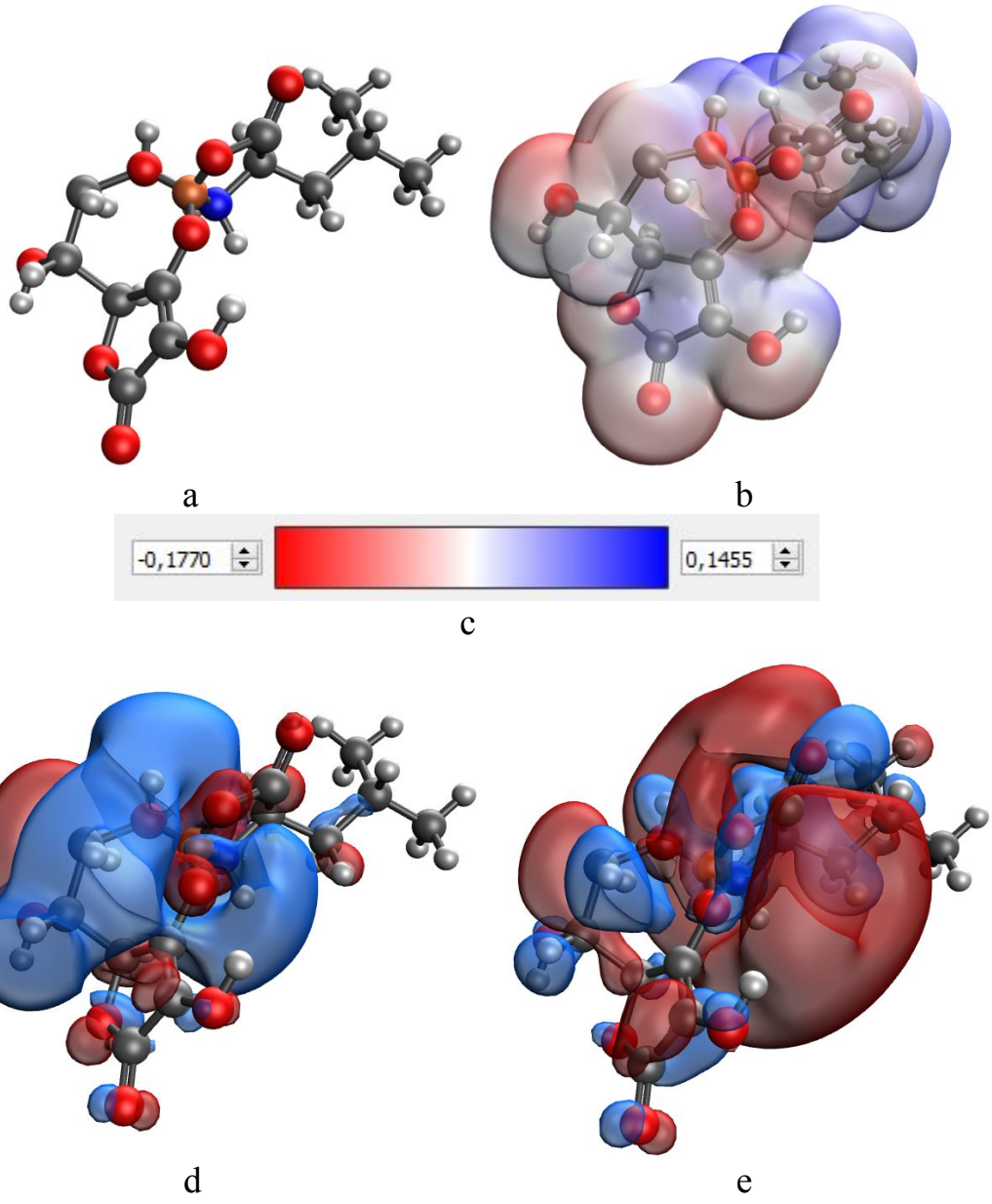

Figure S10. Results of modeling of iron ascorbate leucinate through amino and carboxyl groups of L-leucine and hydroxyl groups attached to C3 and C6 carbon atoms of ascorbic acid: model of the molecular complex (a), electron density distribution (b), electron density distribution gradient (c), HOMO (d), LUMO(e)

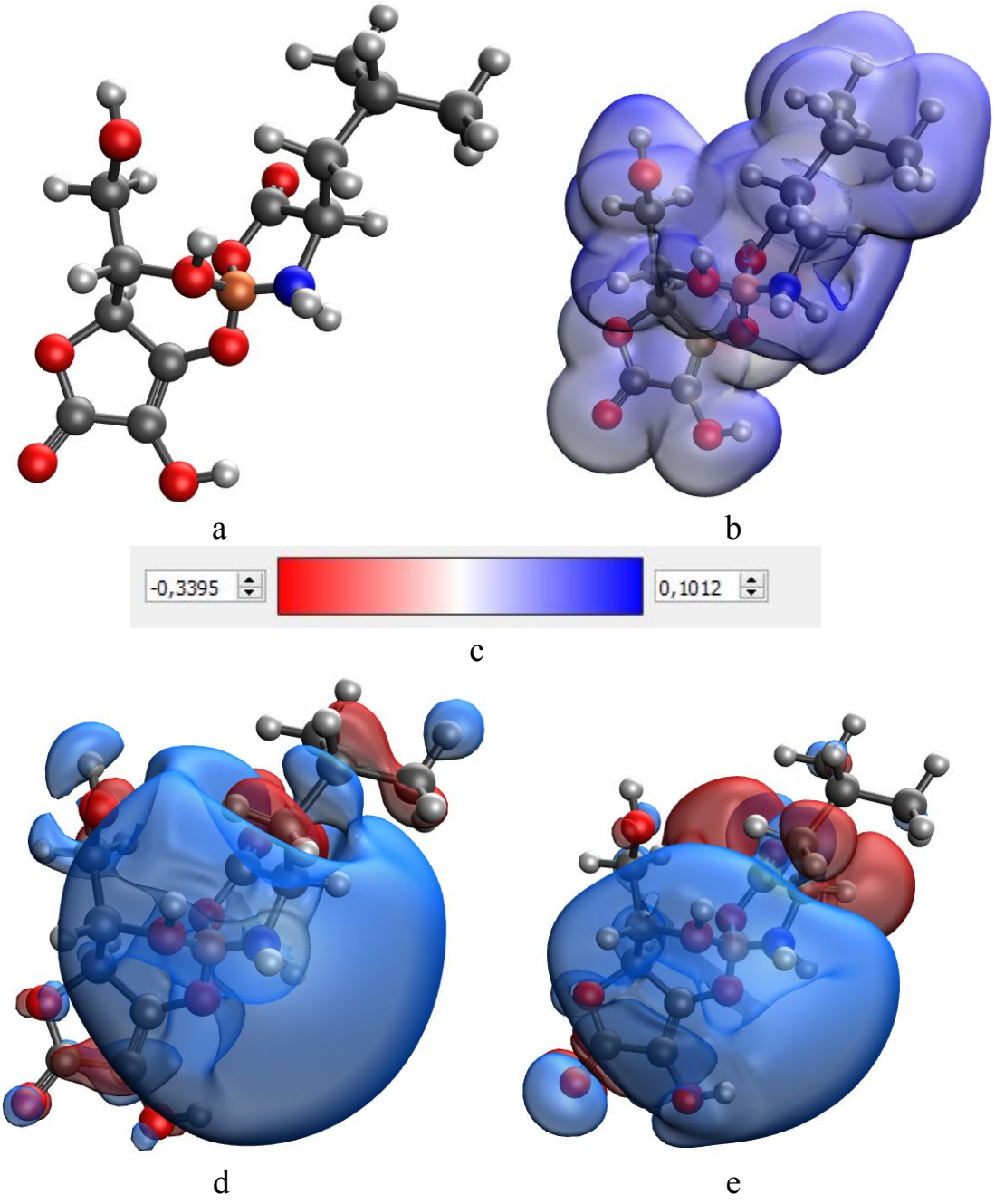

Figure S11. Results of modeling of iron ascorbate leucinate through amino and carboxyl groups of L-leucine and hydroxyl groups attached to C3 and C5 carbon atoms of ascorbic acid: model of the molecular complex (a), electron density distribution (b), electron density distribution gradient (c), HOMO (d), LUMO(e)

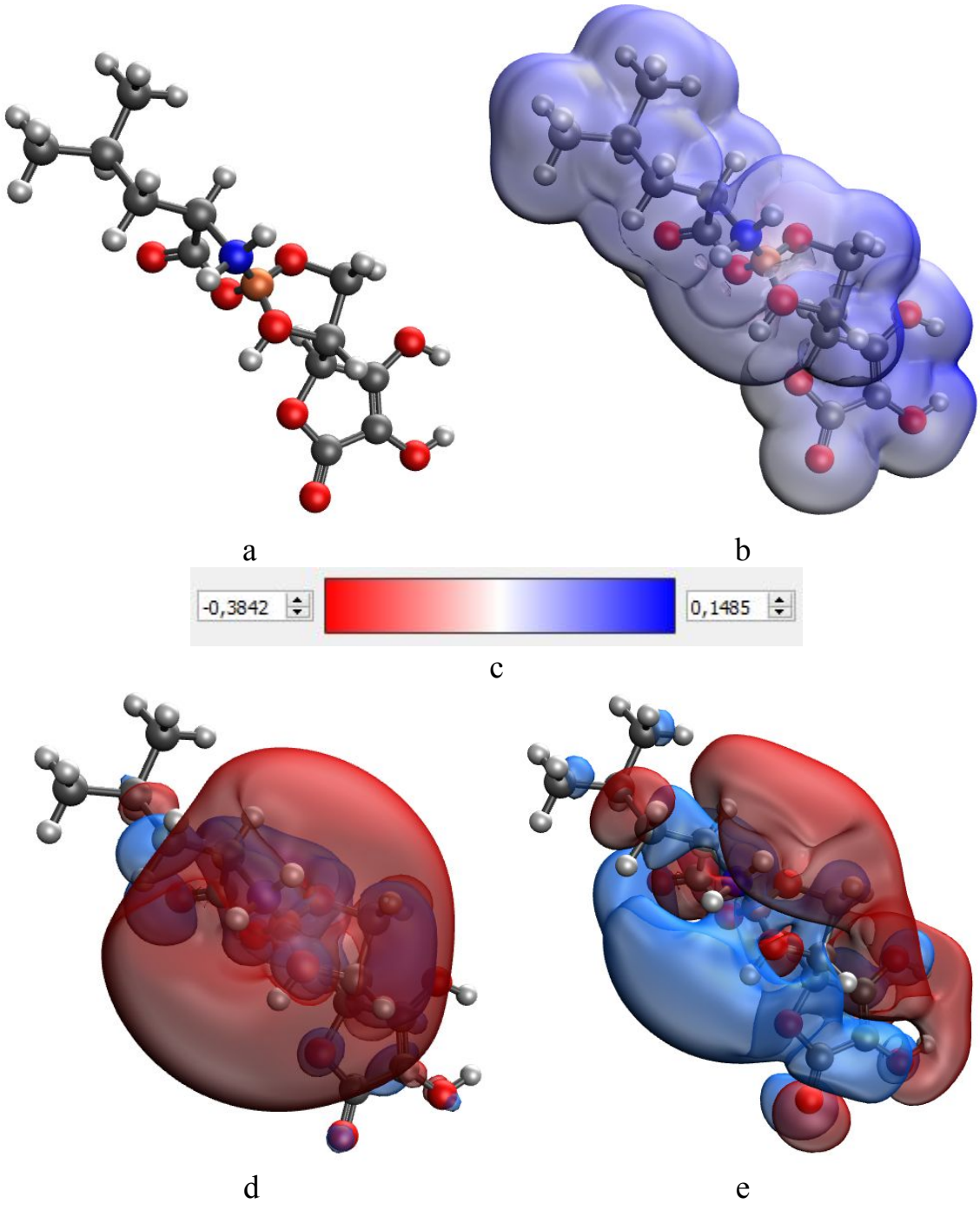

Figure S12. Results of modeling of iron ascorbate leucinate through amino and carboxyl groups of L-leucine and hydroxyl groups attached to C5 and C6 carbon atoms of ascorbic acid: model of the molecular complex (a), electron density distribution (b), electron density distribution gradient (c), HOMO (d), LUMO(e)

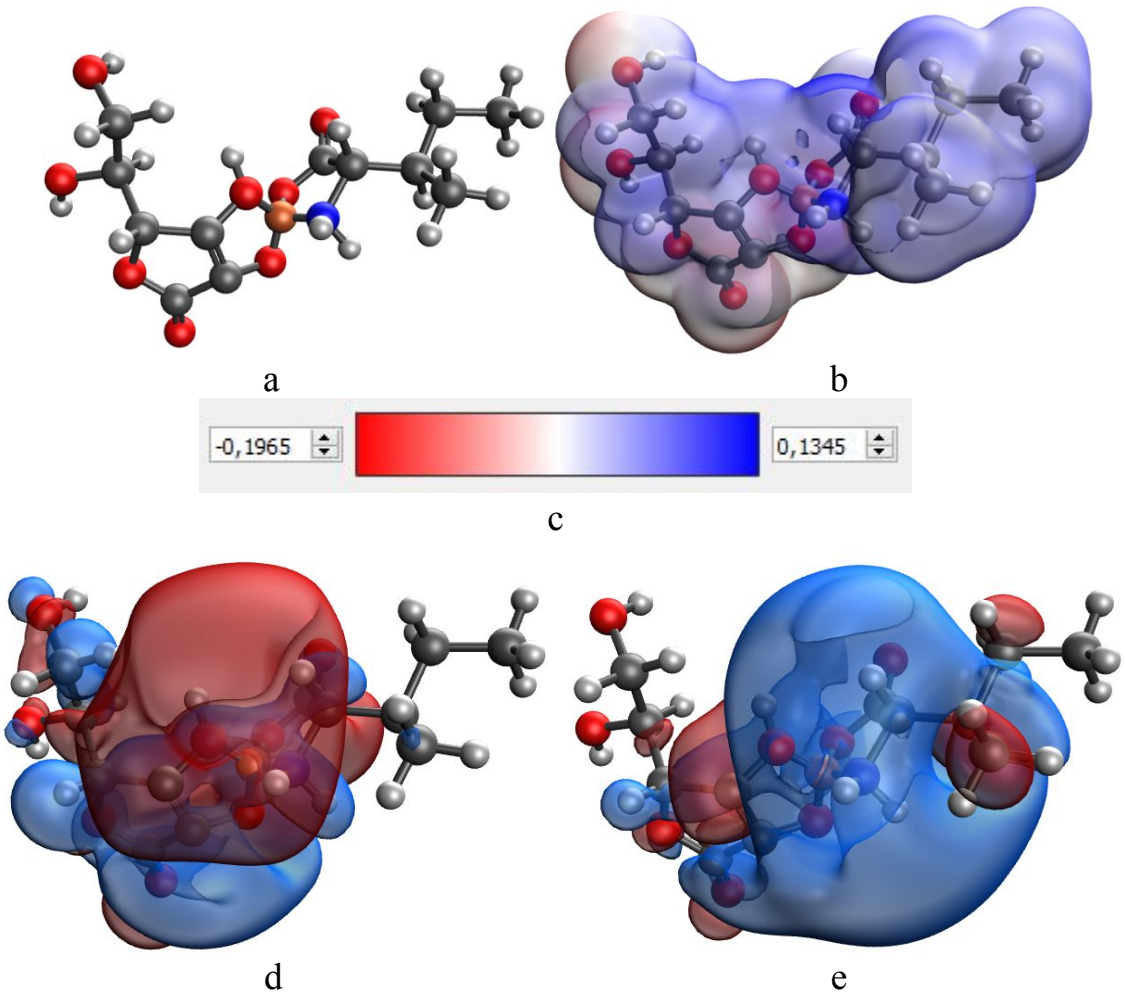

Figure S13. Simulation results of iron ascorbate isoleucinate via amino and carboxyl groups of L-isoleucine and hydroxyl groups attached to C2 and C3 carbon atoms of ascorbic acid: model of the molecular complex (a), electron density distribution (b), electron density distribution gradient (c), HOMO (d), LUMO(e)

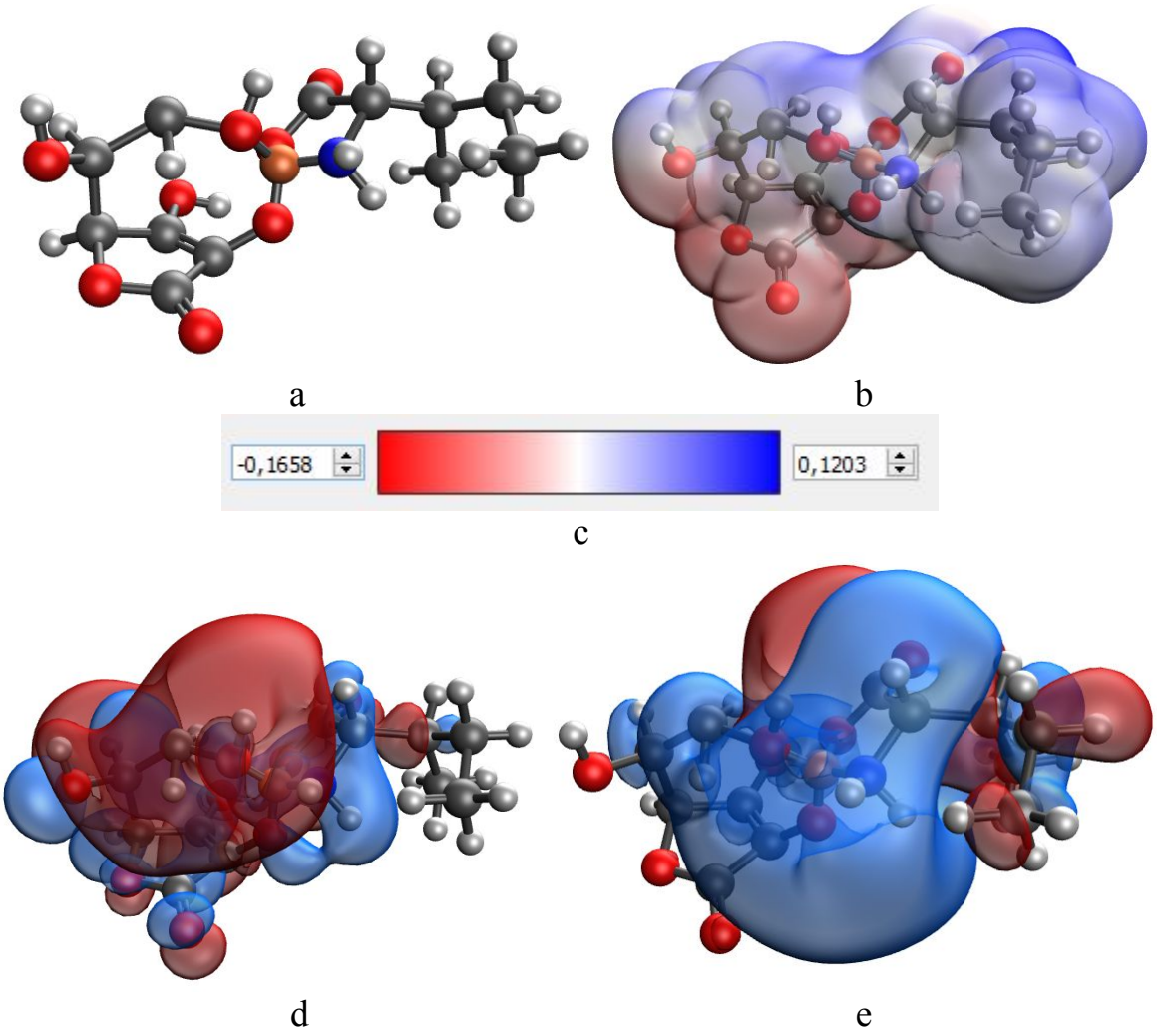

Figure S14. Simulation results of iron ascorbate isoleucinate via amino and carboxyl groups of L-isoleucine and hydroxyl groups attached to C2 and C6 carbon atoms of ascorbic acid: model of the molecular complex (a), electron density distribution (b), electron density distribution gradient (c), HOMO (d), LUMO(e)

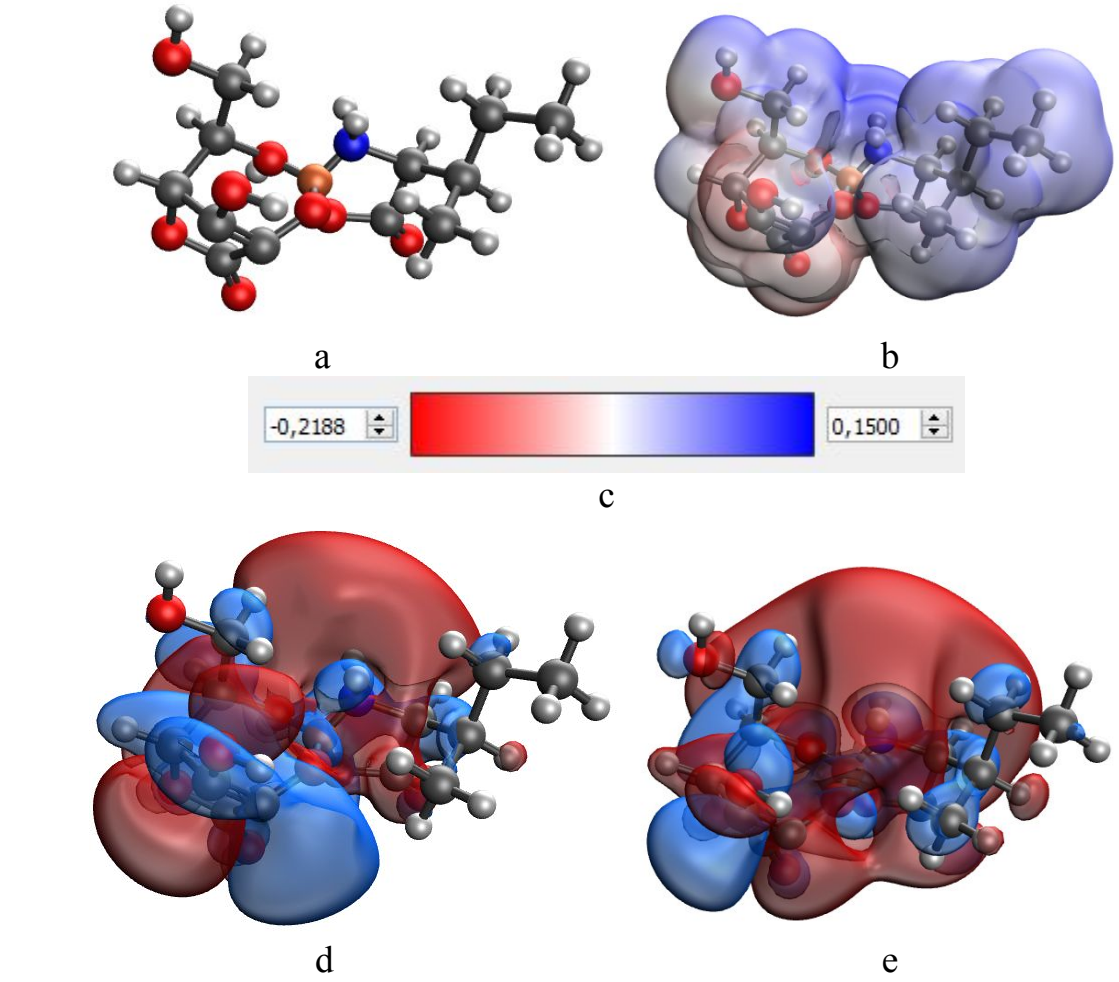

Figure S15. Simulation results of iron ascorbate isoleucinate via amino and carboxyl groups of L-isoleucine and hydroxyl groups attached to C2 and C5 carbon atoms of ascorbic acid: molecular complex model (a), electron density distribution (b), electron density distribution gradient (c), HOMO (d), LUMO(e)

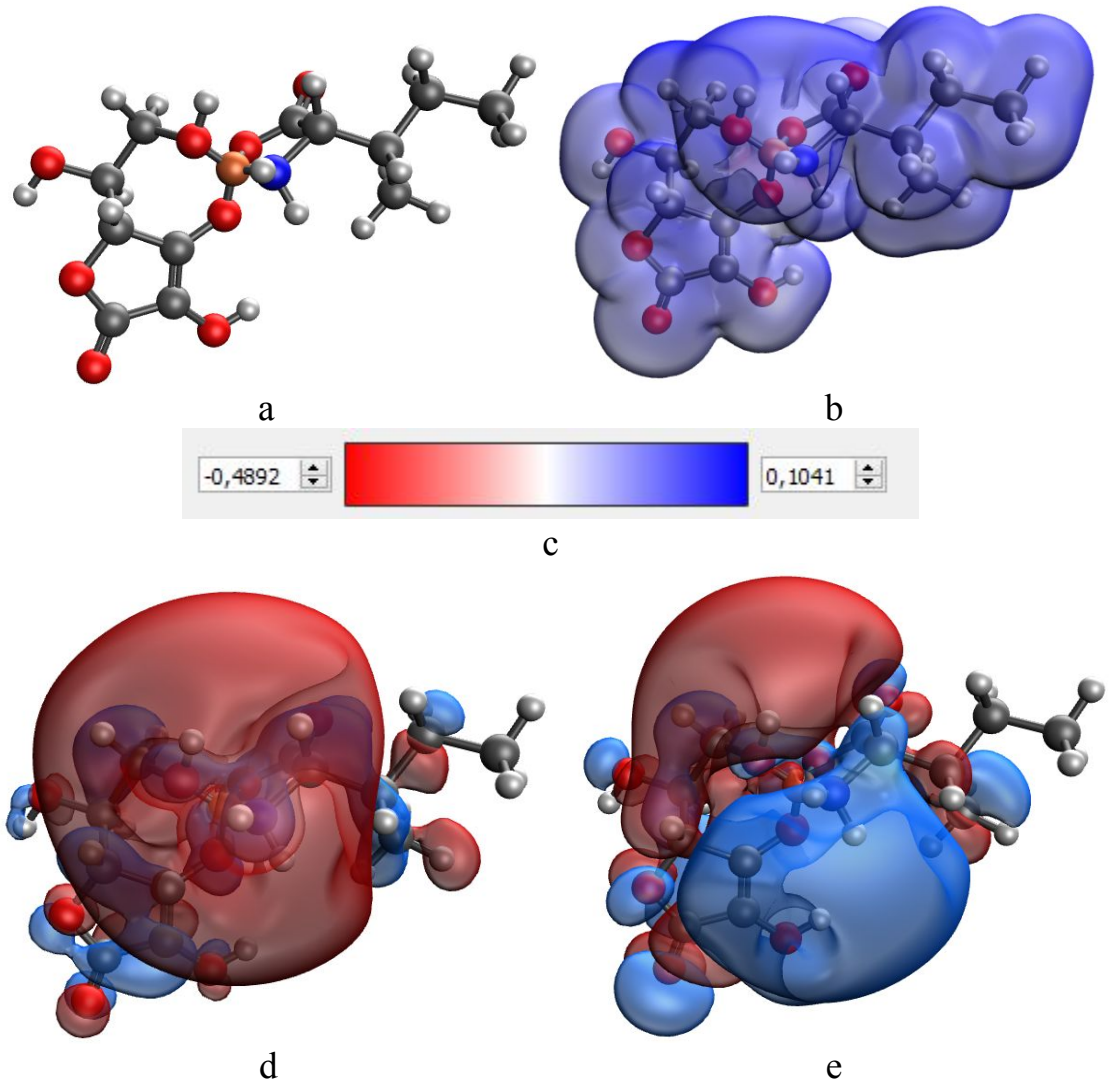

Figure S16. Simulation results of iron ascorbate isoleucinate via amino and carboxyl groups of L-isoleucine and hydroxyl groups attached to C3 and C6 carbon atoms of ascorbic acid: model of the molecular complex (a), electron density distribution (b), electron density distribution gradient (c), HOMO (d), LUMO(e)

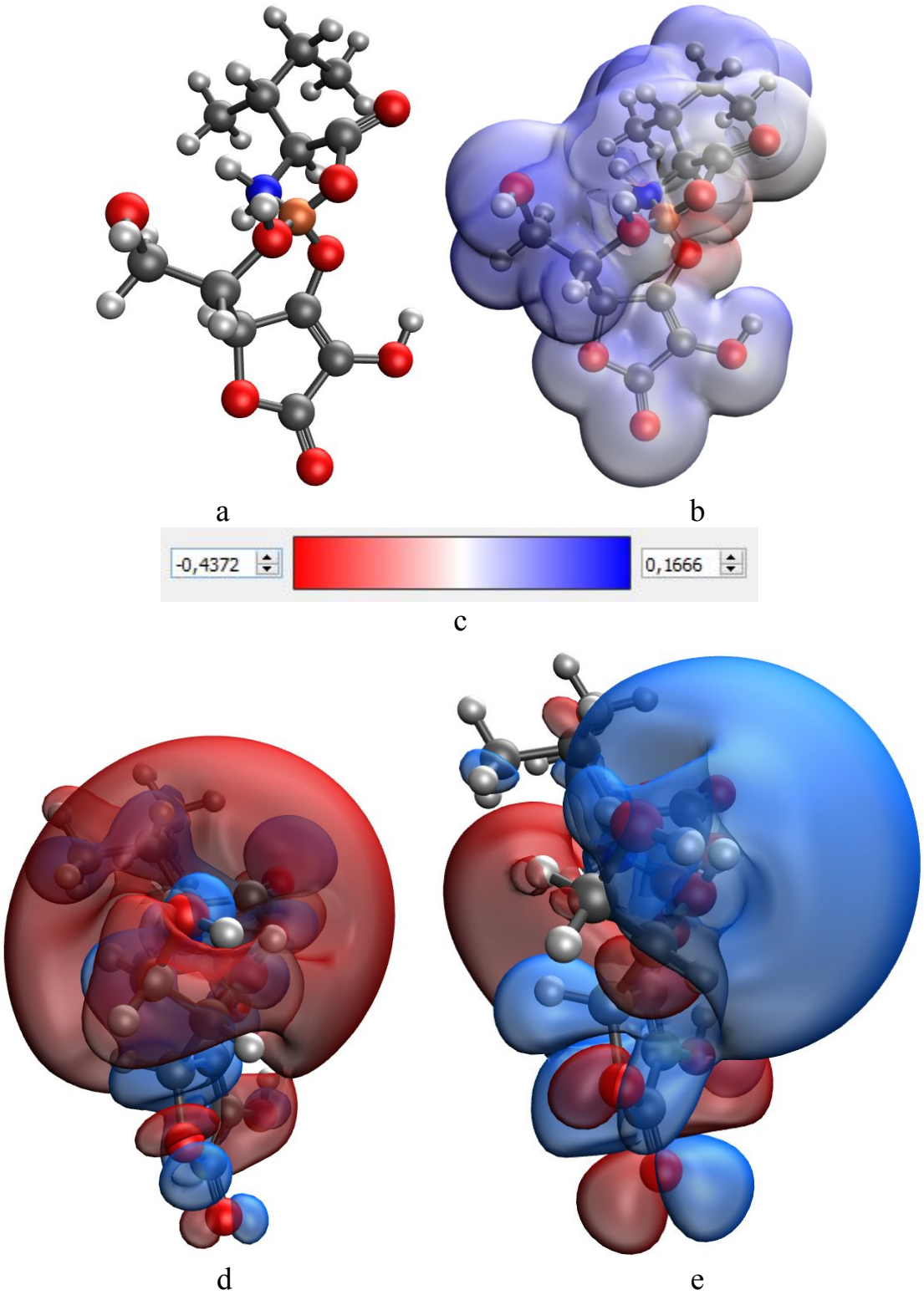

Figure S17. Simulation results of iron ascorbate isoleucinate via amino and carboxyl groups of L-isoleucine and hydroxyl groups attached to C3 and C5 carbon atoms of ascorbic acid: model of the molecular complex (a), electron density distribution (b), electron density distribution gradient (c), HOMO (d), LUMO(e)

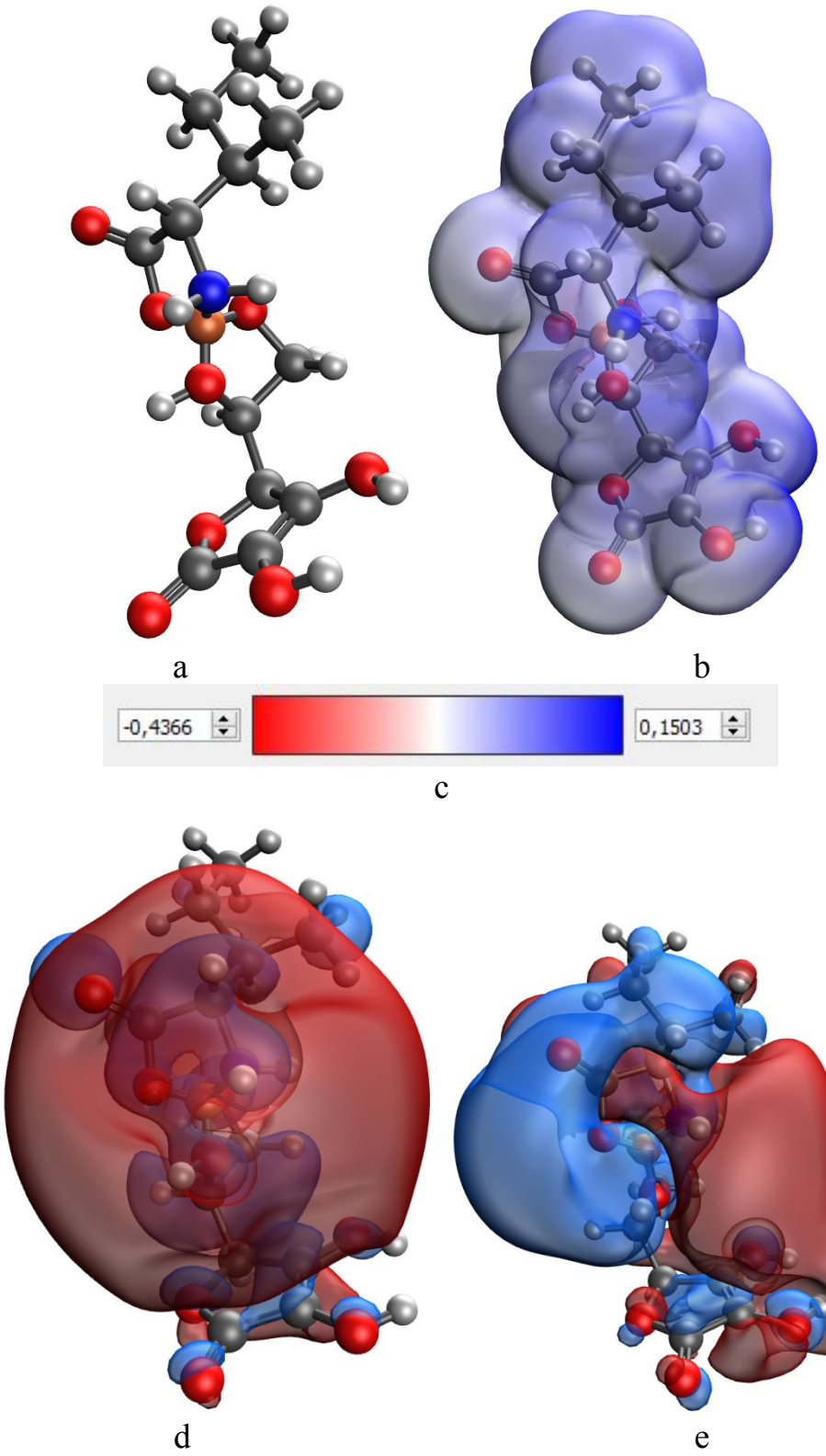

Figure S18. Simulation results of iron ascorbate isoleucinate via amino and carboxyl groups of L-isoleucine and hydroxyl groups attached to C5 and C6 carbon atoms of ascorbic acid: model of the molecular complex (a), electron density distribution (b), electron density distribution gradient (c), HOMO (d), LUMO(e)

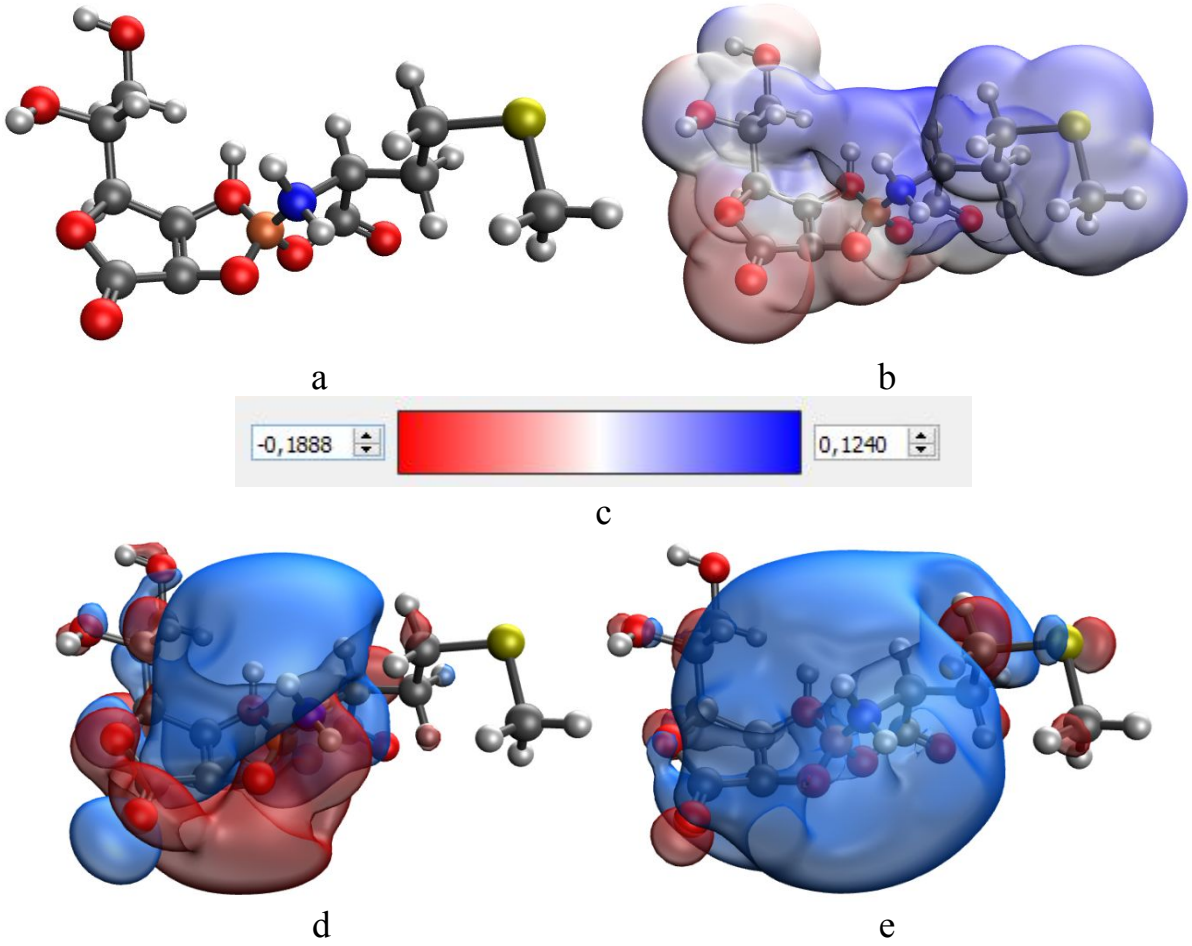

Figure S19. Results of modeling of iron ascorbate methioninate through the amino and carboxyl groups of L-methionine and hydroxyl groups attached to C2 and C3 carbon atoms of ascorbic acid: molecular complex model (a), electron density distribution (b), electron density distribution gradient (c), HOMO (d), LUMO(e)

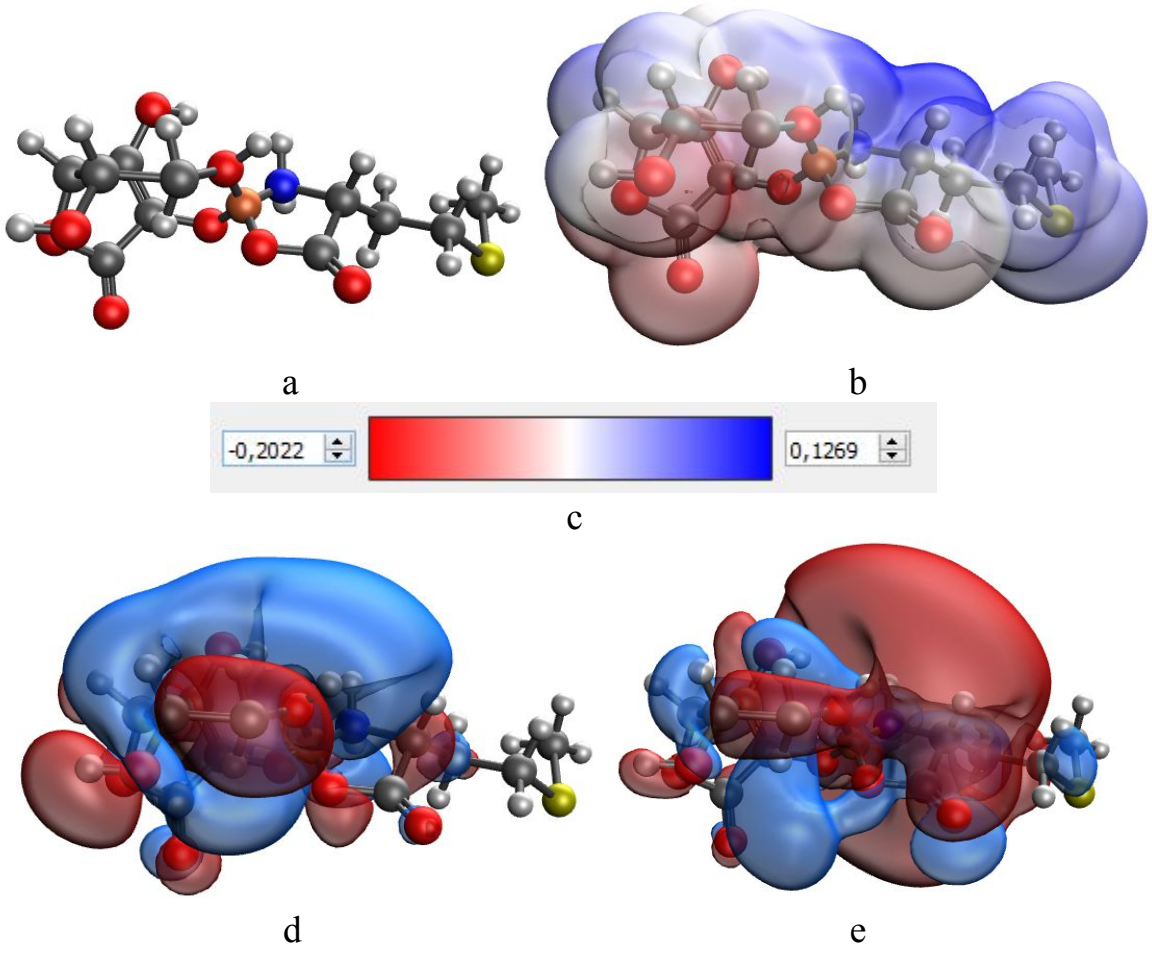

Figure S20. Results of modeling of iron ascorbate methioninate through amino and carboxyl groups of L-methionine and hydroxyl groups attached to C2 and C6 carbon atoms of ascorbic acid: model of the molecular complex (a), electron density distribution (b), electron density distribution gradient (c), HOMO (d), LUMO(e)

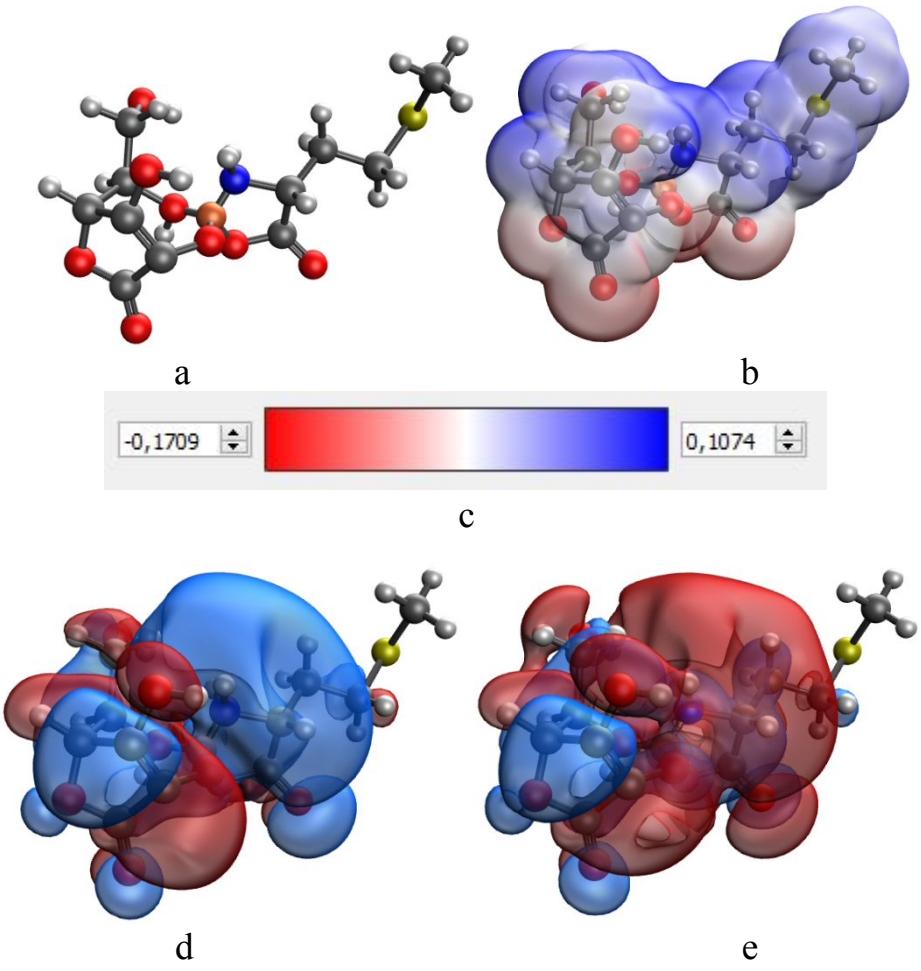

Figure S21. Results of modeling of iron ascorbate methioninate through amino and carboxyl groups of L-methionine and hydroxyl groups attached to C2 and C5 carbon atoms of ascorbic acid: model of the molecular complex (a), electron density distribution (b), electron density distribution gradient (c), HOMO (d), LUMO(e)

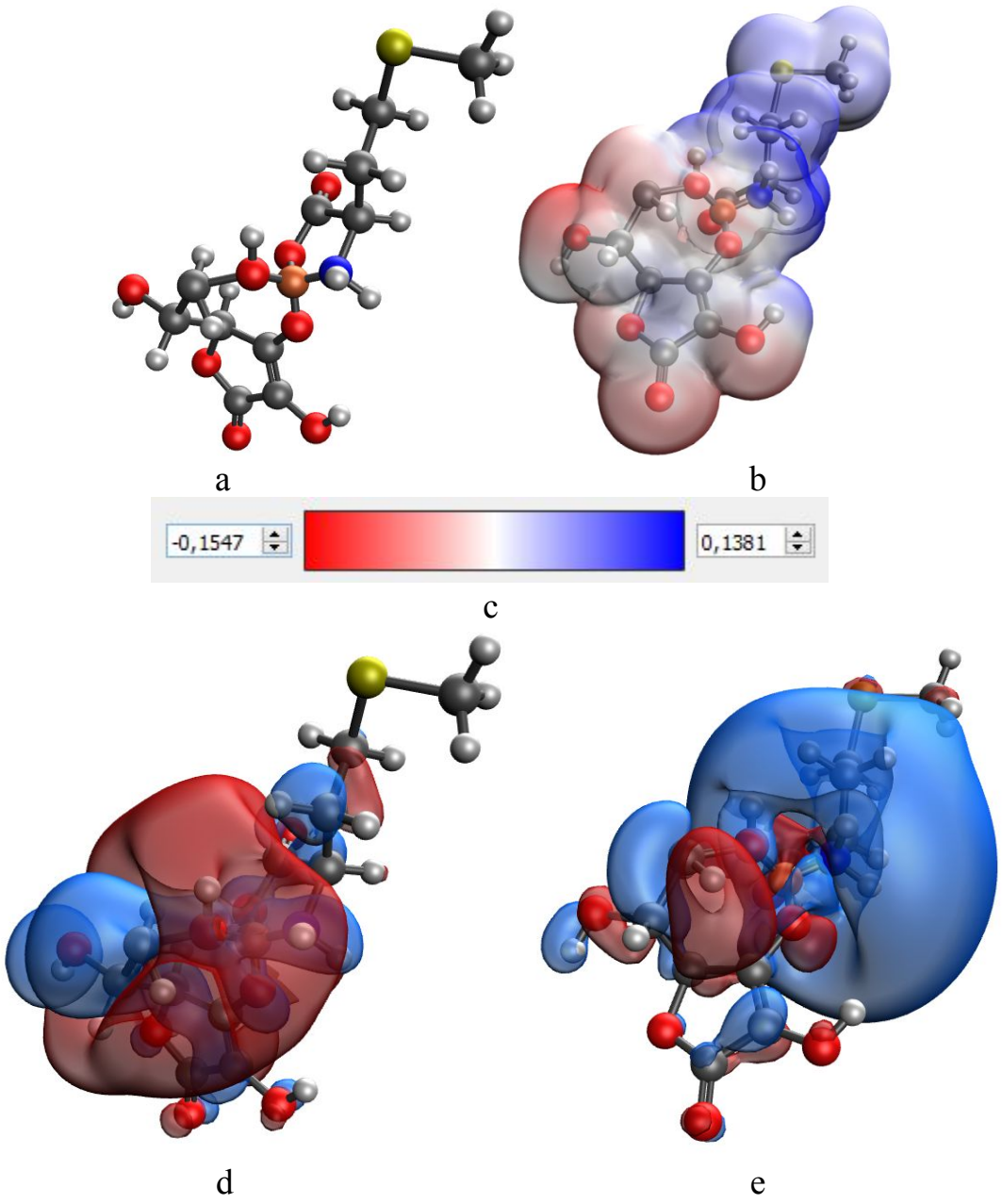

Figure S22. Results of modeling of iron ascorbate methioninate through amino and carboxyl groups of L-methionine and hydroxyl groups attached to C3 and C6 carbon atoms of ascorbic acid: model of the molecular complex (a), electron density distribution (b), electron density distribution gradient (c), HOMO (d), LUMO(e)

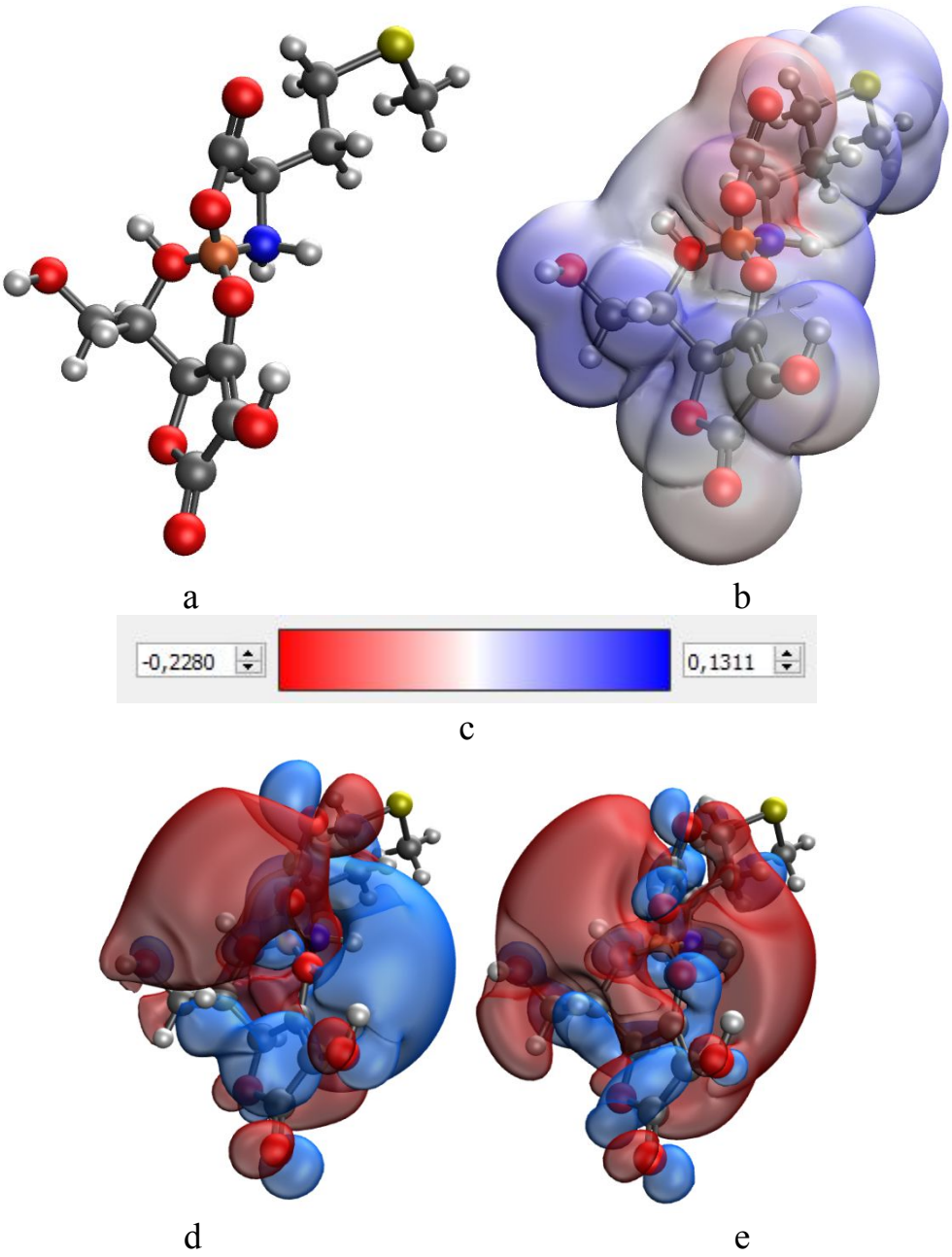

Figure S23. Results of modeling of iron ascorbate methioninate through amino and carboxyl groups of L-methionine and hydroxyl groups attached to C3 and C5 carbon atoms of ascorbic acid: model of the molecular complex (a), electron density distribution (b), electron density distribution gradient (c), HOMO (d), LUMO(e)

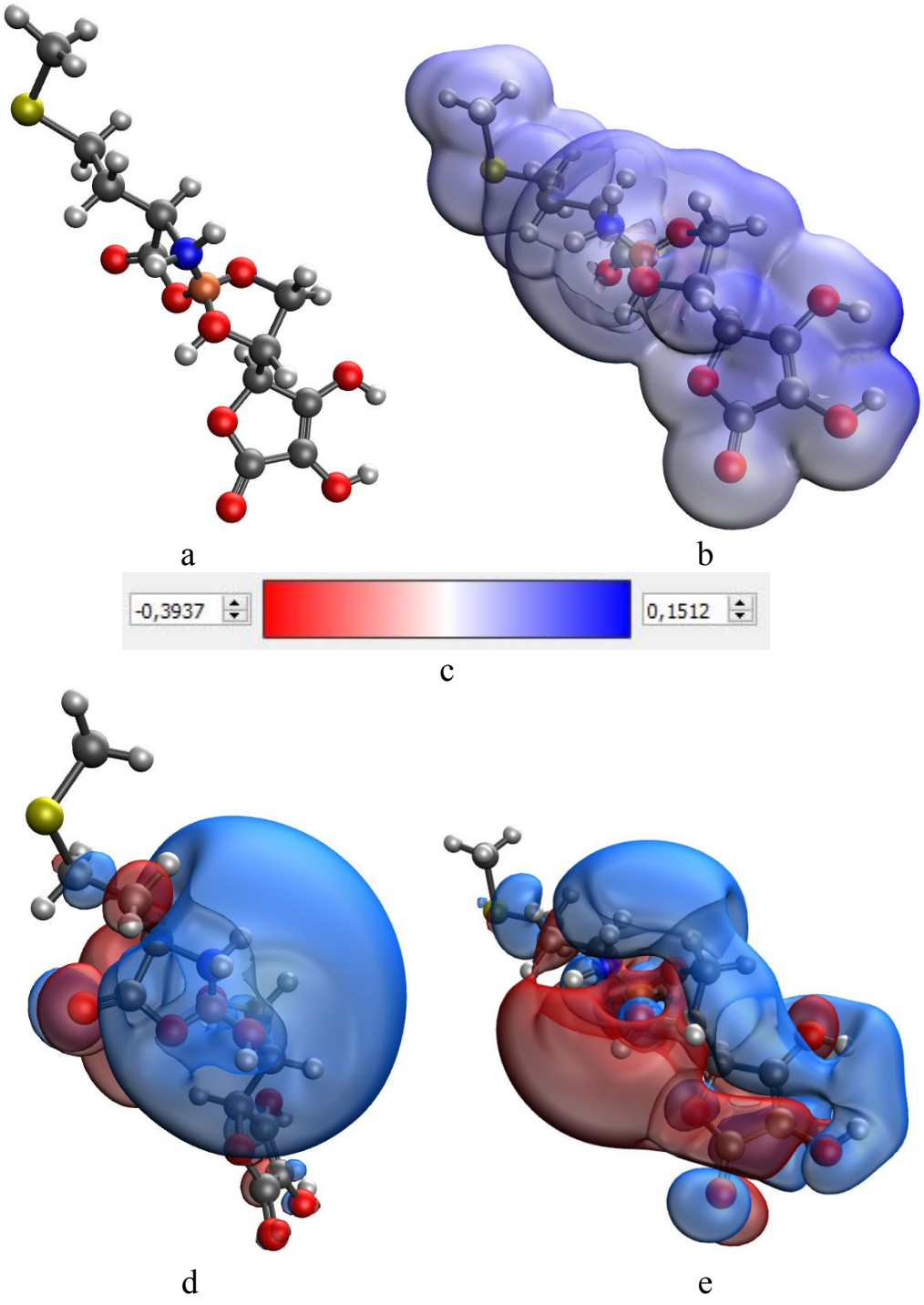

Figure S24. Results of modeling of iron ascorbate methioninate through the amino and carboxyl groups of L-methionine and hydroxyl groups attached to C5 and C6 carbon atoms of ascorbic acid: molecular complex model (a), electron density distribution (b), electron density distribution gradient (c), HOMO (d), LUMO(e)

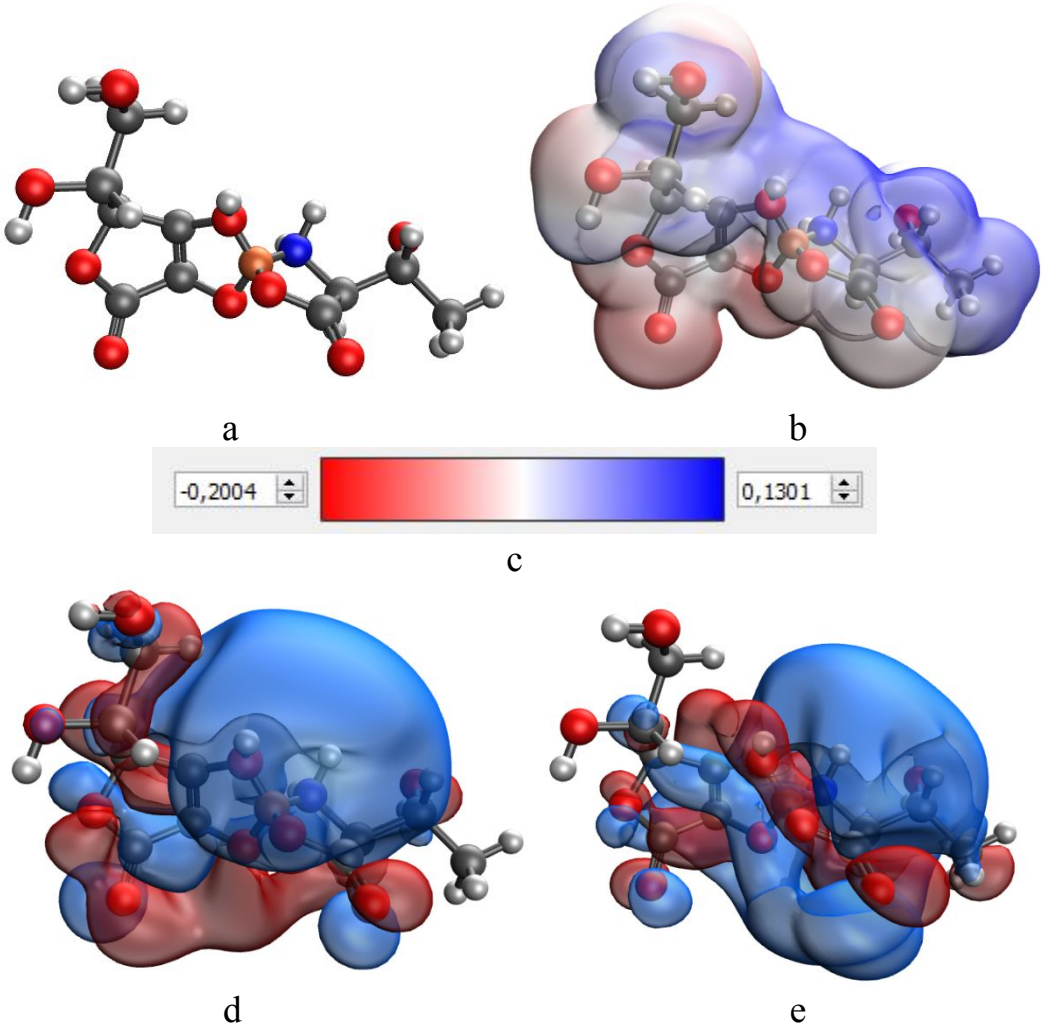

Figure S25. Results of modeling of iron ascorbate threoninate through amino and carboxyl groups of L-threonine and hydroxyl groups attached to C2 and C3 carbon atoms of ascorbic acid: model of the molecular complex (a), electron density distribution (b), electron density distribution gradient (c), HOMO (d), LUMO(e)

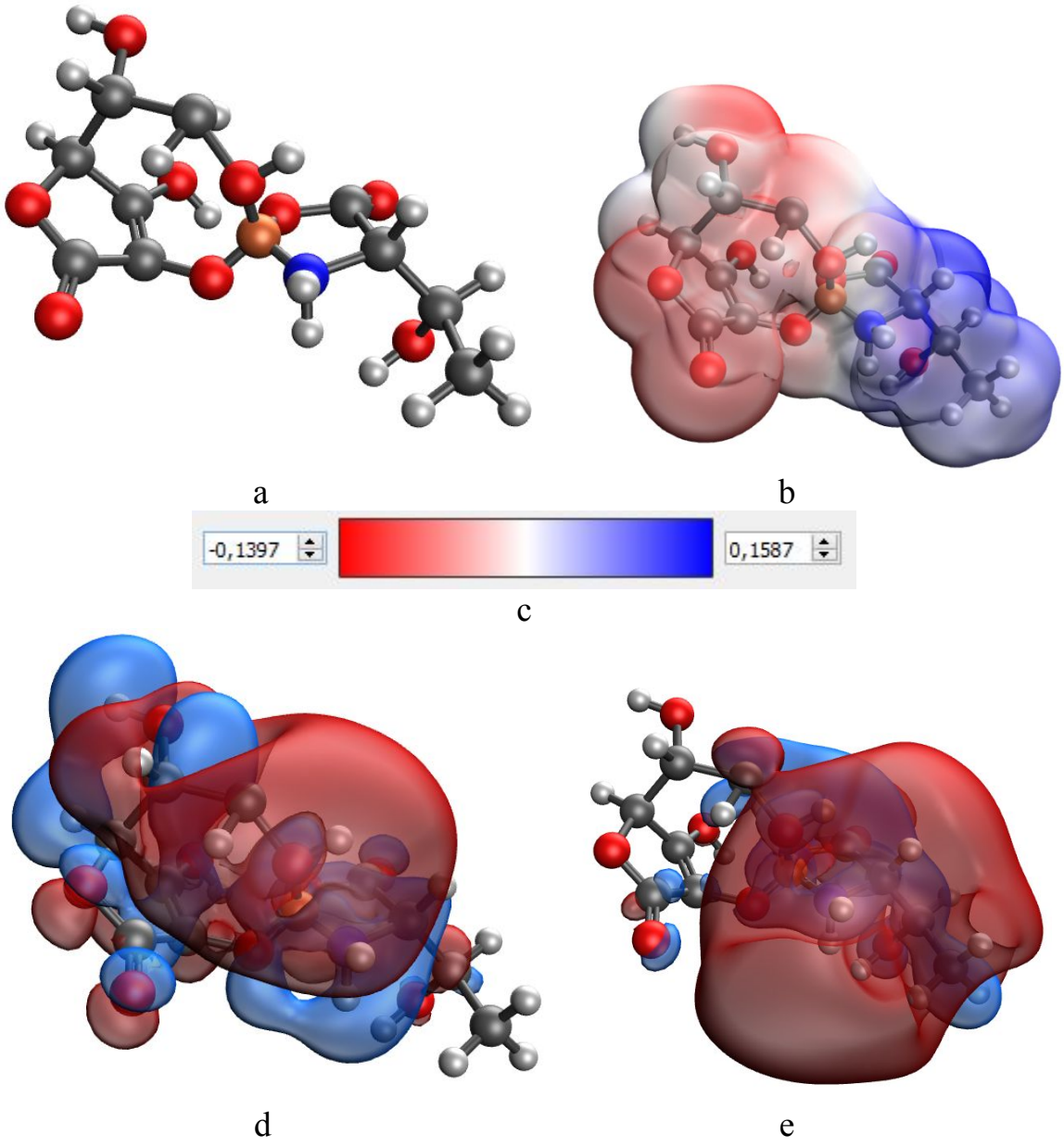

Figure S26. Results of modeling of iron ascorbate threoninate through amino and carboxyl groups of L-threonine and hydroxyl groups attached to C2 and C6 carbon atoms of ascorbic acid: molecular complex model (a), electron density distribution (b), electron density distribution gradient (c), HOMO (d), LUMO(e)

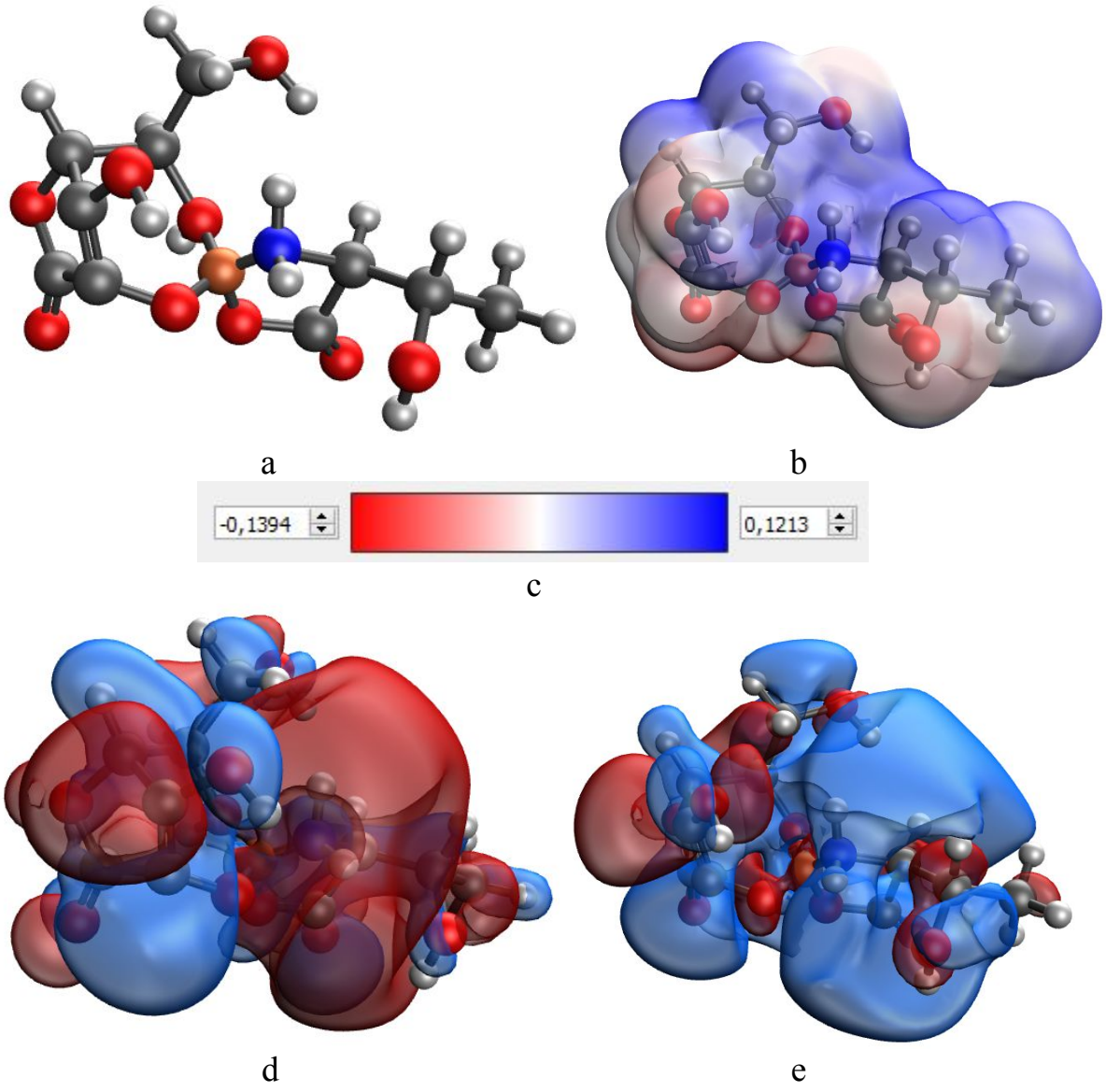

Figure S27. Results of modeling of iron ascorbate threoninate through the amino and carboxyl groups of L-threonine and hydroxyl groups attached to C2 and C5 carbon atoms of ascorbic acid: molecular complex model (a), electron density distribution (b), electron density distribution gradient (c), HOMO (d), LUMO(e)

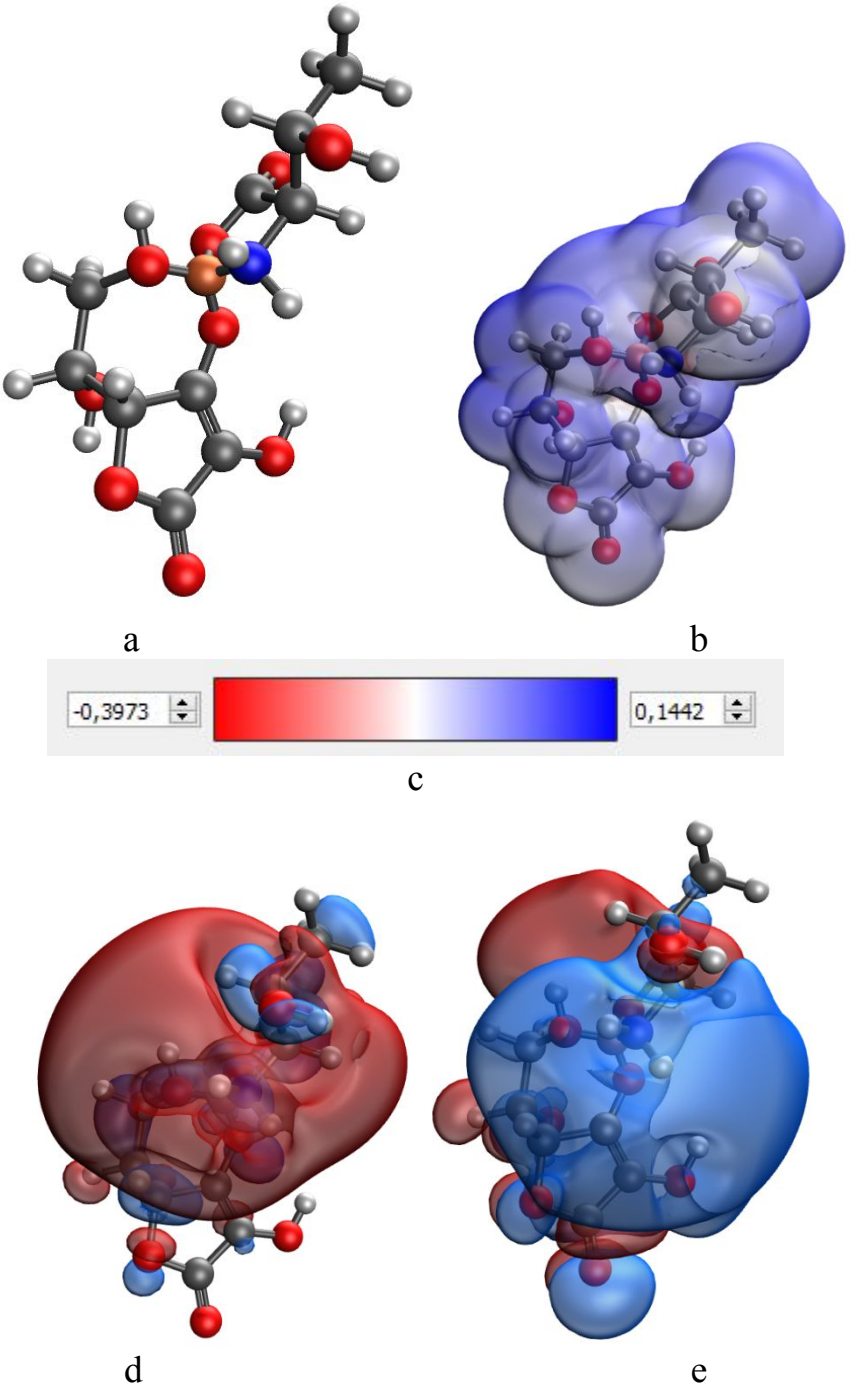

Figure S28. Results of modeling of iron ascorbate threoninate through amino and carboxyl groups of L-threonine and hydroxyl groups attached to C3 and C6 carbon atoms of ascorbic acid: molecular complex model (a), electron density distribution (b), electron density distribution gradient (c), HOMO (d), LUMO(e)

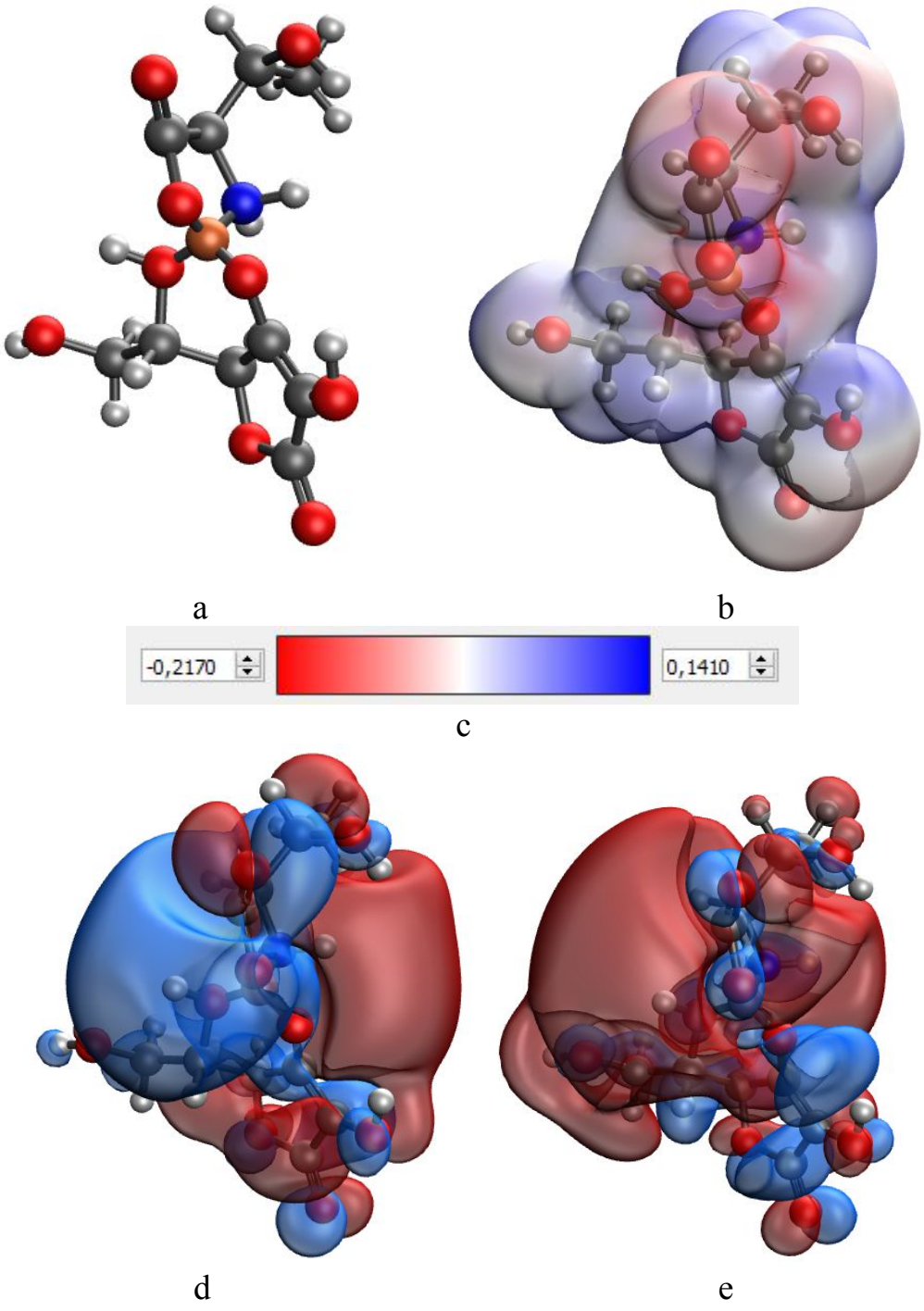

Figure S29. Results of modeling of iron ascorbate threoninate through amino and carboxyl groups of L-threonine and hydroxyl groups attached to C3 and C5 carbon atoms of ascorbic acid: model of the molecular complex (a), electron density distribution (b), electron density distribution gradient (c), HOMO (d), LUMO(e)

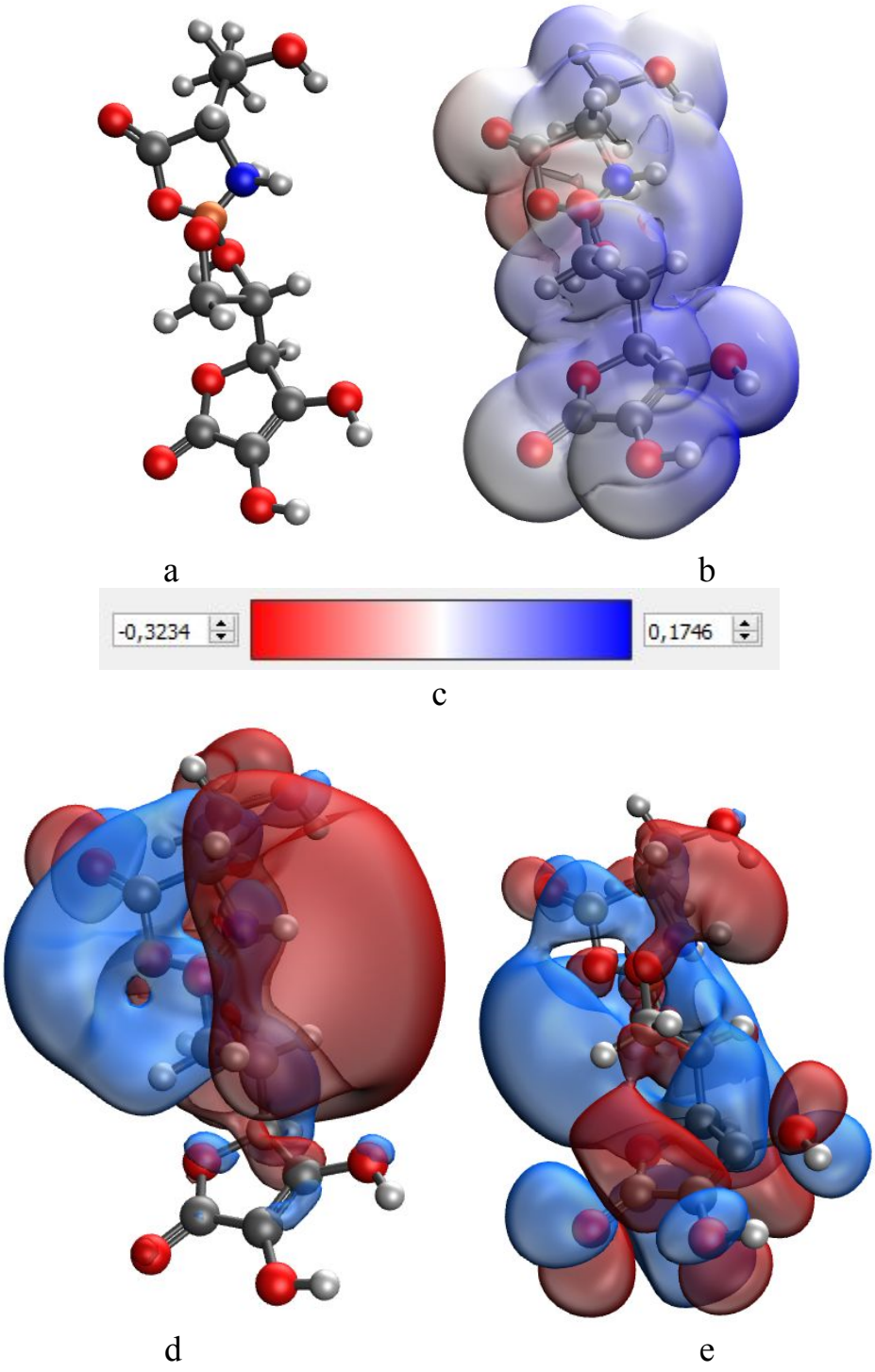

Figure S30. Results of modeling of iron ascorbate threoninate through amino and carboxyl groups of L-threonine and hydroxyl groups attached to C5 and C6 carbon atoms of ascorbic acid: model of the molecular complex (a), electron density distribution (b), electron density distribution gradient (c), HOMO (d), LUMO(e)

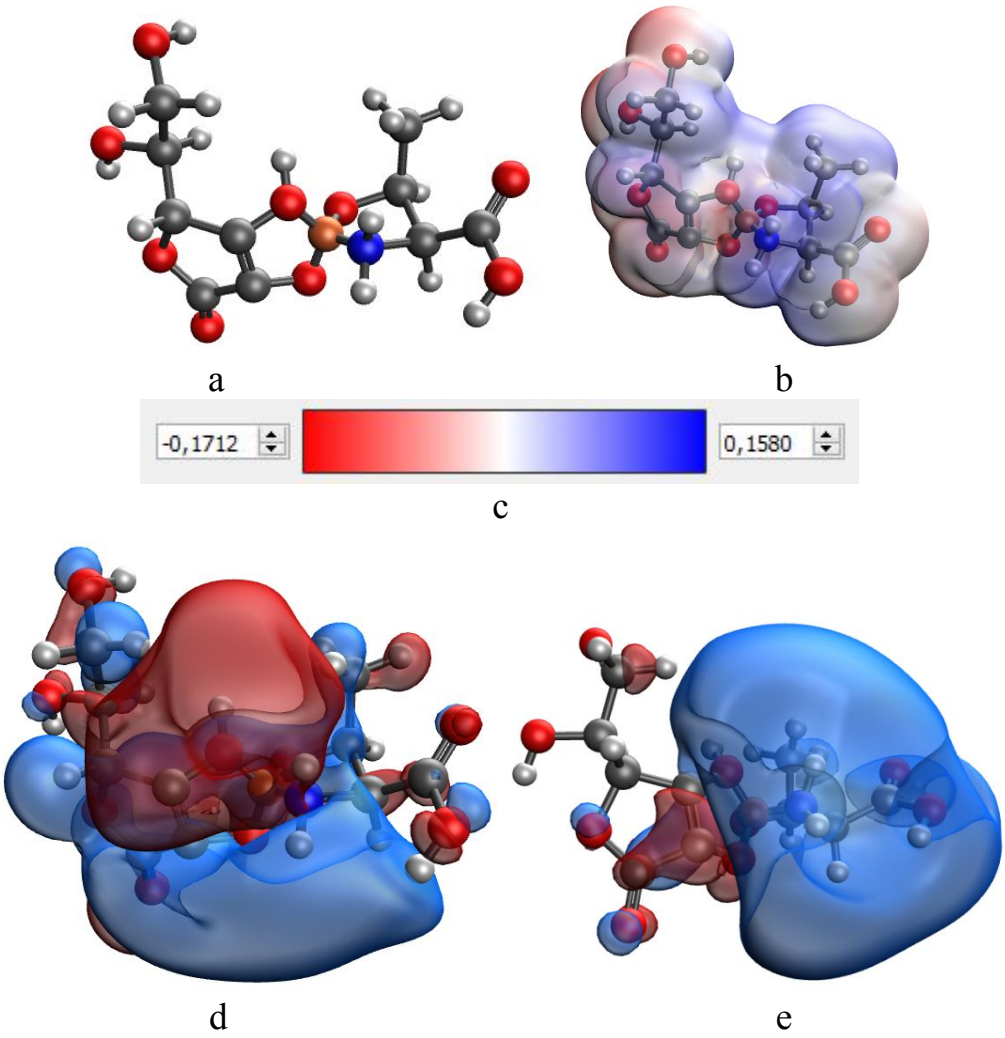

Figure S31. Results of modeling of iron ascorbate threoninate through amino and hydroxyl groups of L-threonine and hydroxyl groups attached to C2 and C3 carbon atoms of ascorbic acid: model of the molecular complex (a), electron density distribution (b), electron density distribution gradient (c), HOMO (d), LUMO(e)

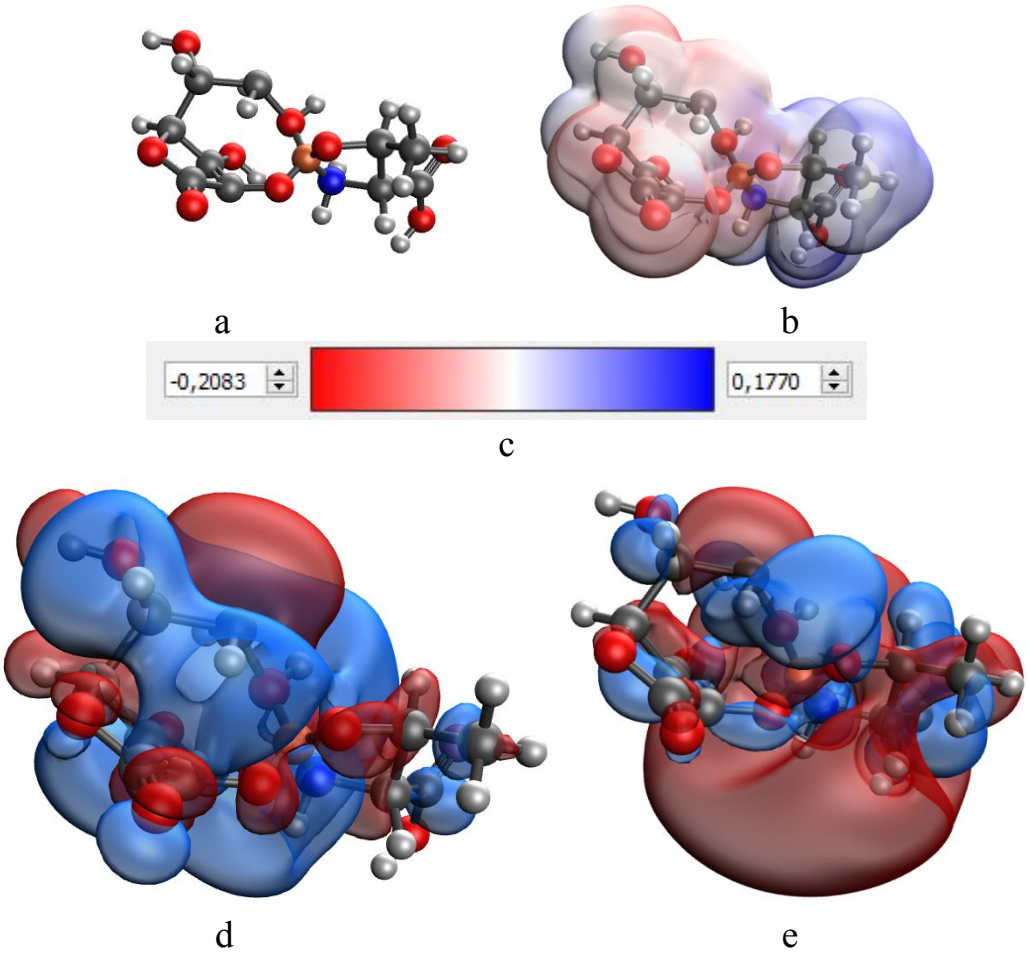

Figure S32. Results of modeling of iron ascorbate threoninate through the amino and hydroxyl groups of L-threonine and hydroxyl groups attached to C2 and C6 carbon atoms of ascorbic acid: molecular complex model (a), electron density distribution (b), electron density distribution gradient (c), HOMO (d), LUMO(e)

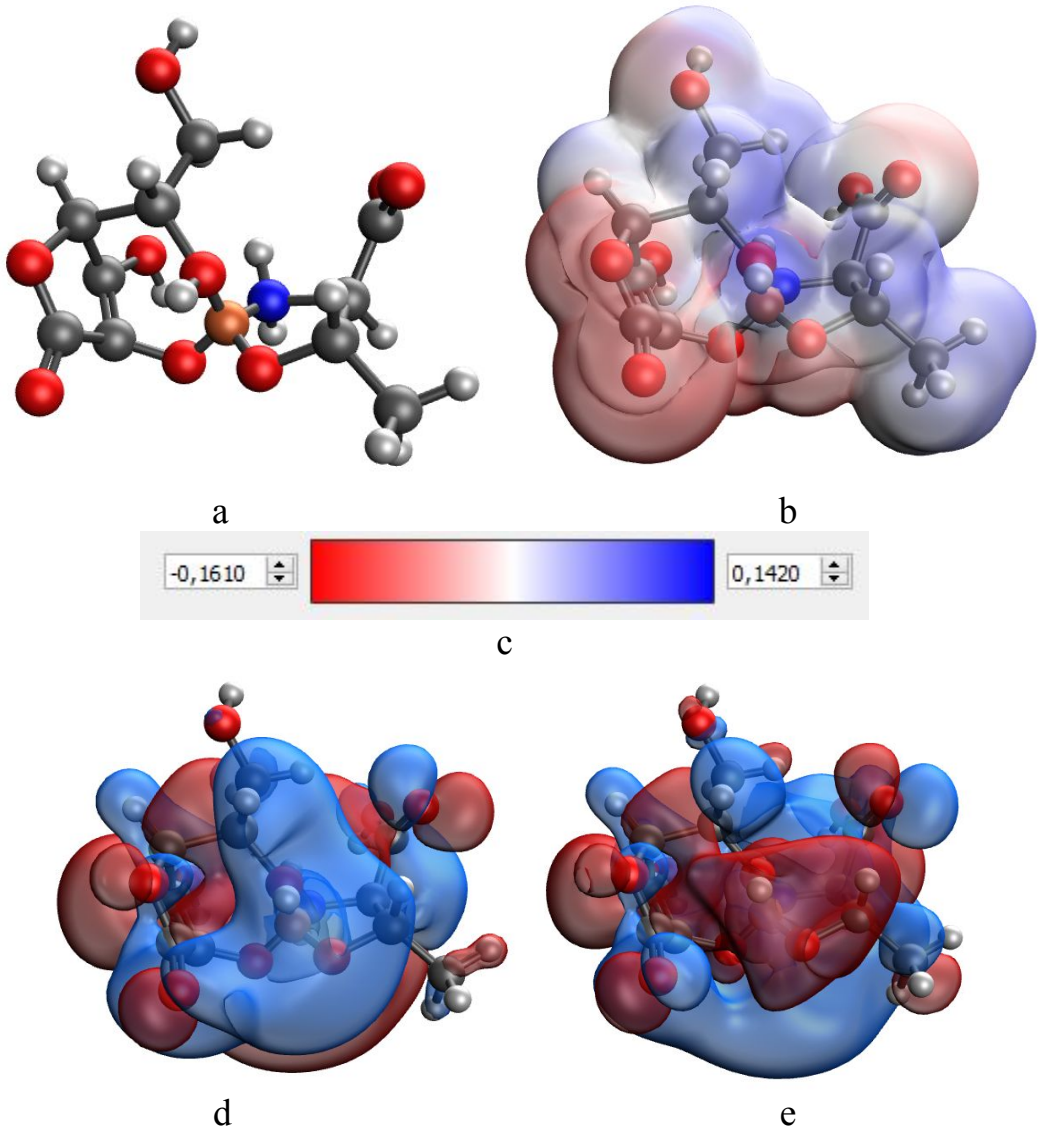

Figure S33. Results of modeling of iron ascorbate threoninate through amino and hydroxyl groups of L-threonine and hydroxyl groups attached to C2 and C5 carbon atoms of ascorbic acid: model of the molecular complex (a), electron density distribution (b), electron density distribution gradient (c), HOMO (d), LUMO(e)

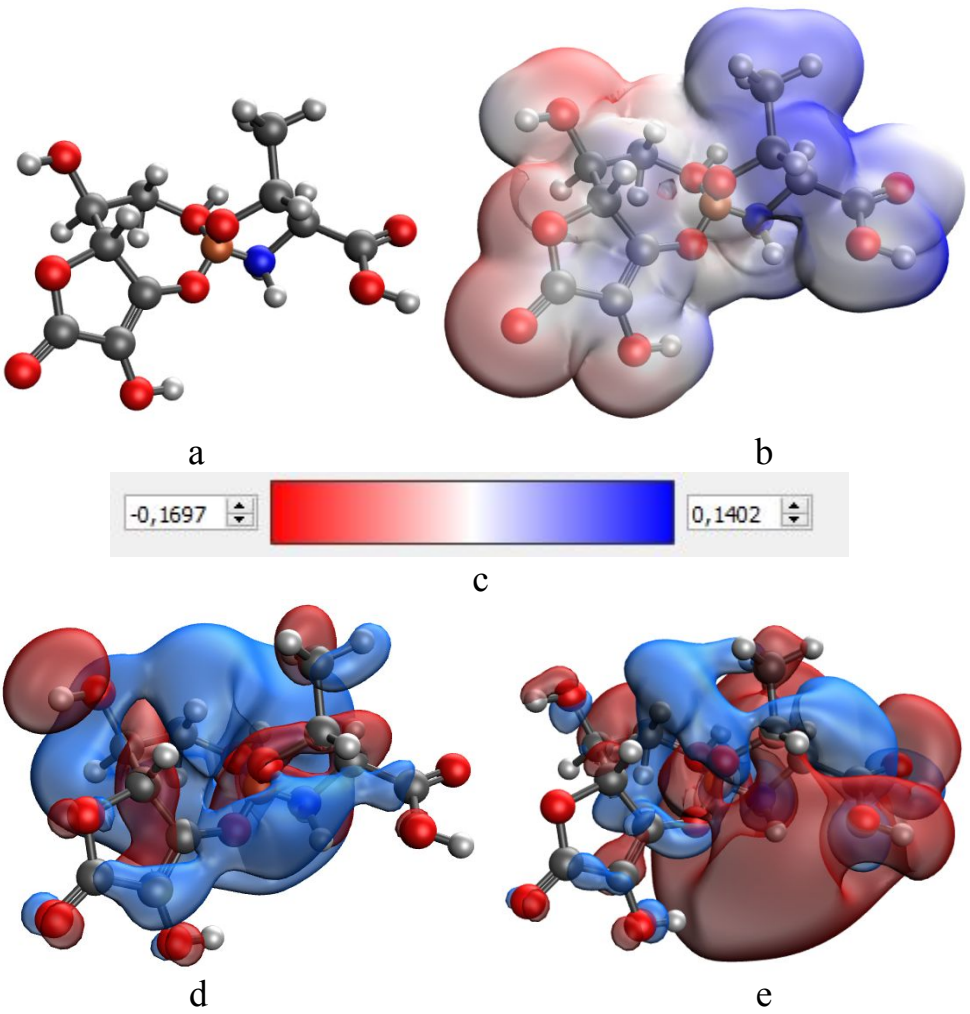

Figure S34. Results of modeling of iron ascorbate threoninate through the amino and hydroxyl groups of L-threonine and hydroxyl groups attached to C3 and C6 carbon atoms of ascorbic acid: molecular complex model (a), electron density distribution (b), electron density distribution gradient (c), HOMO (d), LUMO(e)

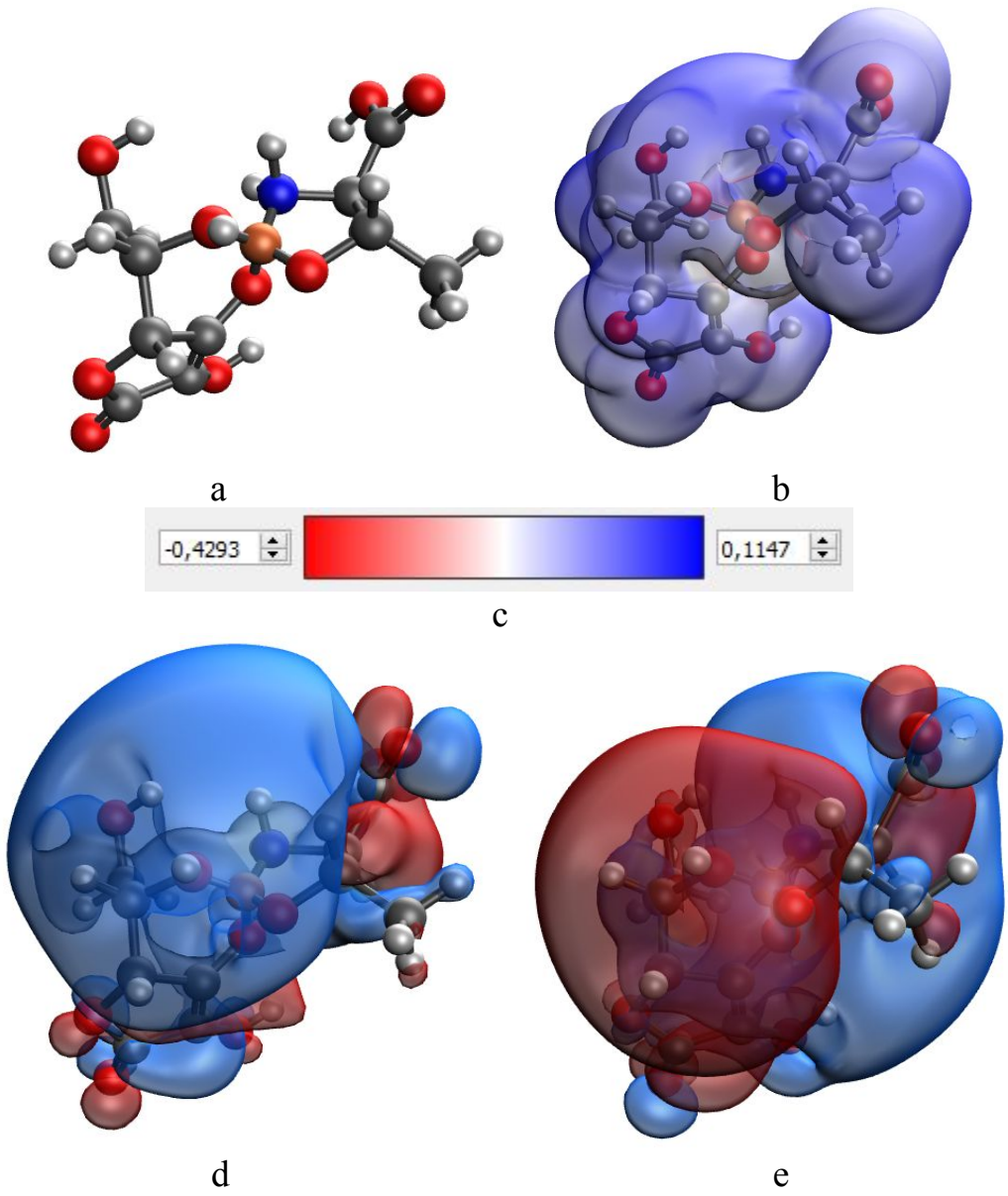

Figure S35. Results of modeling of iron ascorbate threoninate through amino and hydroxyl groups of L-threonine and hydroxyl groups attached to C3 and C5 carbon atoms of ascorbic acid: model of the molecular complex (a), electron density distribution (b), electron density distribution gradient (c), HOMO (d), LUMO(e)

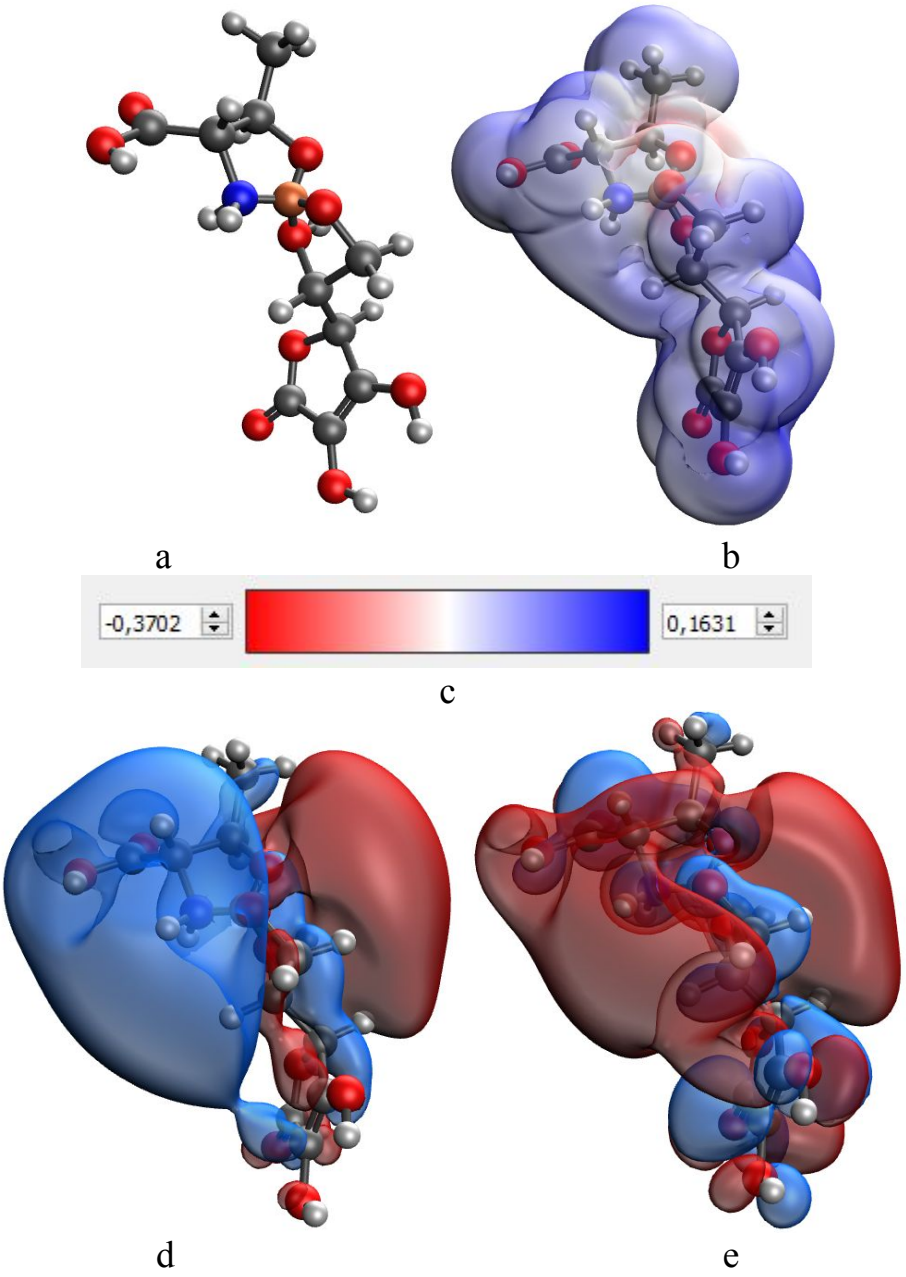

Figure S36. Results of modeling of iron ascorbate threoninate through the amino and hydroxyl groups of L-threonine and hydroxyl groups attached to C5 and C6 carbon atoms of ascorbic acid: molecular complex model (a), electron density distribution (b), electron density distribution gradient (c), HOMO (d), LUMO(e)

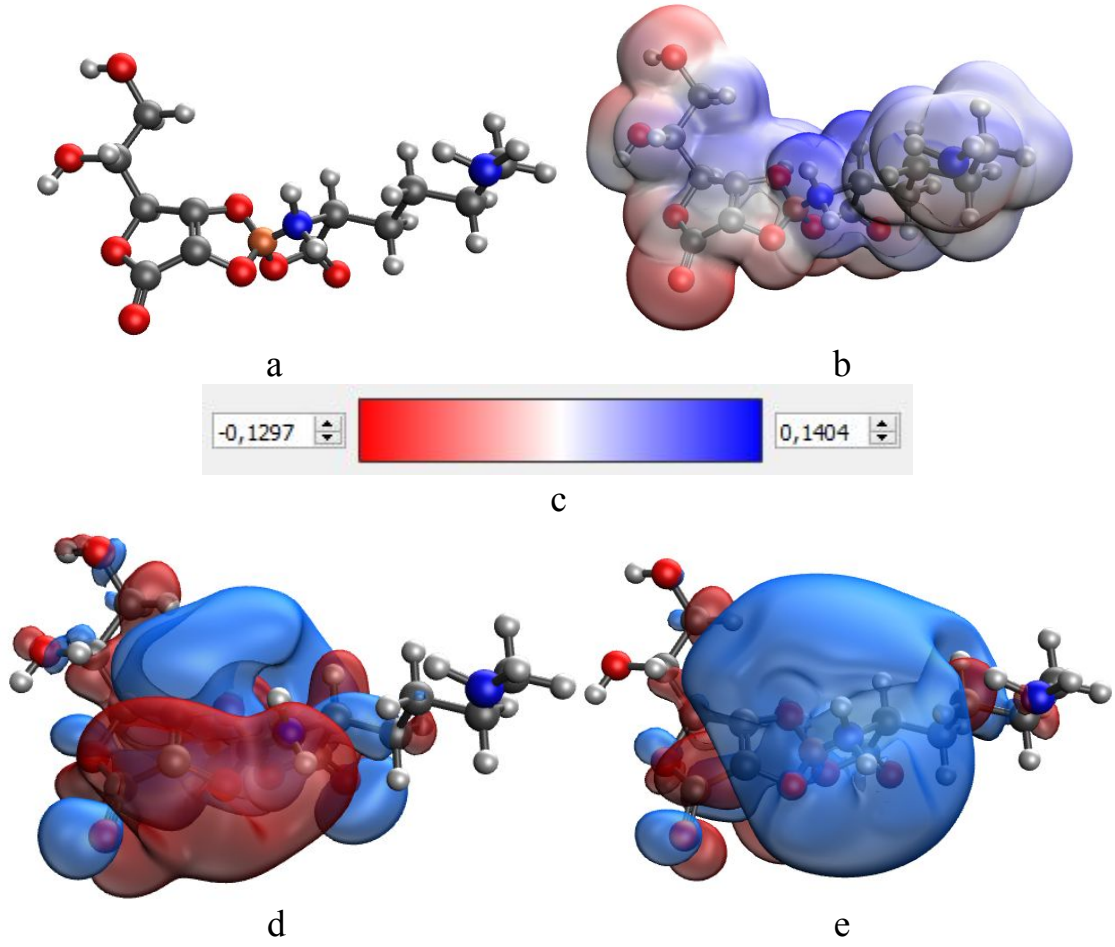

Figure S37. Results of modeling of iron ascorbate lysinate through amino and carboxyl groups of L-lysine and hydroxyl groups attached to C2 and C3 carbon atoms of ascorbic acid: model of the molecular complex (a), electron density distribution (b), electron density distribution gradient (c), HOMO (d), LUMO(e)

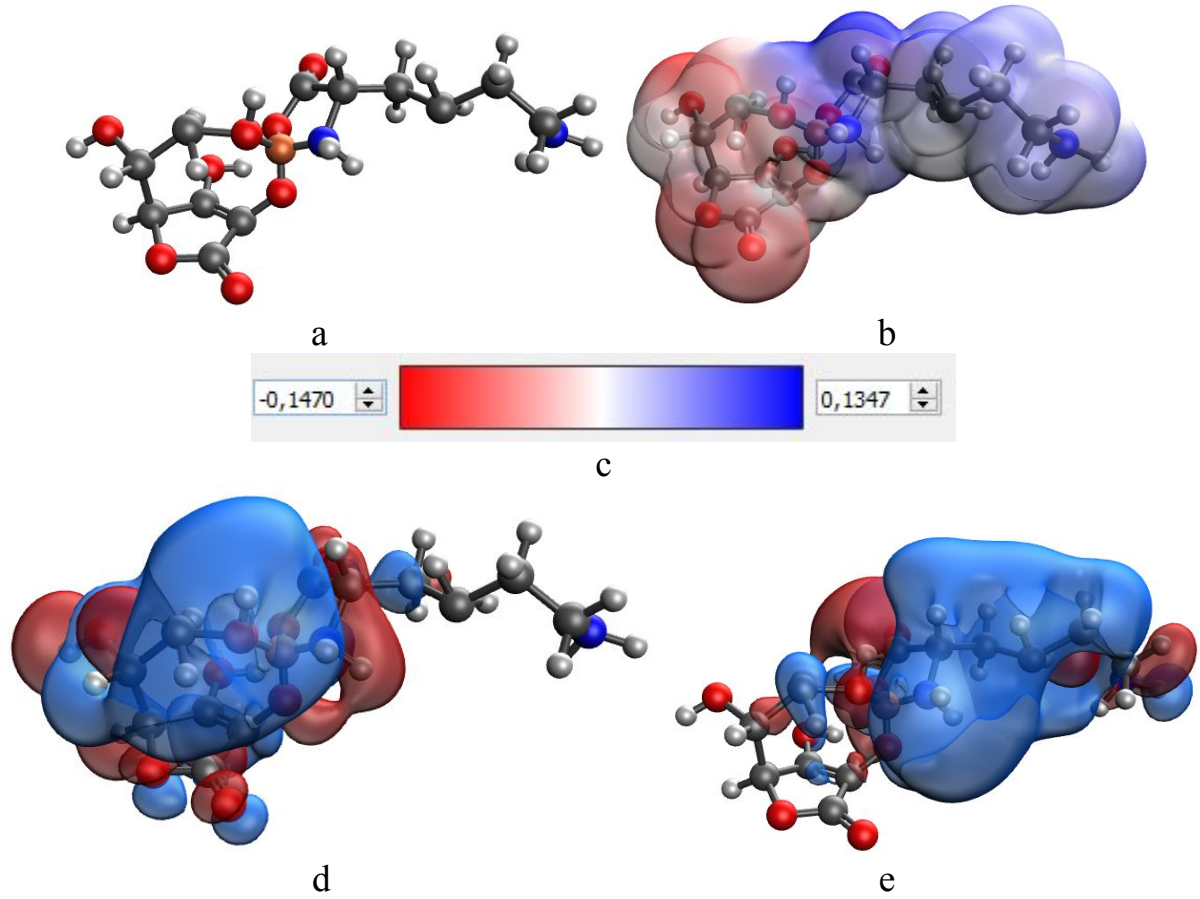

Figure S38. Results of modeling of iron ascorbate lysinate through amino and carboxyl groups of L-lysine and hydroxyl groups attached to C2 and C6 carbon atoms of ascorbic acid: model of the molecular complex (a), electron density distribution (b), electron density distribution gradient (c), HOMO (d), LUMO(e)

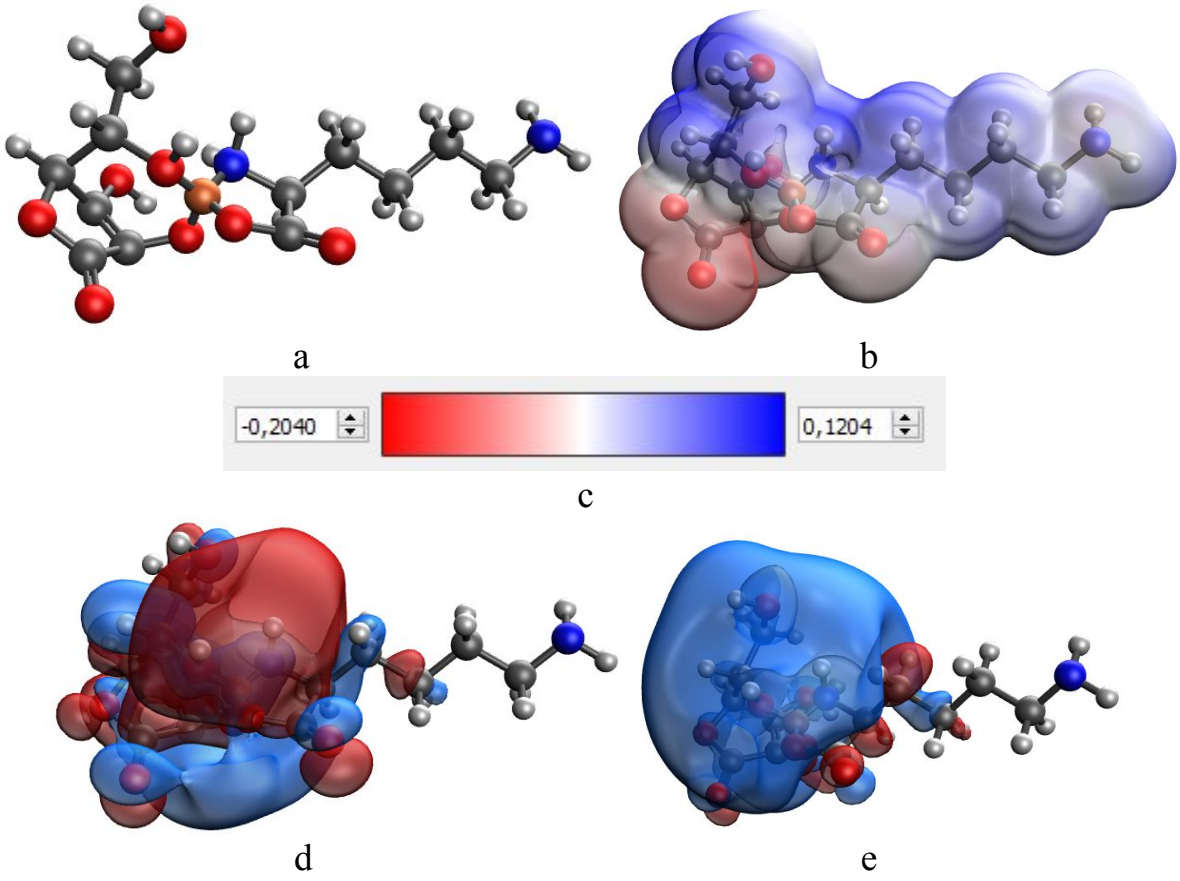

Figure S39. Results of modeling of iron ascorbate lysinate through amino and carboxyl groups of L-lysine and hydroxyl groups attached to C2 and C5 carbon atoms of ascorbic acid: model of the molecular complex (a), electron density distribution (b), electron density distribution gradient (c), HOMO (d), LUMO(e)

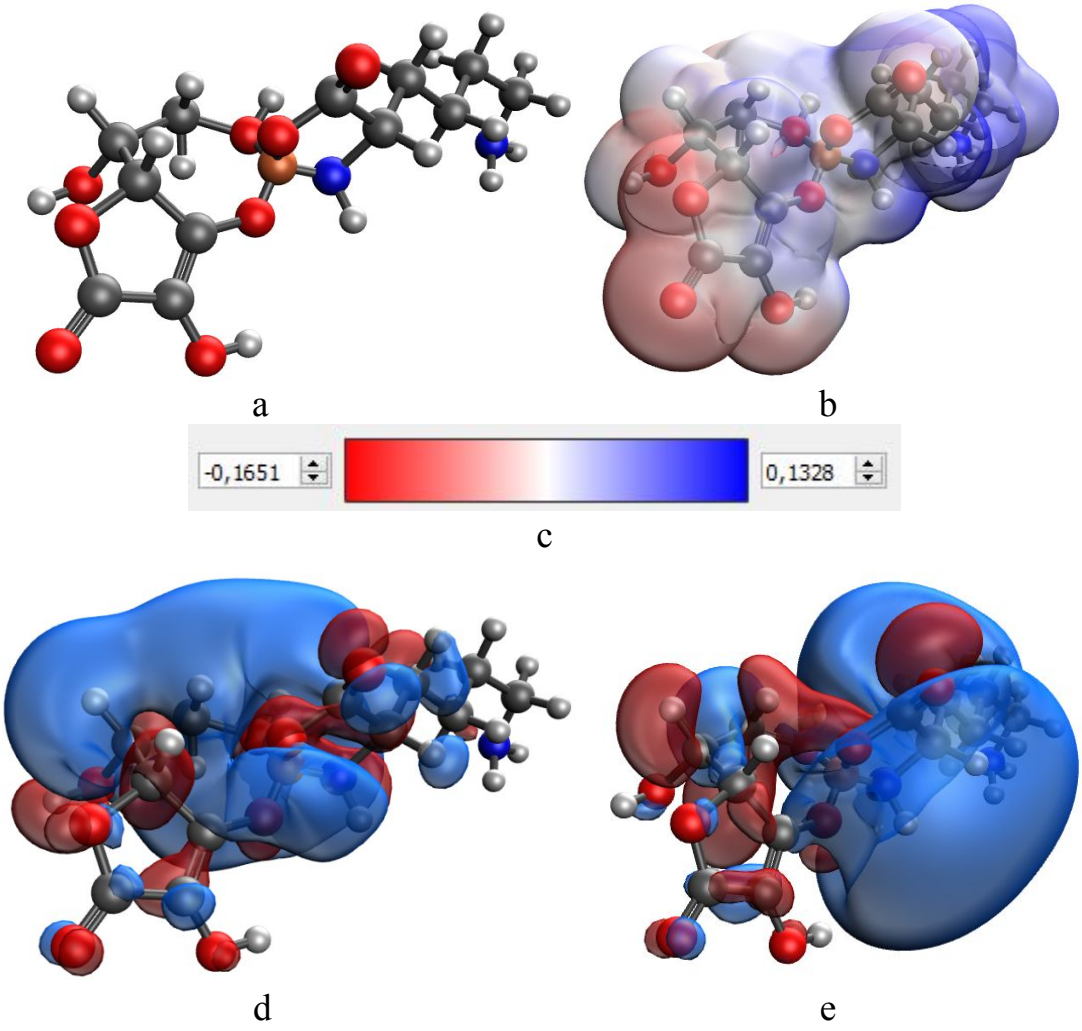

Figure S40. Results of modeling of iron ascorbate lysinate through the amino and carboxyl groups of L-lysine and hydroxyl groups attached to C3 and C6 carbon atoms of ascorbic acid: molecular complex model (a), electron density distribution (b), electron density distribution gradient (c), HOMO (d), LUMO(e)

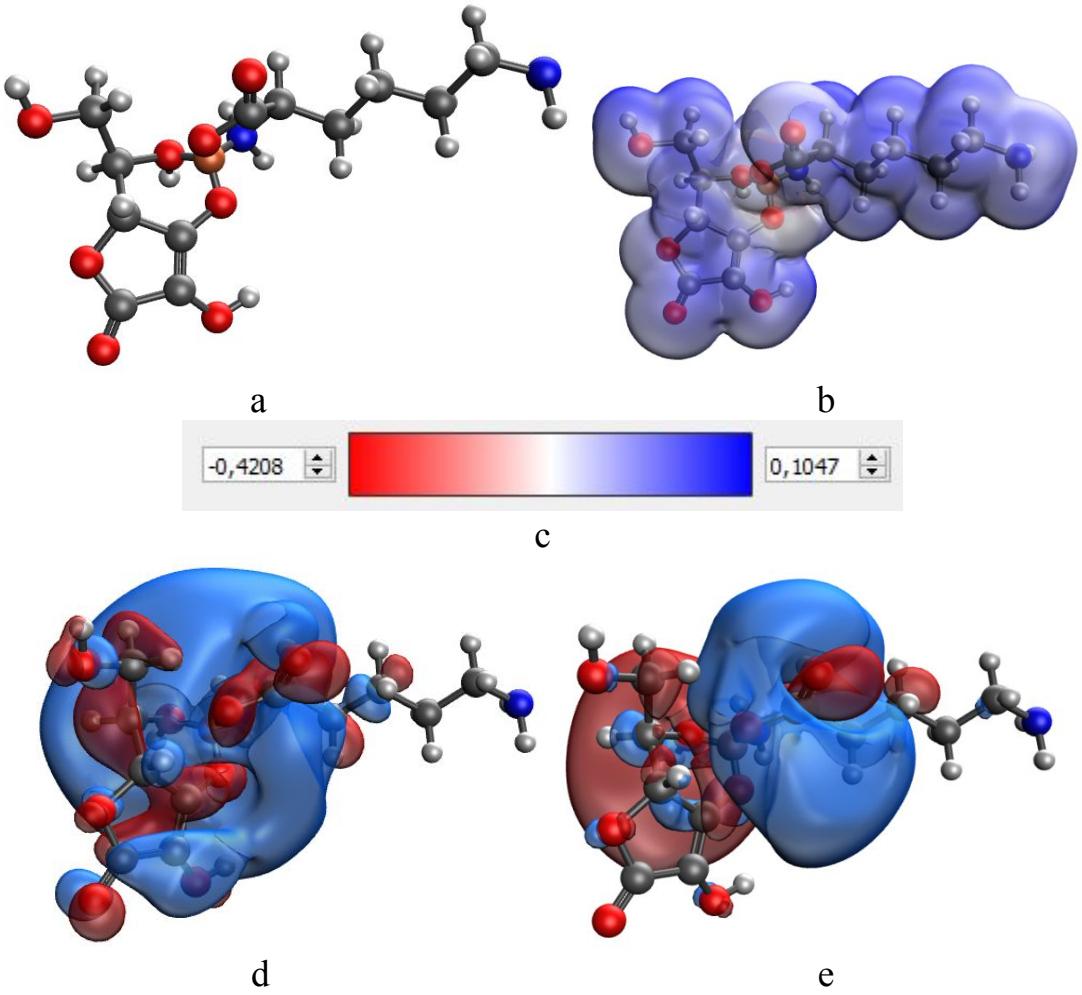

Figure S41. Results of modeling of iron ascorbate lysinate through amino and carboxyl groups of L-lysine and hydroxyl groups attached to C3 and C5 carbon atoms of ascorbic acid: model of the molecular complex (a), electron density distribution (b), electron density distribution gradient (c), HOMO (d), LUMO(e)

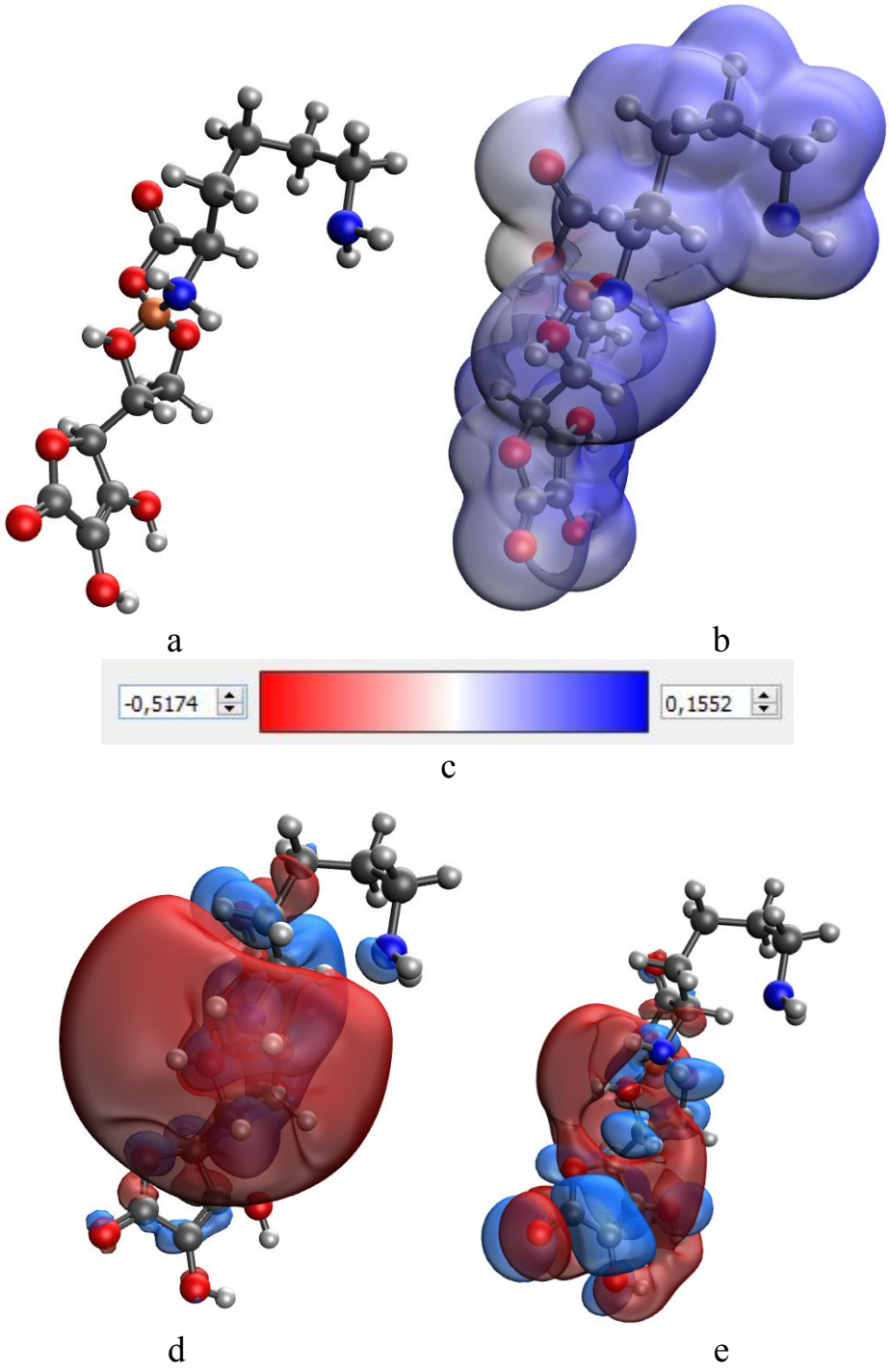

Figure S42. Results of modeling of iron ascorbate lysinate through amino- and g carboxyl groups of L-lysine and hydroxyl groups attached to C5 and C6 carbon atoms of ascorbic acid: molecular complex model (a), electron density distribution (b), electron density distribution gradient (c), HOMO (d), LUMO(e)

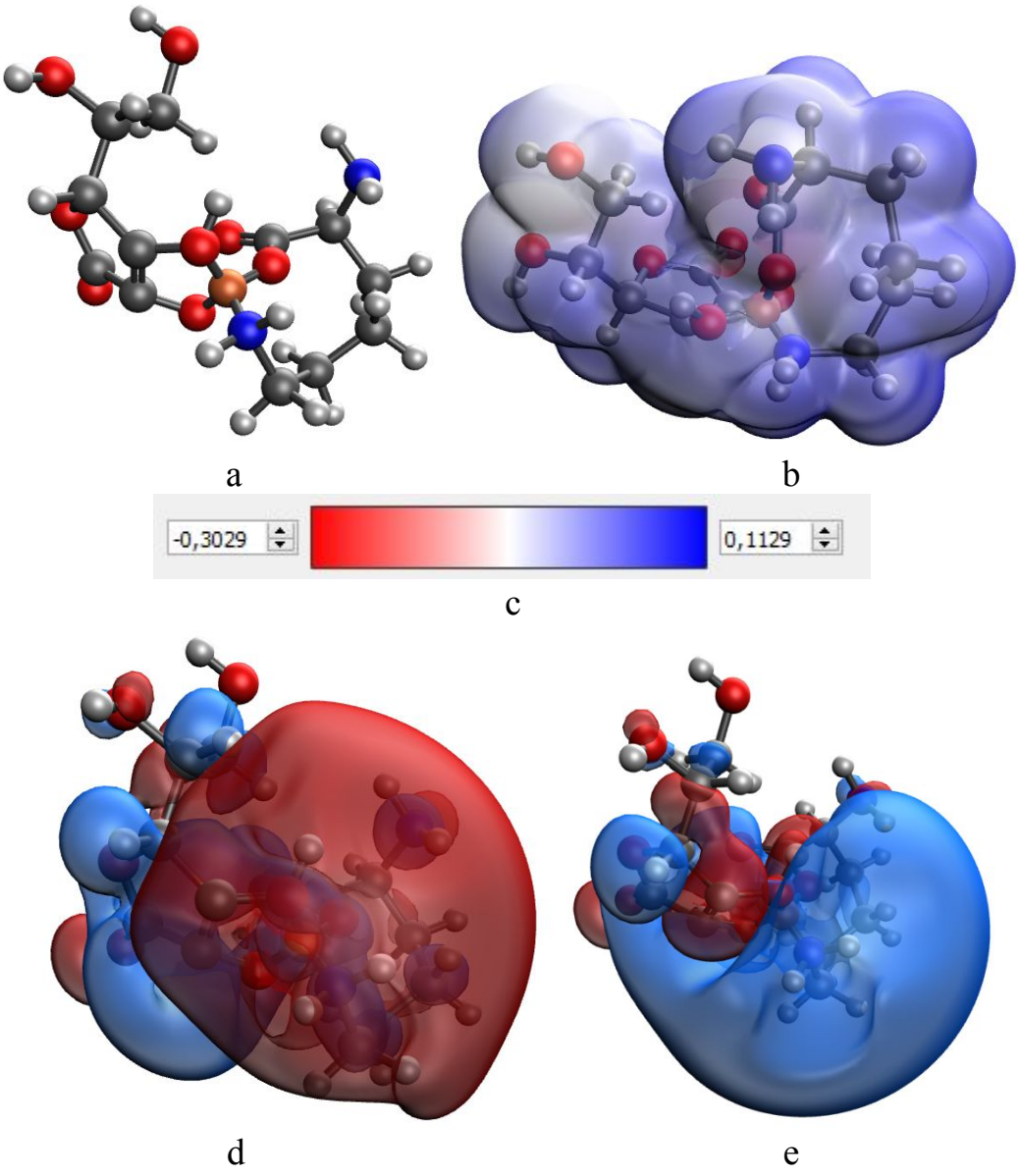

Figure S43. Results of modeling of iron ascorbate lysinate through the amino and hydroxyl groups of L-lysine and hydroxyl groups attached to C2 and C3 carbon atoms of ascorbic acid: molecular complex model (a), electron density distribution (b), electron density distribution gradient (c), HOMO (d), LUMO(e)

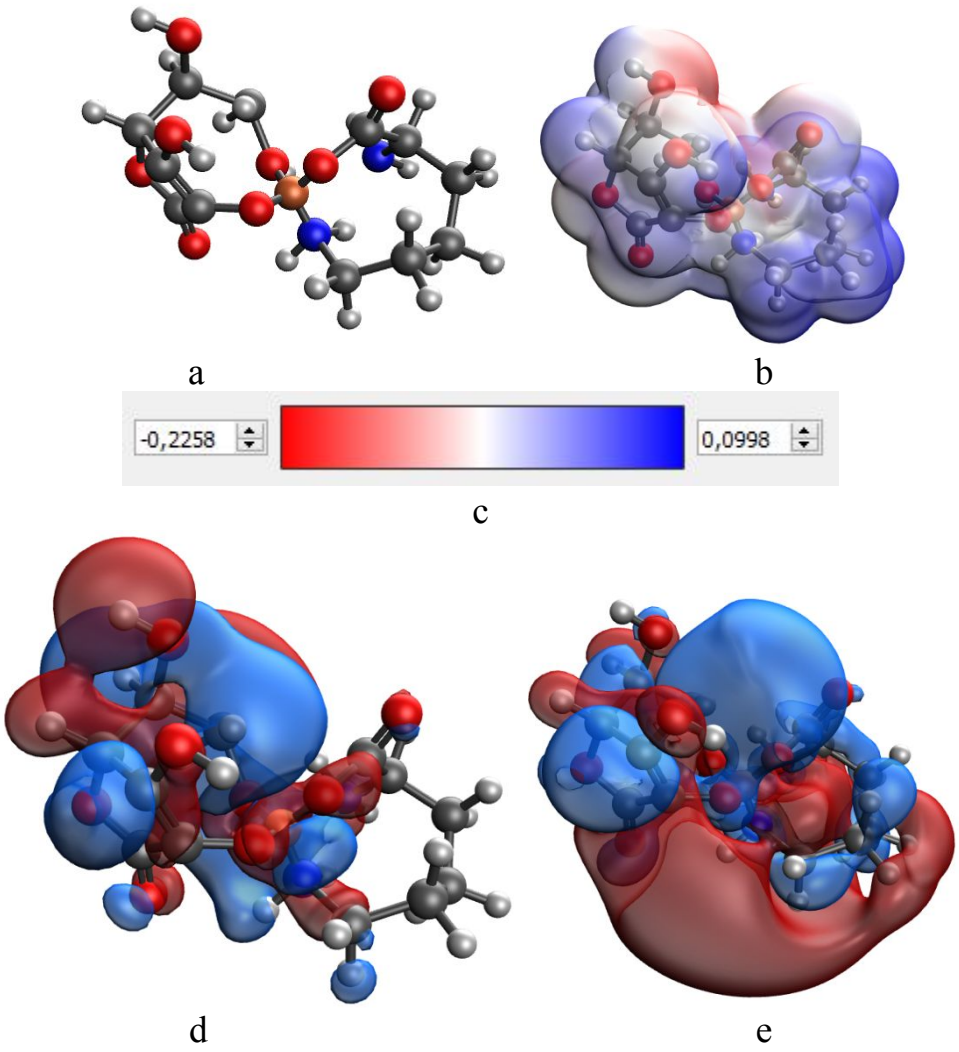

Figure S44. Results of modeling of iron ascorbate lysinate through amino and hydroxyl groups of L-lysine and hydroxyl groups attached to C2 and C6 carbon atoms of ascorbic acid: model of the molecular complex (a), electron density distribution (b), electron density distribution gradient (c), HOMO (d), LUMO(e)

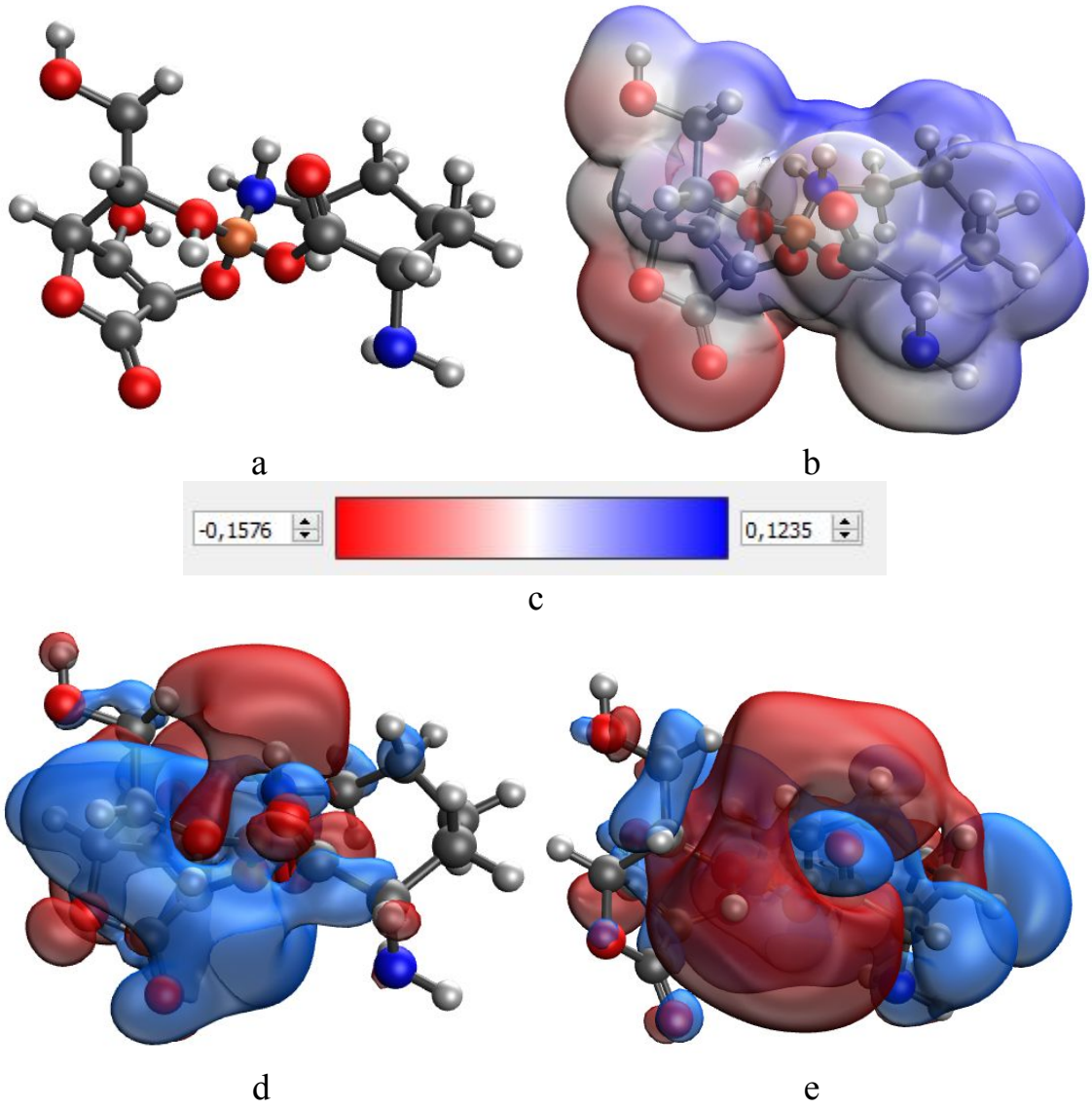

Figure S45. Results of modeling of iron ascorbate lysinate through the amino and hydroxyl groups of L-lysine and hydroxyl groups attached to C2 and C5 carbon atoms of ascorbic acid: molecular complex model (a), electron density distribution (b), electron density distribution gradient (c), HOMO (d), LUMO(e)

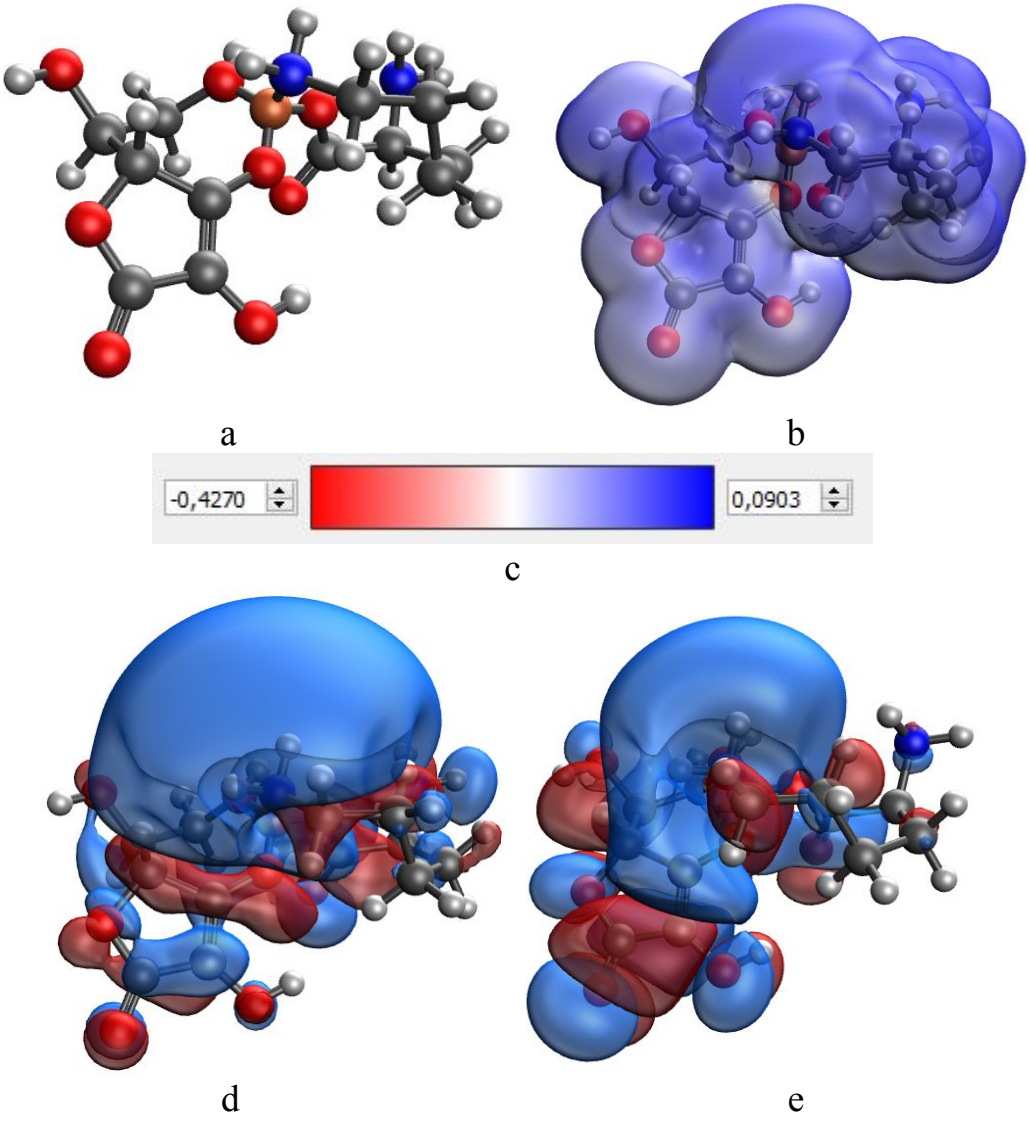

Figure S46. Results of modeling of iron ascorbate lysinate through amino and hydroxyl groups of L-lysine and hydroxyl groups attached to C3 and C6 carbon atoms of ascorbic acid: model of the molecular complex (a), electron density distribution (b), electron density distribution gradient (c), HOMO (d), LUMO(e)

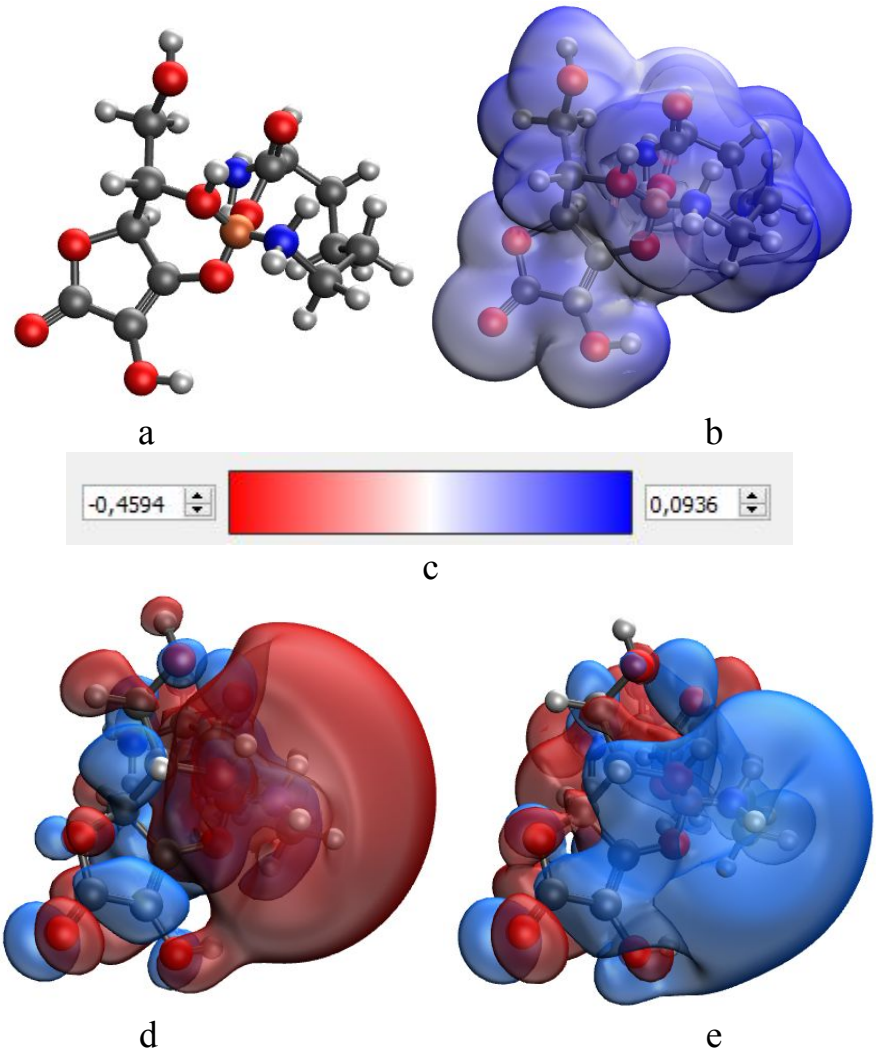

Figure S47. Results of modeling of iron ascorbate lysinate through the amino and hydroxyl groups of L-lysine and hydroxyl groups attached to C3 and C5 carbon atoms of ascorbic acid: molecular complex model (a), electron density distribution (b), electron density distribution gradient (c), HOMO (d), LUMO(e)

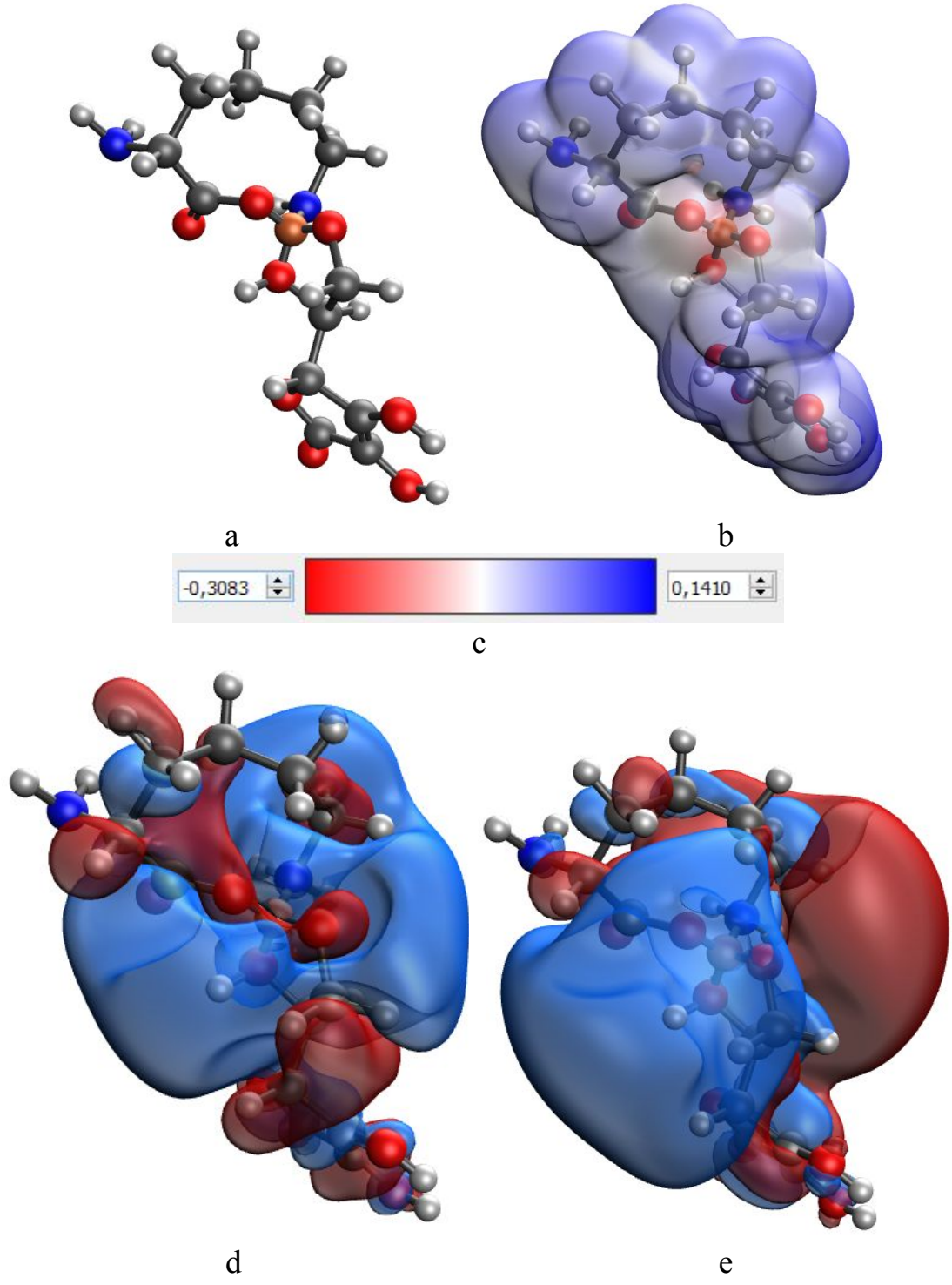

Figure S48. Results of modeling of iron ascorbate lysinate through the amino and hydroxyl groups of L-lysine and hydroxyl groups attached to C5 and C6 carbon atoms of ascorbic acid: molecular complex model (a), electron density distribution (b), electron density distribution gradient (c), HOMO (d), LUMO(e)

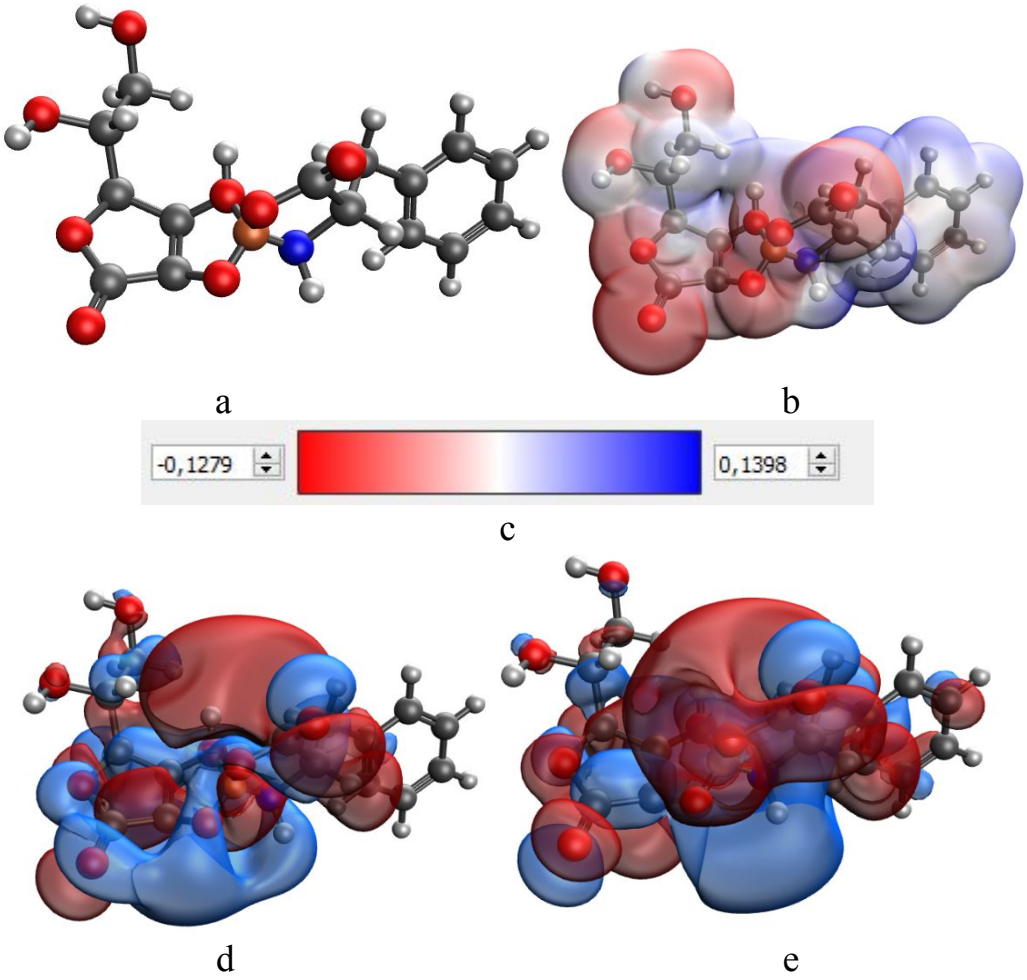

Figure S49. Results of modeling of iron ascorbate phenylalaninate through amino and carboxyl groups of L-phenylalanine and hydroxyl groups attached to C2 and C3 carbon atoms of ascorbic acid: molecular complex model (a), electron density distribution (b), electron density distribution gradient (c), HOMO (d), LUMO(e)

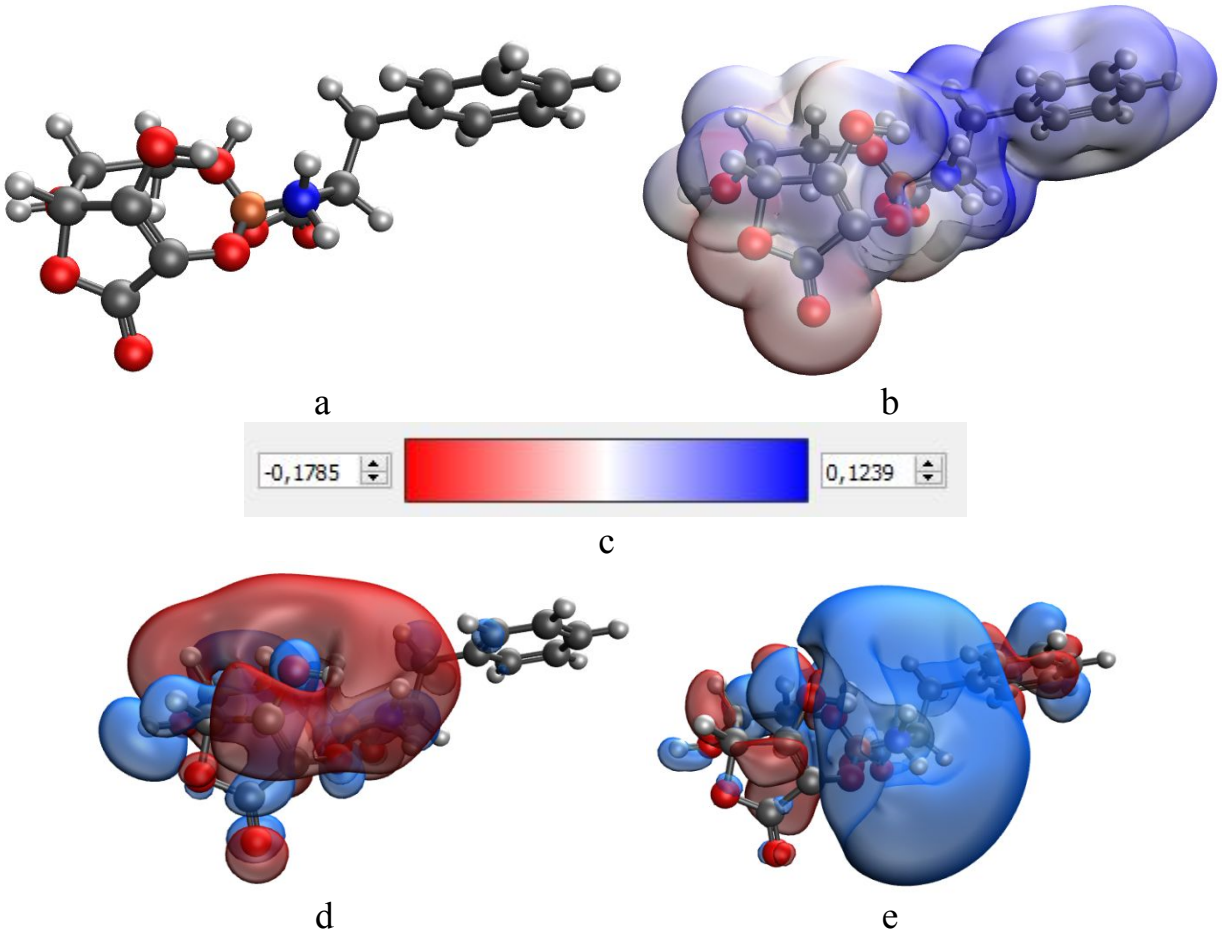

Figure S50. Results of modeling of iron ascorbate phenylalaninate through amino and carboxyl groups of L-phenylalanine and hydroxyl groups attached to C2 and C6 carbon atoms of ascorbic acid: molecular complex model (a), electron density distribution (b), electron density distribution gradient (c), HOMO (d), LUMO(e)

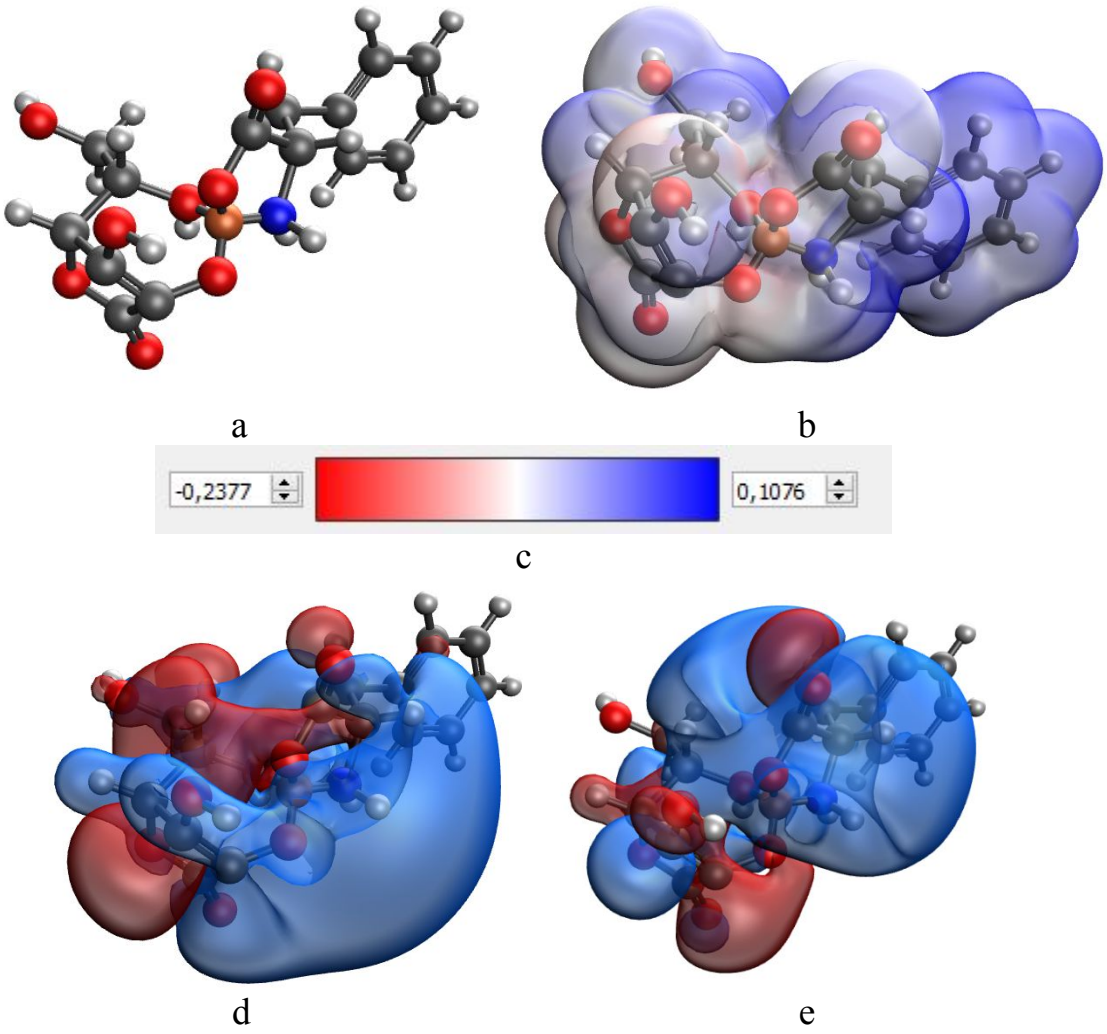

Figure S51. Results of modeling of iron ascorbate phenylalaninate through amino and carboxyl groups of L-phenylalanine and hydroxyl groups attached to C2 and C5 carbon atoms of ascorbic acid: molecular complex model (a), electron density distribution (b), electron density distribution gradient (c), HOMO (d), LUMO(e)

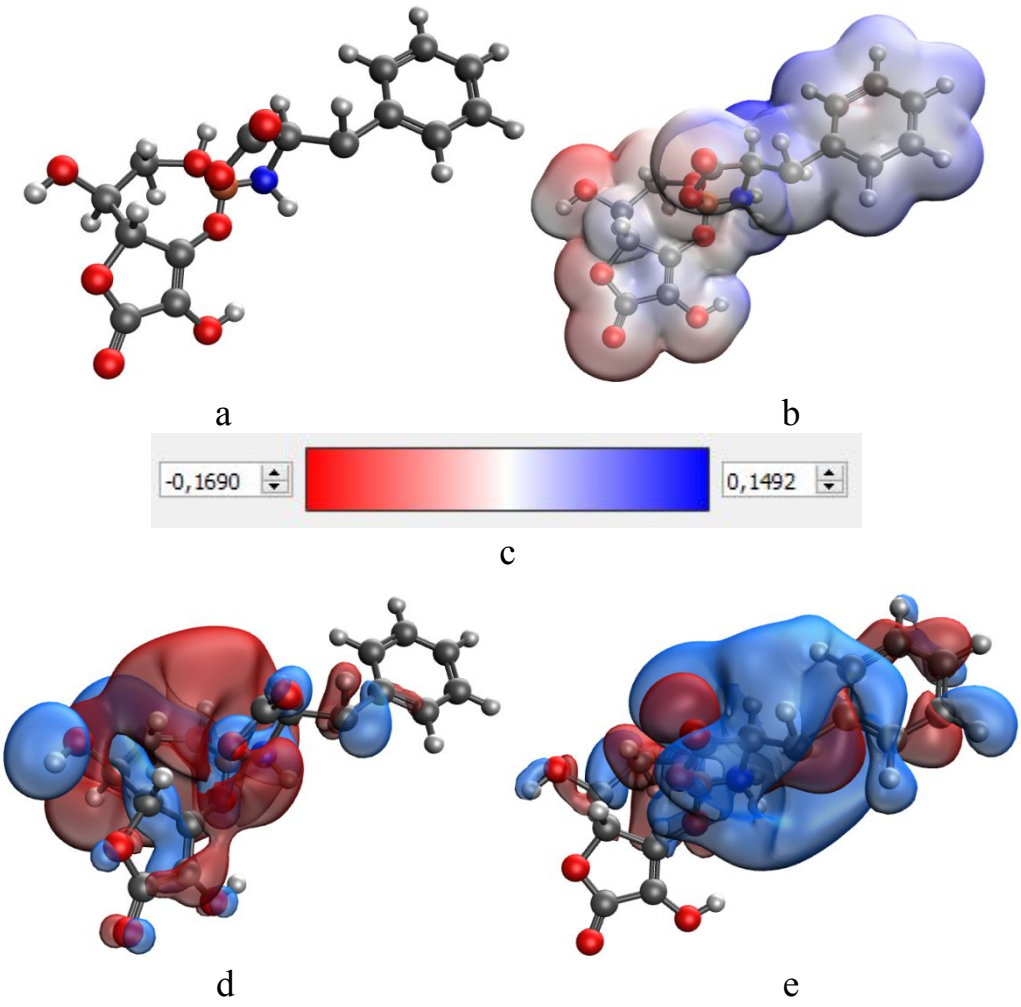

Figure S52. Results of modeling of iron ascorbate phenylalaninate through amino and carboxyl groups of L-phenylalanine and hydroxyl groups attached to C3 and C6 carbon atoms of ascorbic acid: molecular complex model (a), electron density distribution (b), electron density distribution gradient (c), HOMO (d), LUMO(e)

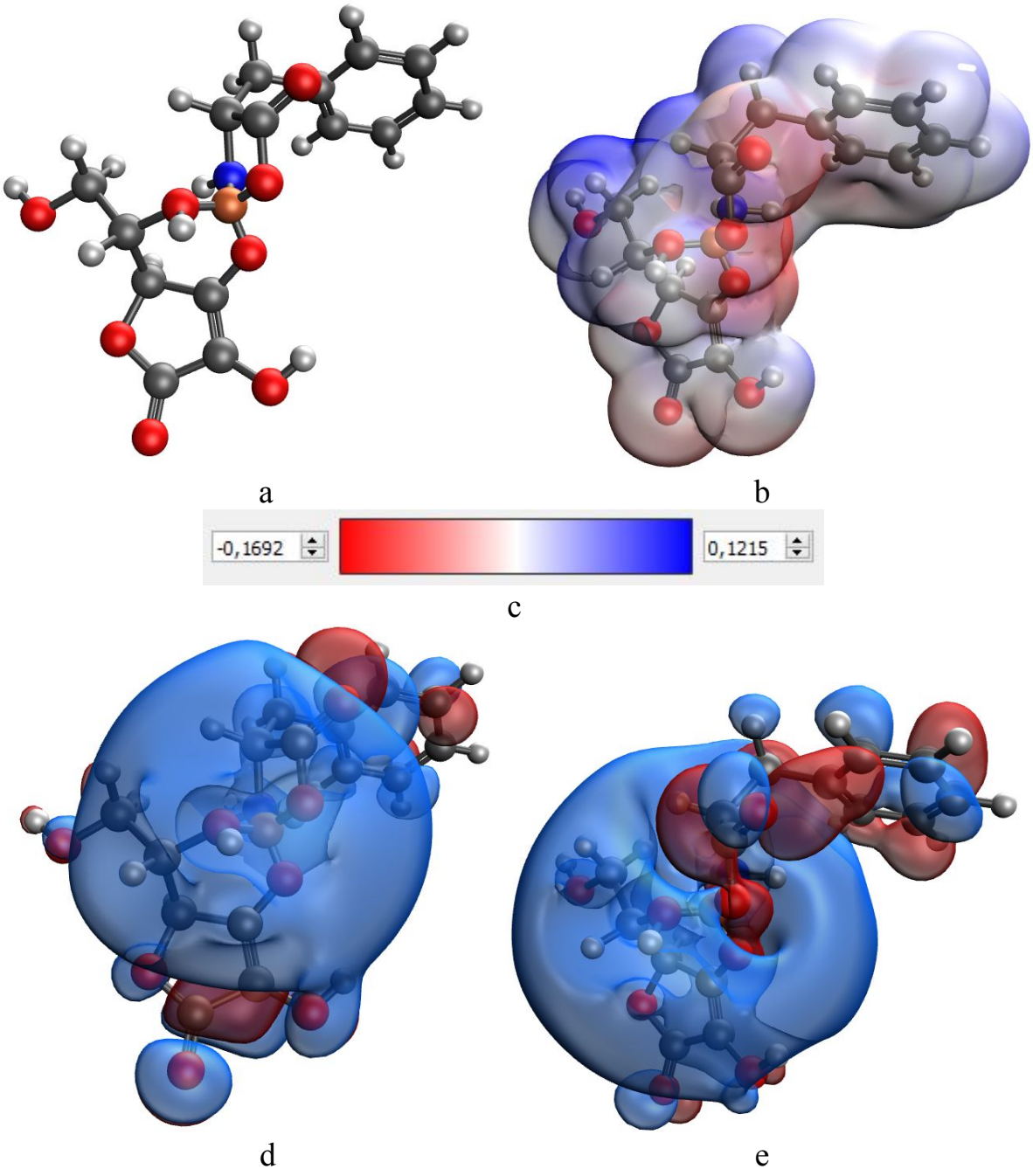

Figure S53. Results of modeling of iron ascorbate phenylalaninate through amino and carboxyl groups of L-phenylalanine and hydroxyl groups attached to C3 and C5 carbon atoms of ascorbic acid: molecular complex model (a), electron density distribution (b), electron density distribution gradient (c), HOMO (d), LUMO(e)

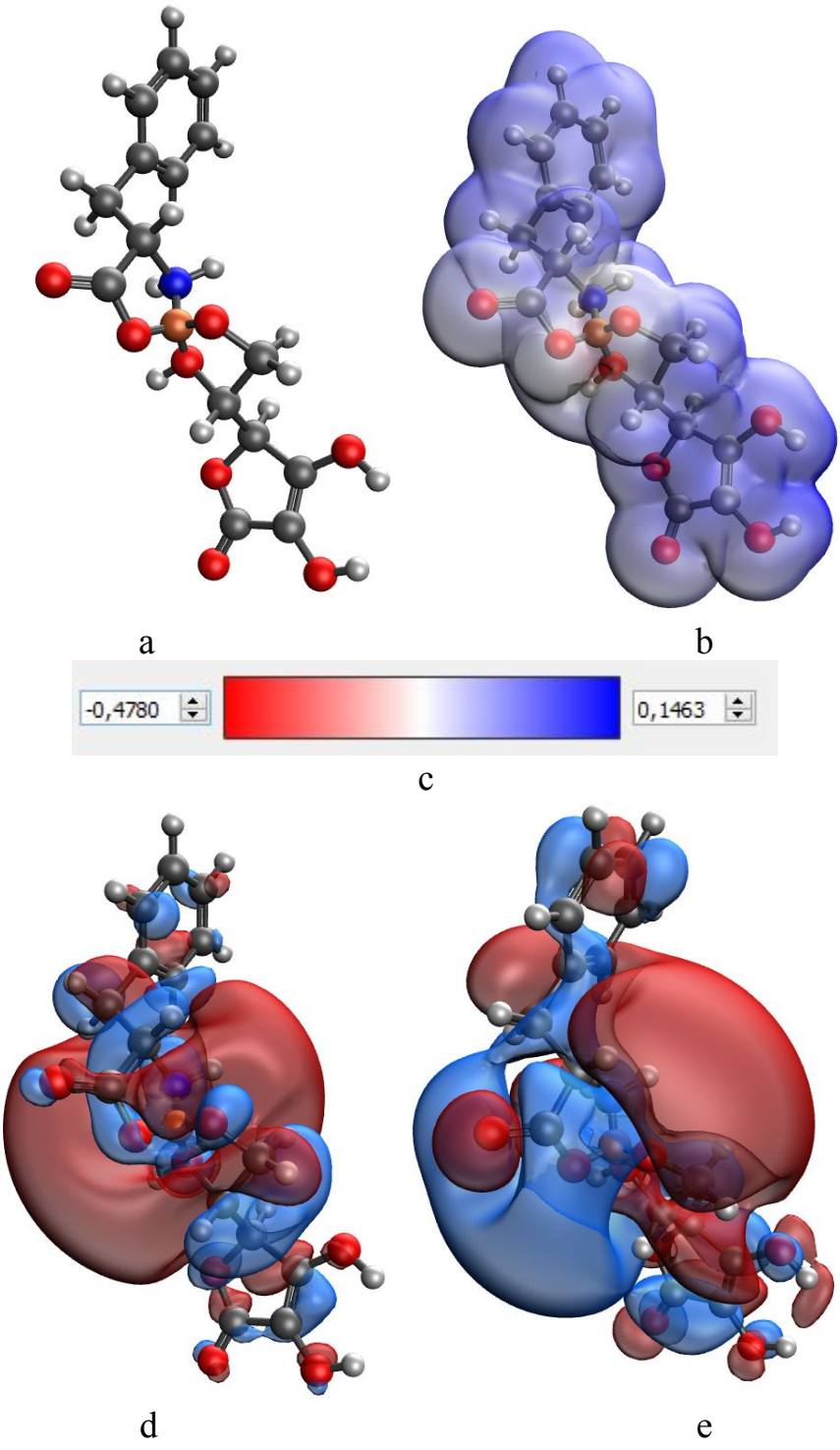

Figure S54. Results of modeling of iron ascorbate phenylalaninate through amino and carboxyl groups of L-phenylalanine and hydroxyl groups attached to C5 and C6 carbon atoms of ascorbic acid: molecular complex model (a), electron density distribution (b), electron density distribution gradient (c), HOMO (d), LUMO(e)

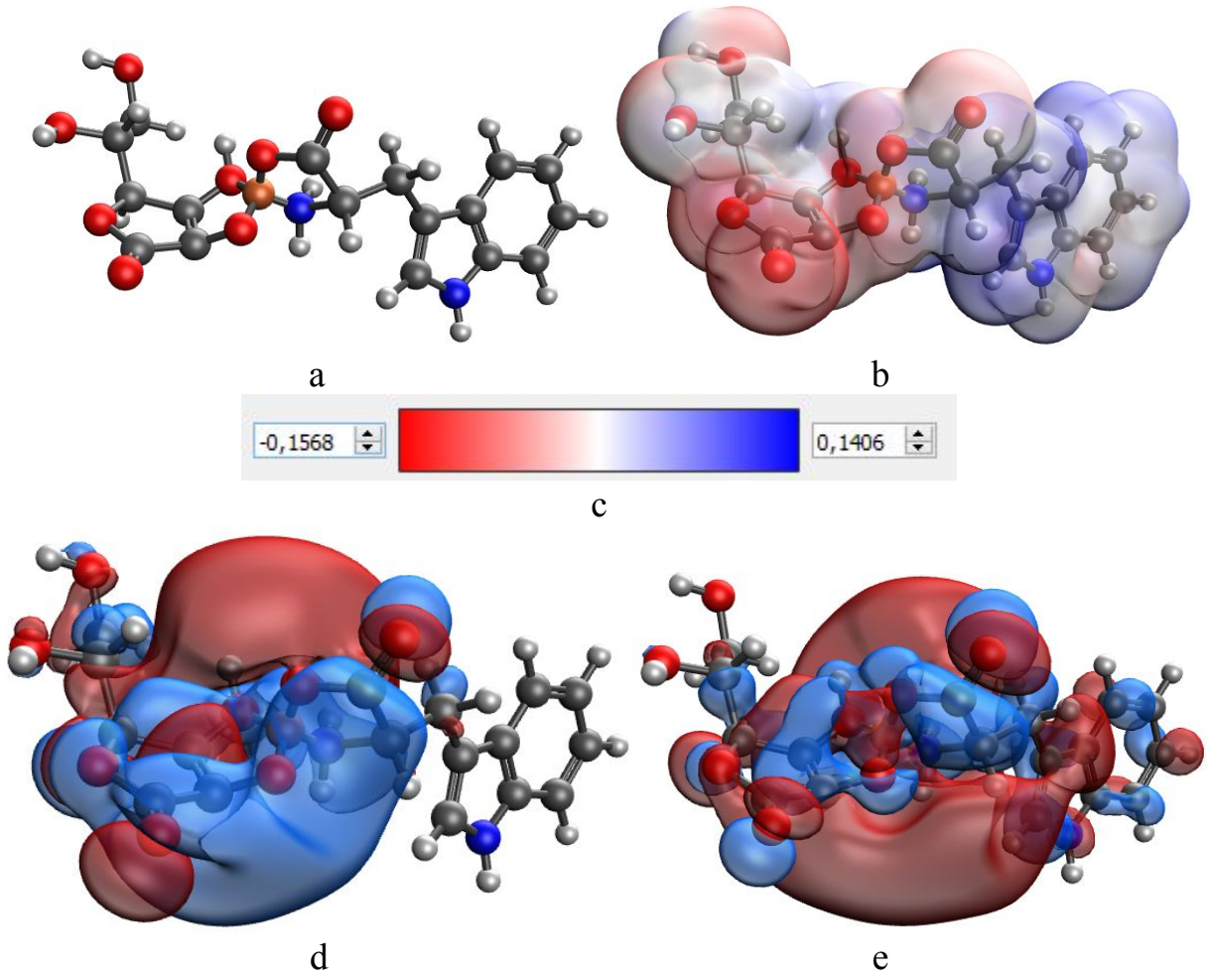

Figure S55. Results of modeling of iron ascorbate tryptophanate through amino and carboxyl groups of L-tryptophan and hydroxyl groups attached to C2 and C3 carbon atoms of ascorbic acid: molecular complex model (a), electron density distribution (b), electron density distribution gradient (c), HOMO (d), LUMO(e)

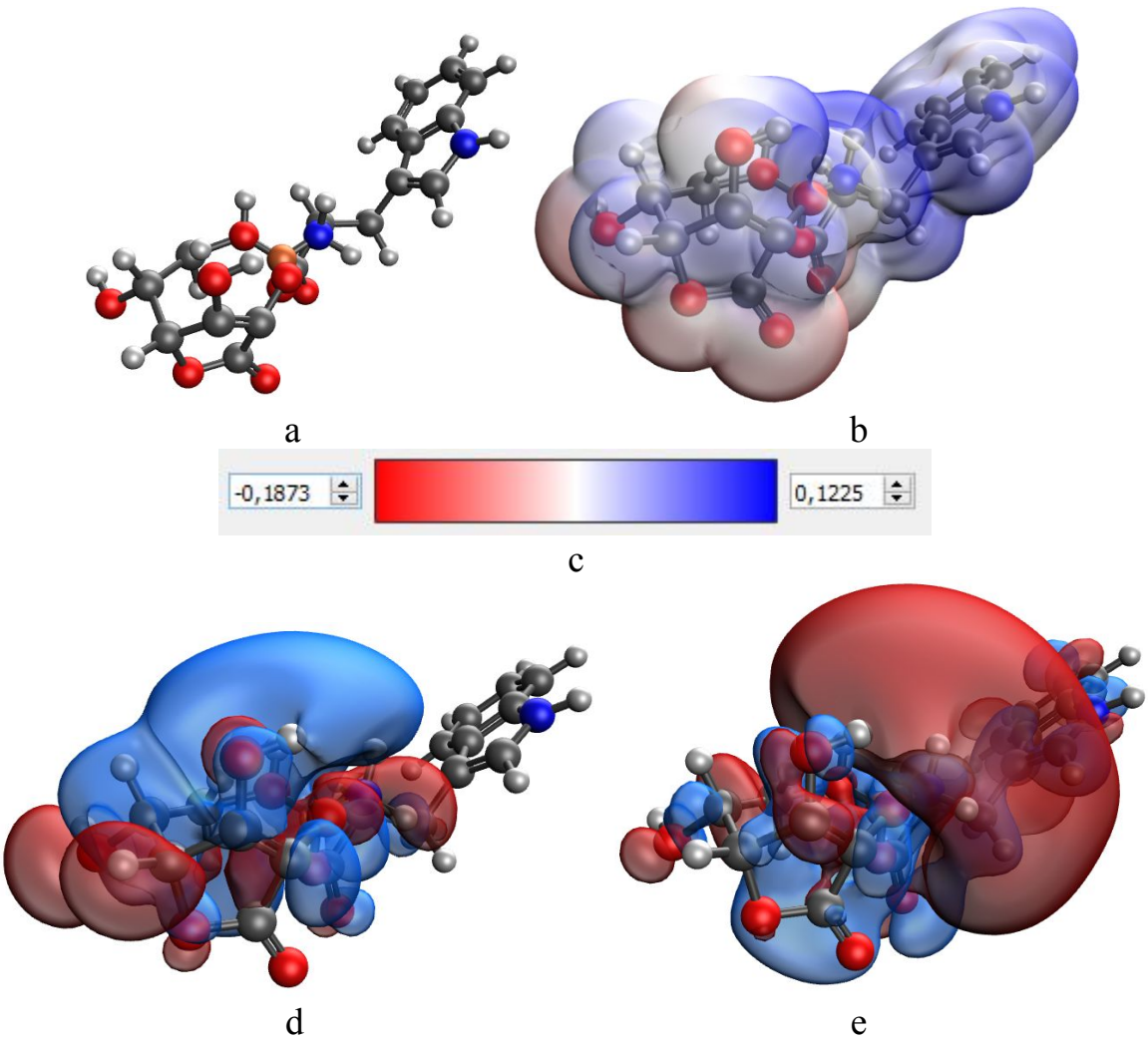

Figure S56. Results of modeling of iron ascorbate tryptophanate through the amino and carboxyl groups of L-tryptophan and hydroxyl groups attached to C2 and C6 carbon atoms of ascorbic acid: molecular complex model (a), electron density distribution (b), electron density distribution gradient (c), HOMO (d), LUMO(e)

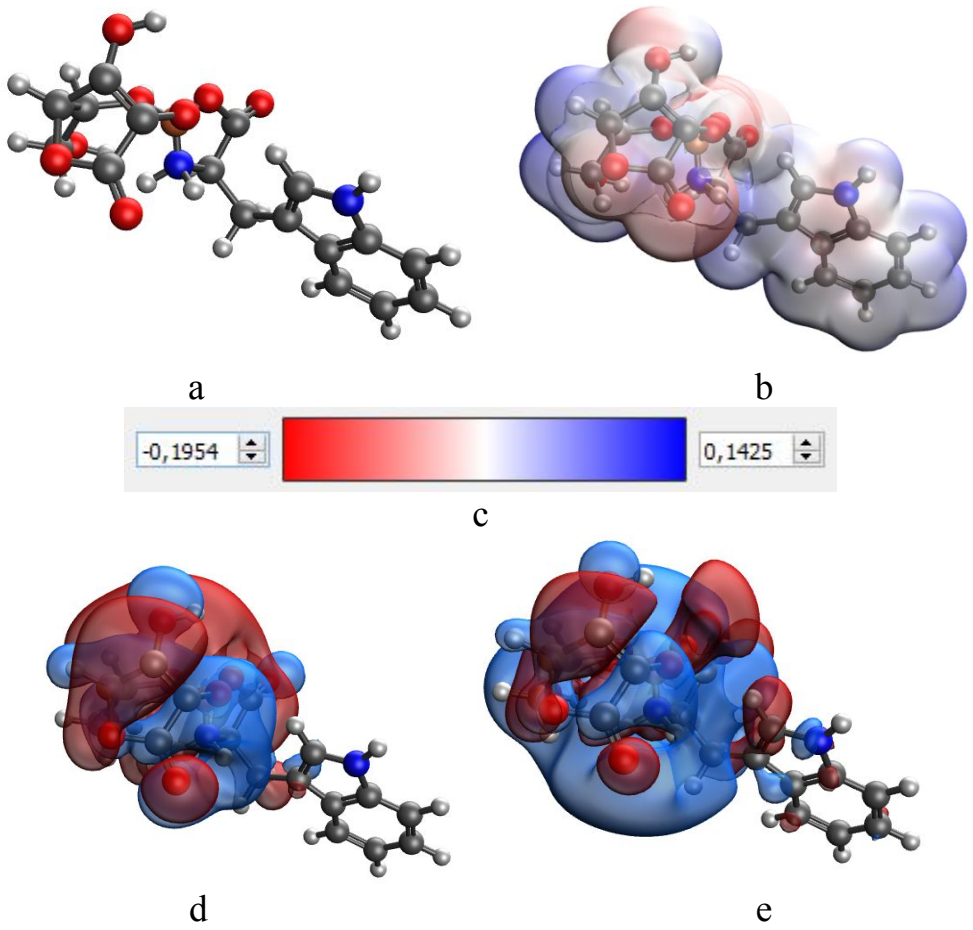

Figure S57. Results of modeling of iron ascorbate tryptophanate through the amino and carboxyl groups of L-tryptophan and hydroxyl groups attached to C2 and C5 carbon atoms of ascorbic acid: molecular complex model (a), electron density distribution (b), electron density distribution gradient (c), HOMO (d), LUMO(e)

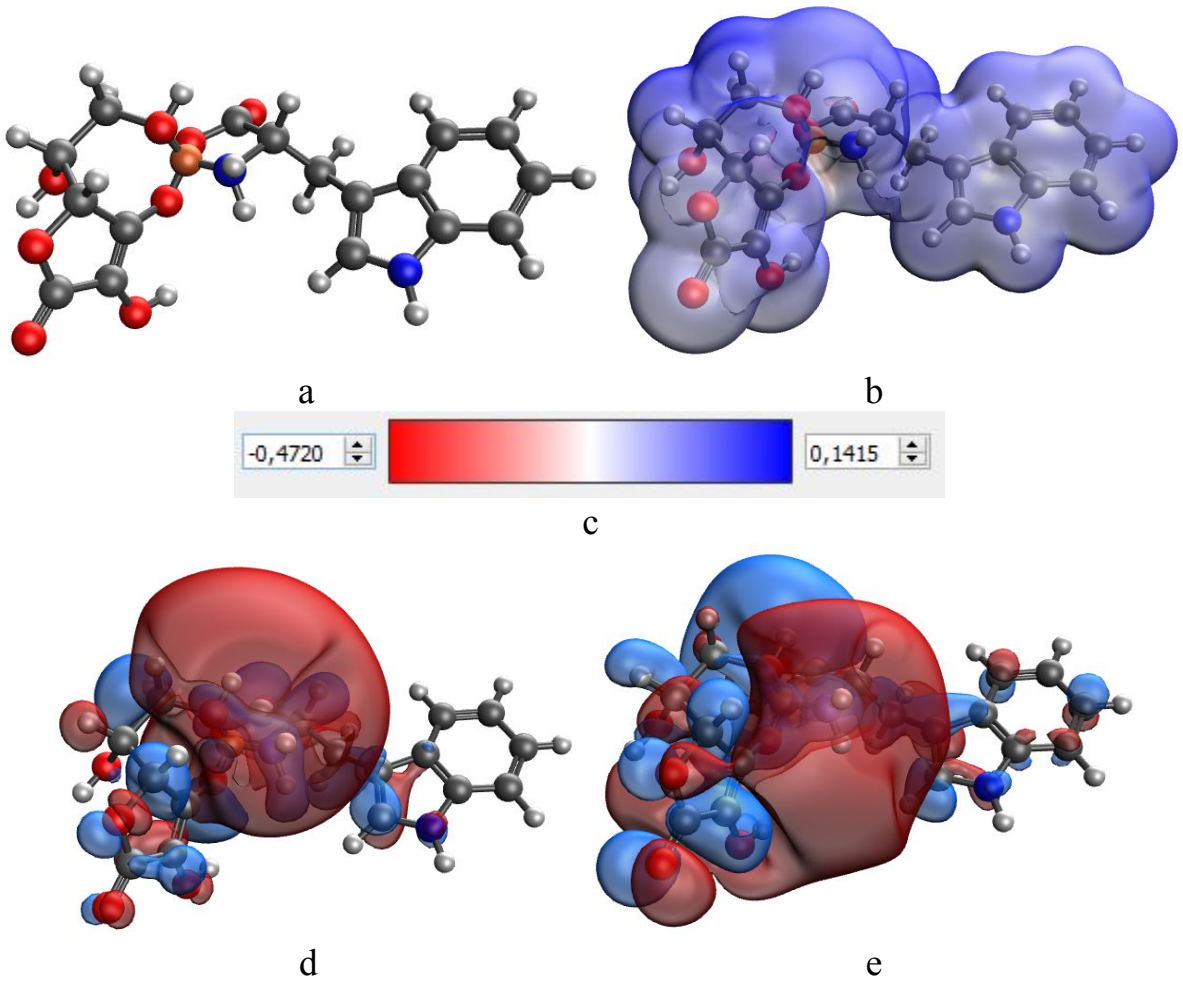

Figure S58. Results of modeling of iron ascorbate tryptophanate through the amino and carboxyl groups of L-tryptophan and hydroxyl groups attached to C3 and C6 carbon atoms of ascorbic acid: molecular complex model (a), electron density distribution (b), electron density distribution gradient (c), HOMO (d), LUMO(e)

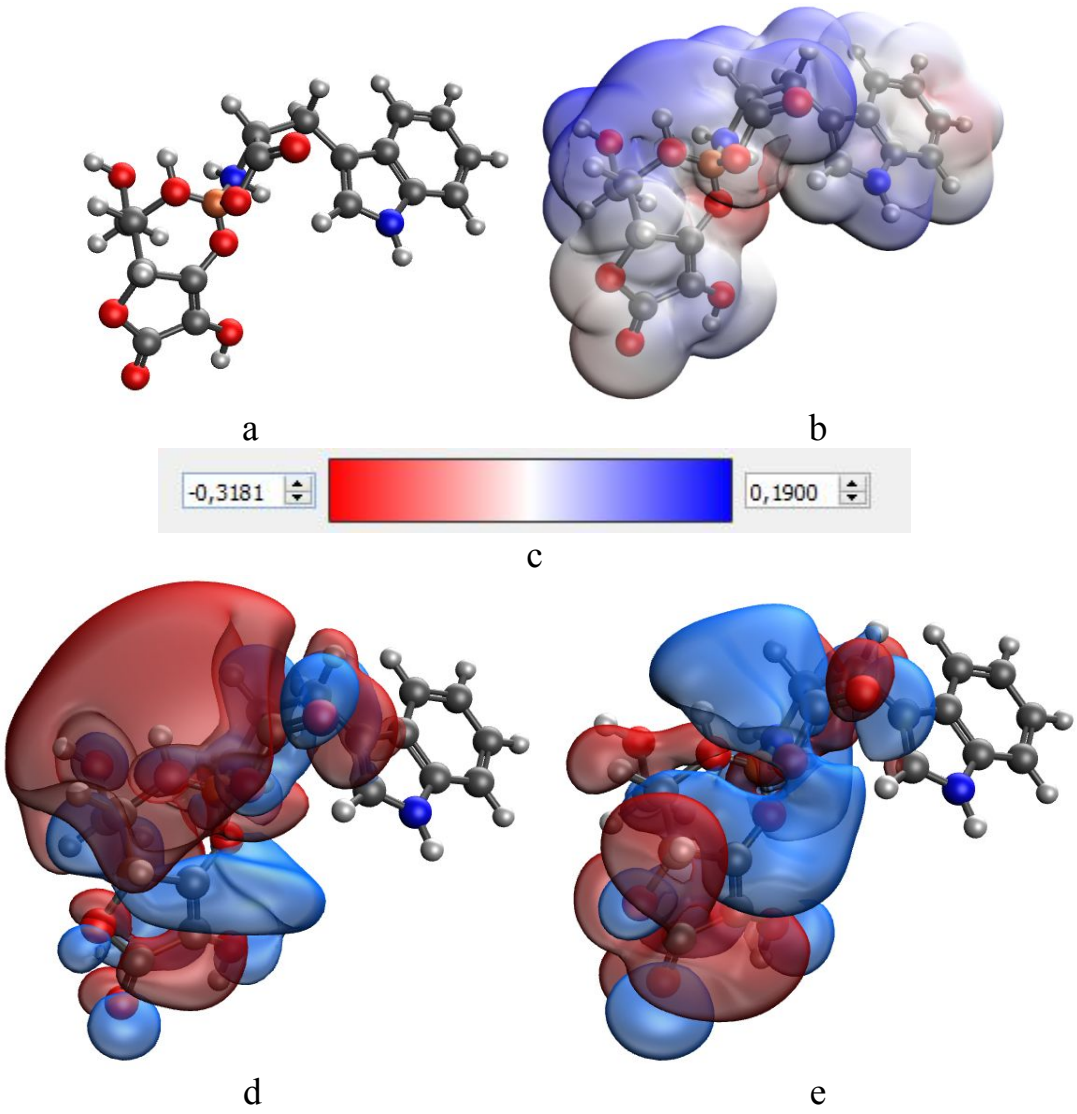

Figure S59. Results of modeling of iron ascorbate tryptophanate through the amino and carboxyl groups of L-tryptophan and hydroxyl groups attached to C3 and C5 carbon atoms of ascorbic acid: molecular complex model (a), electron density distribution (b), electron density distribution gradient (c), HOMO (d), LUMO(e)

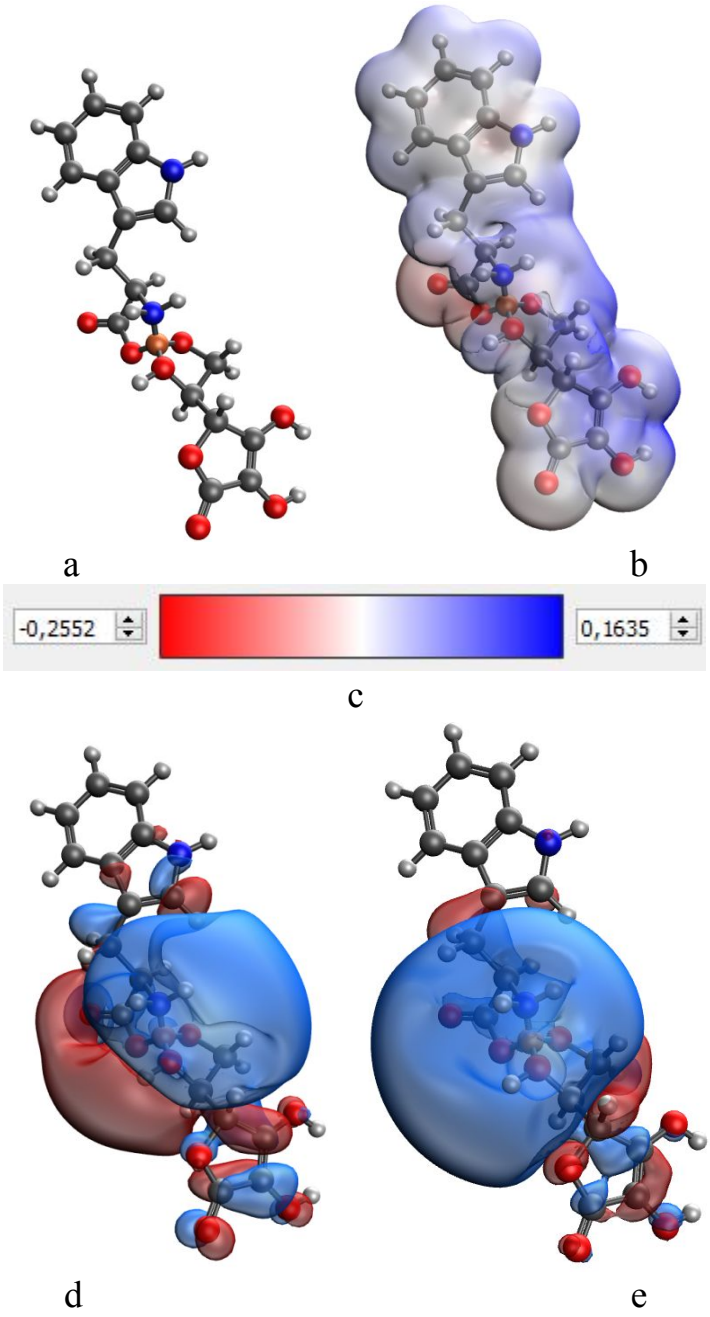

Figure S60. Results of modeling of iron ascorbate tryptophanate through the amino and carboxyl groups of L-tryptophan and hydroxyl groups attached to C5 and C6 carbon atoms of ascorbic acid: molecular complex model (a), electron density distribution (b), electron density distribution gradient (c), HOMO (d), LUMO(e)

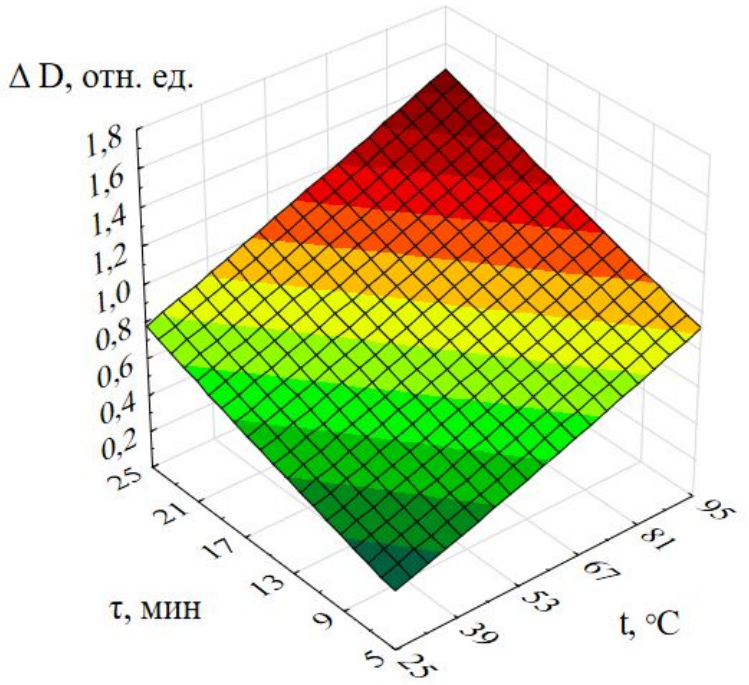

a

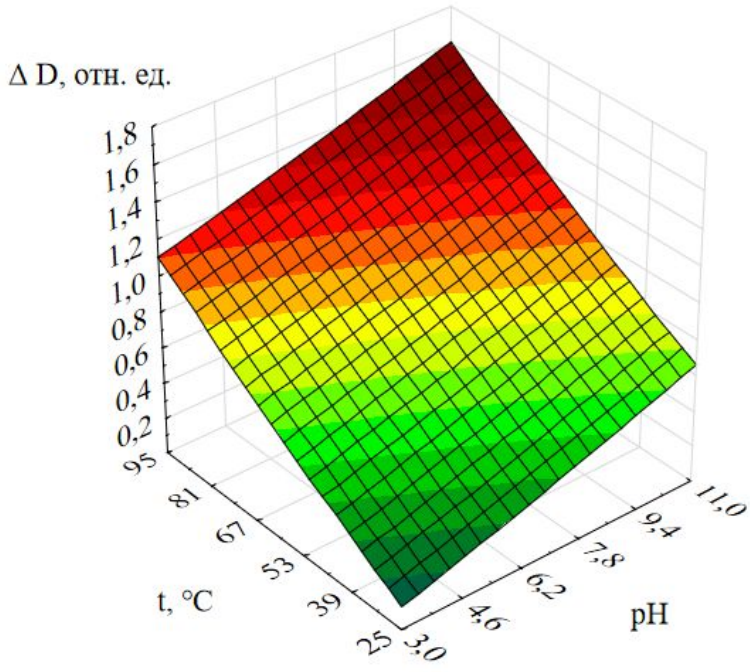

b

Figure S61. Stability of iron ascorbate threoninate: dependences of changes in optical density on technological parameters of temperature and exposure time (a), pH and temperature (b)

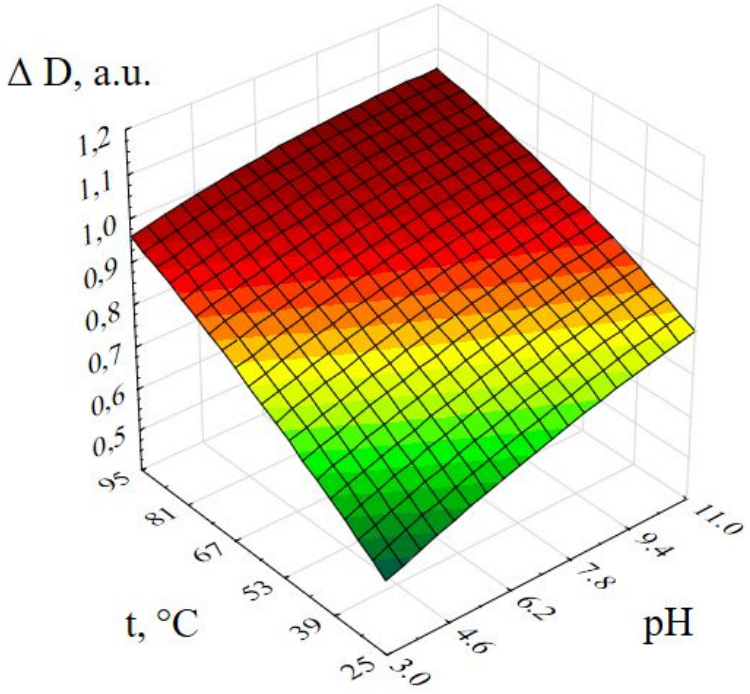

a

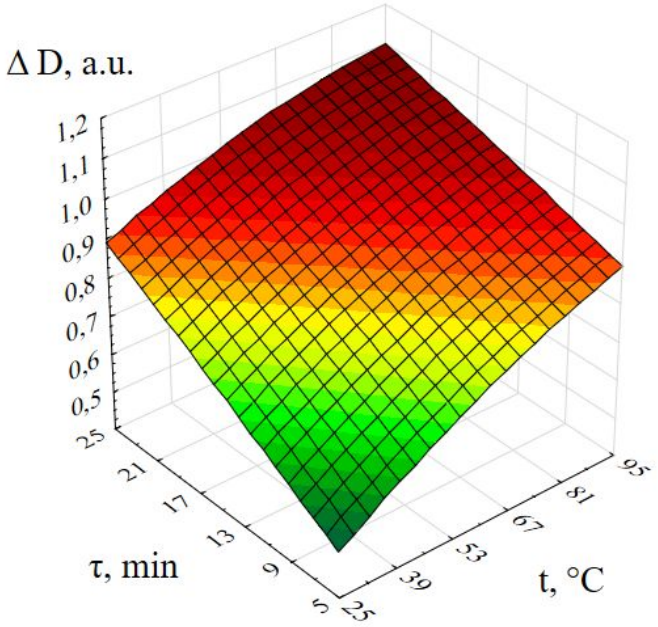

b

Figure S62. Stability of iron ascorbate isoleucinate: dependences of changes in optical density on technological parameters of pH and temperature (a), temperature and exposure time (b)

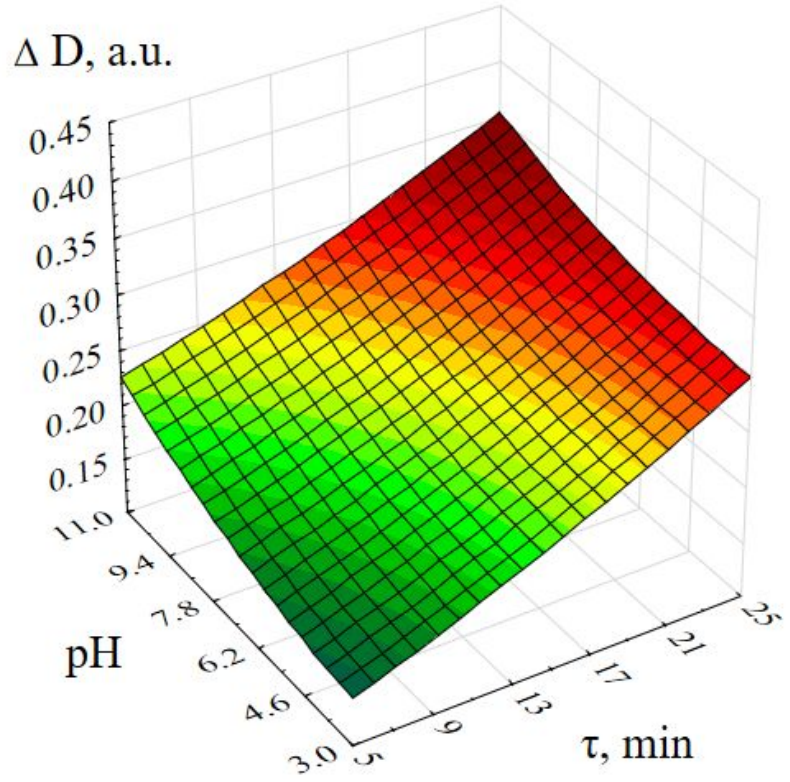

a

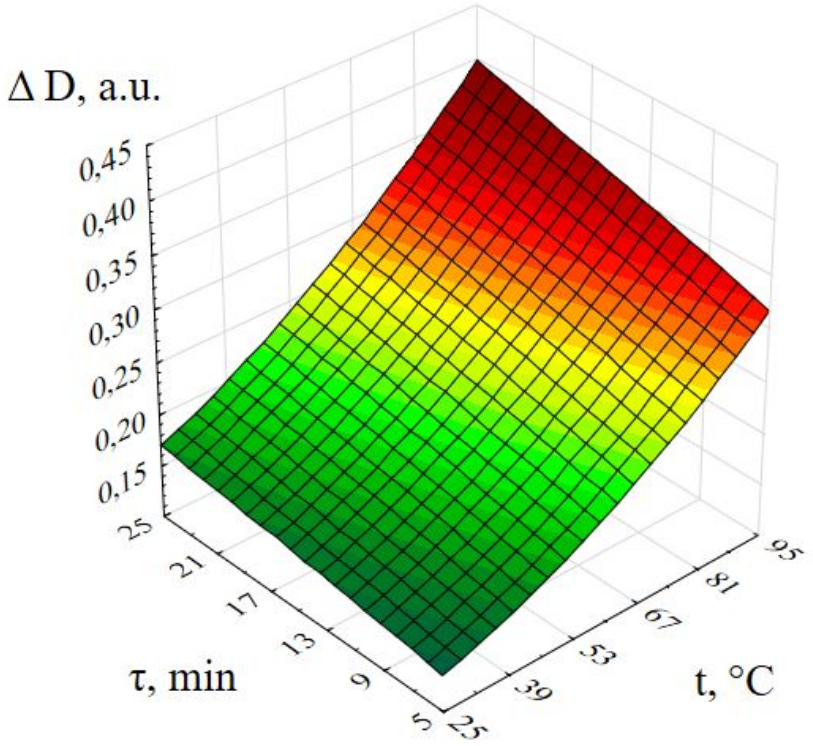

b

Figure S63. Stability of iron ascorbate leucinate: dependences of changes in optical density on technological parameters of pH and exposure time (a), temperature and exposure time (b)

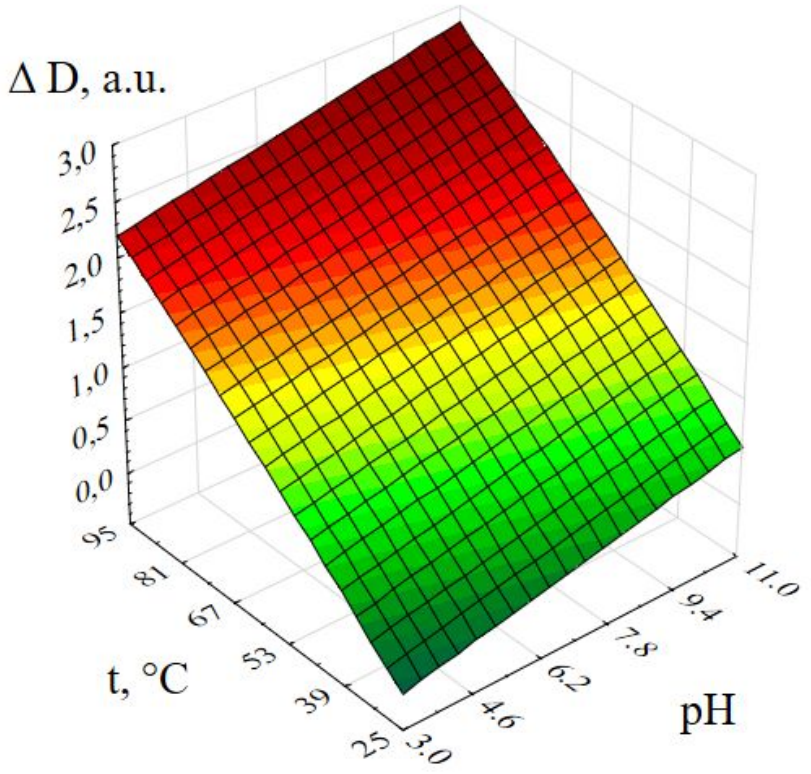

a

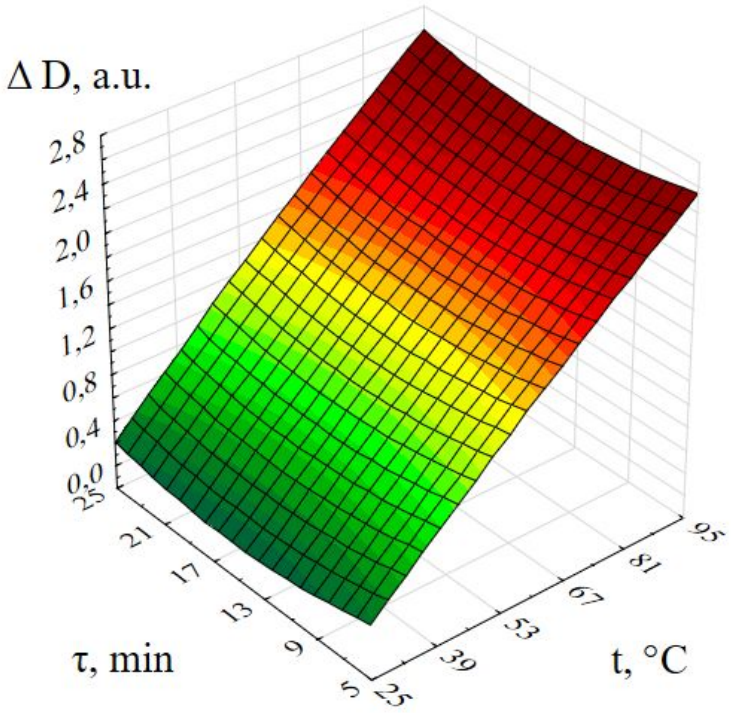

b

Figure S64. Stability of iron ascorbate methioninate: dependences of changes in optical density on technological parameters of pH and temperature (a), temperature and exposure time (b)

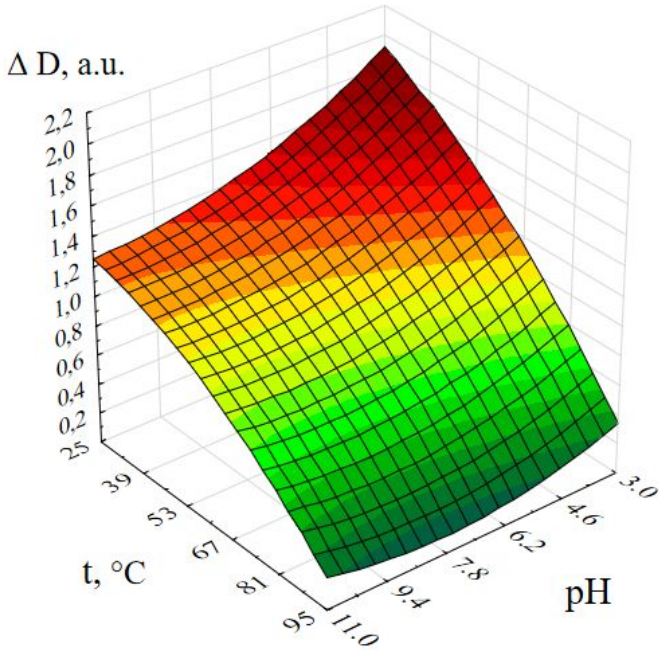

a

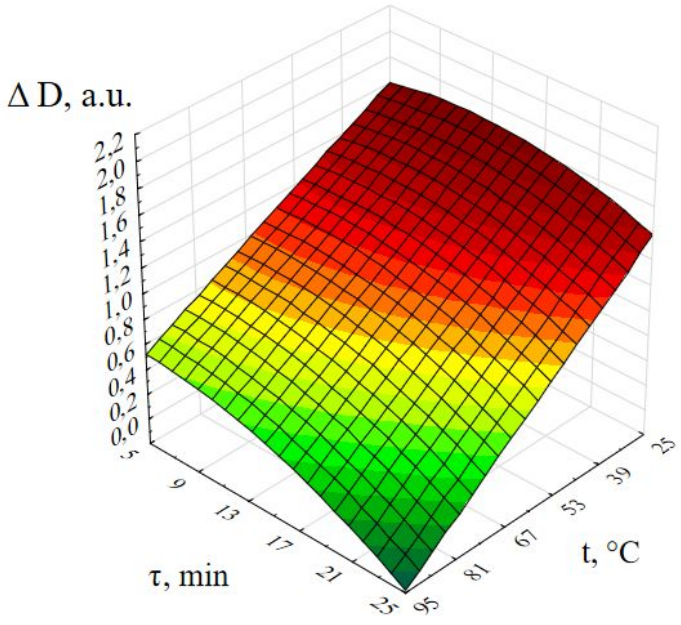

b

Figure S65. Stability of iron ascorbate valinate: dependences of changes in optical density on technological parameters of pH and temperature (a), temperature and exposure time (b)

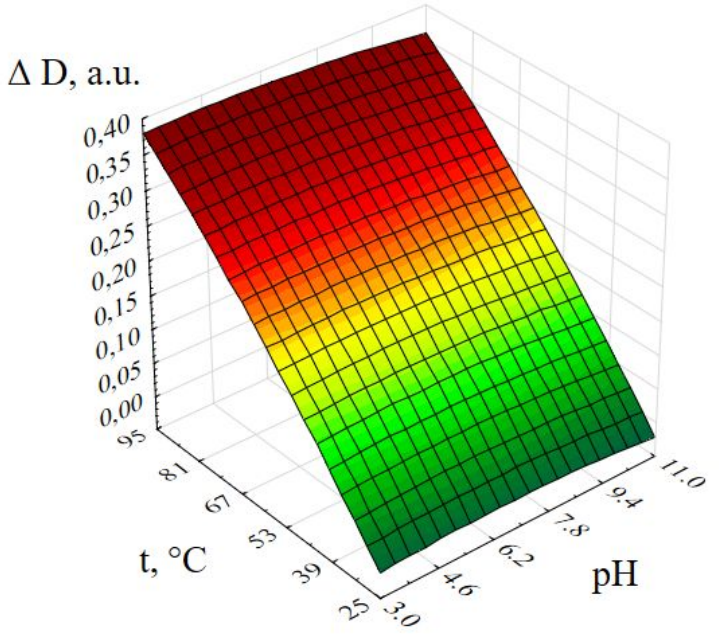

a

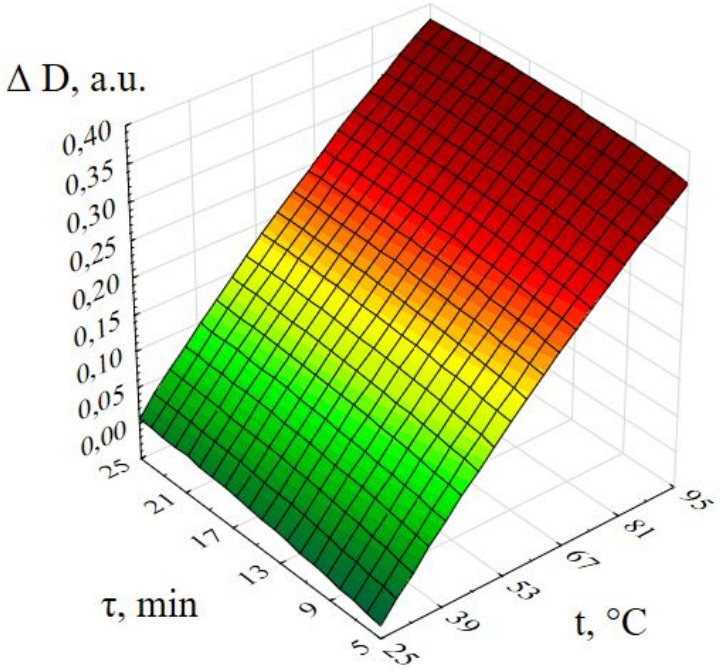

b

Figure S66. Stability of iron ascorbate phenylalaninate: dependences of changes in optical density on technological parameters of pH and temperature (a), temperature and exposure time (b)

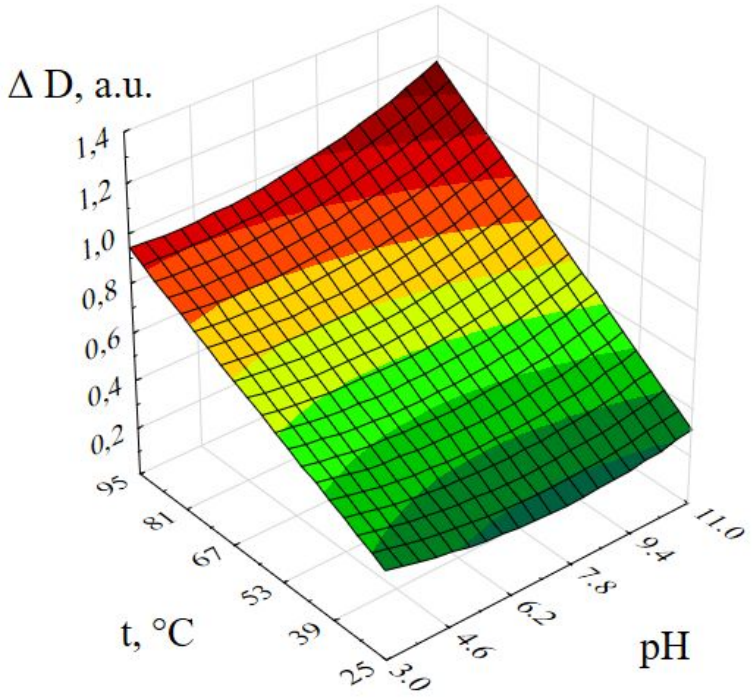

a

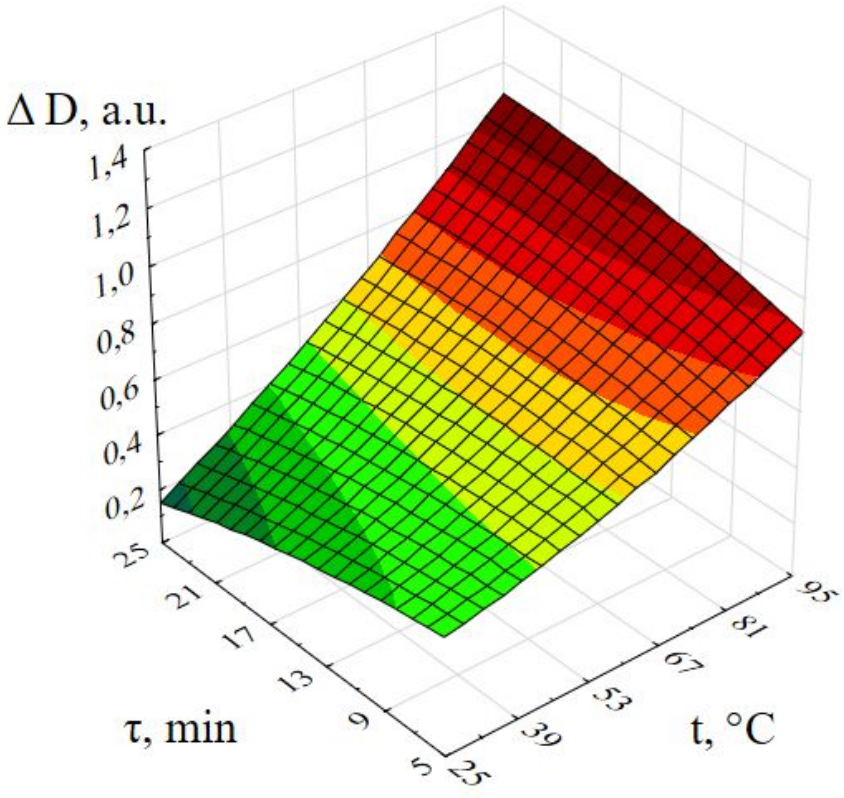

b

Figure S67. Stability of iron ascorbate threoninate: dependences of changes in optical density on technological parameters of pH and temperature (a), temperature and exposure time (b)